ไฮโดรจิเนชันอิมัลชันพอลิไอโซพรีนขนาดนาโนเมตรและน้ำยางธรรมชาติในวัฏภาคน้ำ โดยใช้ตัวเร่งปฏิกิริยาโรเดียม

นายพรเลิศ ปิยะอารีธรรม

วิทยานิพนธ์นี้เป็นส่วนหนึ่งของการศึกษาตามหลักสูตรปริญญาวิทยาศาสตรดุษฎีบัณฑิต
สาขาวิชาเคมีเทคนิค ภาควิชาเคมีเทคนิค
คณะวิทยาศาสตร์ จุฬาลงกรณ์มหาวิทยาลัย
ปีการศึกษา 2556

AQUEOUS-PHASE HYDROGENATION OF NANOSIZED POLYISOPRENE EMULSION AND NATURAL RUBBER LATEX USING RHODIUM CATALYSTS

Mr. Pornlert Piya-areetham

A Dissertation Submitted in Partial Fulfillment of the Requirements
for the Degree of Doctor of Philosophy Program in Chemical Technology
Department of Chemical Technology
Faculty of Science
Chulalongkorn University
Academic Year 2013

Thesis Title	AQUEOUS-PHASE HYDROGENATION OF NANOSIZED POLYISOPRENE EMULSION AND NATURAL RUBBER LATEX USING RHODIUM CATALYSTS
By	Mr. Pornlert Piya-areetham
Field of Study	Chemical Technology
Thesis Advisor	Professor Pattarapan Prasassarakich, Ph.D.
Thesis Co-Advisor	Professor Garry L. Rempel, Ph.D.

Accepted by the Faculty of Science, Chulalongkorn University in Partial Fulfillment of the Requirements for the Doctoral Degree

.....Dean of the Faculty of Science

(Professor Supot Hannongbua, Dr. rer. nat.)

THESIS COMMITTEE

.....Chairman

(Associate Professor Kejvalee Pruksathorn, Ph.D.)

.....Thesis Advisor

(Professor Pattarapan Prasassarakich, Ph.D.)

.....Thesis Co-Advisor

(Professor Garry L. Rempel, Ph.D.)

.....Examiner

(Assistant Professor Napida Hinchiranan, Ph.D.)

.....Examiner

(Assistant Professor Sirilux Poompradub, Ph.D.)

.....External Examiner

(Suwadee Kongparakul, Ph.D.)

พรเลิศ ปิยะอารีธรรม : ไฮโดรจิเนชันอิมัลชันพอลิไอโซพรีนขนาดนาโนเมตรและน้ำยางธรรมชาติในวัฏภาคน้ำโดยใช้ตัวเร่งปฏิกิริยาโรเดียม. (AQUEOUS-PHASE HYDROGENATION OF NANOSIZED POLYISOPRENE EMULSION AND NATURAL RUBBER LATEX USING RHODIUM CATALYSTS) อ.ที่ปรึกษาวิทยานิพนธ์หลัก: ศ. ดร.ภัทรพรรณ ประศาสน์สารกิจ, อ.ที่ปรึกษาวิทยานิพนธ์ร่วม: Prof. Garry L. Rempel Ph.D., 116 หน้า.

งานวิจัยนี้เป็นการปรับปรุงสมบัติทางความร้อนและสมบัติเชิงกลของยางธรรมชาติและอนุภาคนาโนพอลิไอโซพรีนด้วยไฮโดรจิเนชันปราศจากตัวทำละลายอินทรีย์โดยใช้ตัวเร่งปฏิกิริยาโรเดียมที่ละลายน้ำได้ โครงสร้าง C=C พันธะคู่ในน้ำยางธรรมชาติและพอลิไอโซพรีนอิมัลชันสังเคราะห์ขนาดอนุภาค 49 นาโนเมตรถูกไฮโดรจิเนตโดยใช้สารประกอบเชิงซ้อนโรเดียม ($RhCl_3/PPh_3$, $RhCl_3$/TPPTS และ $RhCl_3$/TPPMS) จากการศึกษาไฮโดรจิเนชันปราศจากตัวทำละลายอินทรีย์พบว่า ระดับไฮโดรจิเนชันของยางธรรมชาติและพอลิไอโซพรีนสังเคราะห์มีค่าสูงสุดเมื่อใช้ $RhCl_3$/TPPMS เป็นตัวเร่งปฏิกิริยา คือร้อยละ 85.8 และ 96.0 ตามลำดับ ซึ่งสามารถอธิบายพฤติกรรมการเร่งปฏิกิริยาได้ด้วยตัวแบบฮาร์ทเลย์ไอออนิกไมเซล ระดับไฮโดรจิเนชันสูงขึ้นเมื่อมีการเพิ่มของความเข้มข้นของตัวเร่งปฏิกิริยา อุณหภูมิ และความดันไฮโดรเจน จากการศึกษาเพิ่มเติมพบว่าความสามารถของตัวเร่งปฏิกิริยา $RhCl_3$/TPPMS ในไฮโดรจิเนชันน้ำยางธรรมชาติมีค่าต่ำกว่าในไฮโดรจิเนชันพอลิไอโซพรีนอิมัลชันสังเคราะห์ที่ทุกภาวะเนื่องจากในน้ำยางธรรมชาตินั้นมีสารมลทิน เช่น โปรตีน จากการศึกษาจลนพลศาสตร์พบว่าไฮโดรจิเนชันอนุภาคนาโนพอลิไอโซพรีนเป็นปฏิกิริยาอันดับหนึ่งขึ้นกับปริมาณพันธะคู่ ค่าคงที่อัตราเร็วขึ้นกับความเข้มข้นของตัวเร่งปฏิกิริยา อุณหภูมิ ความดันไฮโดรเจน และขนาดอนุภาคพอลิไอโซพรีน ค่าพลังงานกระตุ้นของปฏิกิริยาที่ช่วงอุณหภูมิ 120 ถึง 140 องศาเซลเซียส มีค่า 117.0 กิโลจูล/โมล ยางธรรมชาติและพอลิไอโซพรีนไฮโดรจิเนตให้ค่าความเสถียรความร้อนสูง กล่าวคือมีค่าอุณหภูมิสลายตัวสูงสุดที่ 466 และ 462 องศาเซลเซียส จากการวิเคราะห์สมบัติเชิงกลพลวัตพบว่ายางเอทิลีนพรอพิลีนให้ค่ามอดูลัสสูงที่สุดเนื่องจากโครงสร้างอิ่มตัวสายโซ่พอลิเมอร์ การผสมพอลิไอโซพรีนไฮโดรจิเนตลงในยางธรรมชาติช่วยเพิ่มความทนต่อความร้อนและโอโซนของยางธรรมชาติผสม

ภาควิชา เคมีเทคนิค ลายมือชื่อนิสิต .....

สาขาวิชา เคมีเทคนิค ลายมือชื่อ อ.ที่ปรึกษาวิทยานิพนธ์หลัก .....

ปีการศึกษา 2556 ลายมือชื่อ อ.ที่ปรึกษาวิทยานิพนธ์ร่วม .....

5273879023 : MAJOR CHEMICAL TECHNOLOGY
KEYWORDS: NATURAL RUBBER LATEX / NANOSIZED POLYISOPRENE / HYDROGENATION / RHODIUM / AQUOUS-PHASE

PORNLERT PIYA-AREETHAM: AQUEOUS-PHASE HYDROGENATION OF NANOSIZED POLYISOPRENE EMULSION AND NATURAL RUBBER LATEX USING RHODIUM CATALYSTS. ADVISOR: PROF. PATTARAPAN PRASASSARAKICH, Ph.D., CO-ADVISOR: PROF. GARRY L. REMPEL, Ph.D., 116 pp.

A water-soluble rhodium catalyst is an efficient catalyst for hydrogenation of unsaturated polymers in the absence of organic solvent. Natural rubber (NR) latex and nanosized polyisoprene (PIP) emulsion were hydrogenated using rhodium complexes ($RhCl_3/PPh_3$, $RhCl_3$/TPPTS and $RhCl_3$/TPPMS) as a catalyst precursor. A high hydrogenation degree (HD) (85.8% for NR, 96.0% for PIP) was achieved by using $RhCl_3$/TPPMS. The catalytic behavior could be well explained by the Hartley ionic spherical micelle model. The HD increased with increasing catalyst amount, reaction temperature and H_2 pressure. The catalyst activity in NR hydrogenation was found to be lower than that in PIP hydrogenation for all conditions due to impurities in the latex, including protein. Kinetic experiments for PIP hydrogenation indicate that the hydrogenation rate is first order with respect to catalyst and carbon– carbon double bond concentration. The rate constant was dependent on catalyst concentration, temperature and hydrogen pressure, and PIP particle size. The apparent activation energy over the temperature range of 120–140°C was found to be 117.0 kJ/mol. The hydrogenated NR (HNR) and PIP (HPIP) has high thermal stability with a maximum decomposition temperature of 466 and 462°C, respectively. In addition, HNR and HPIP had a maximum storage modulus due to the saturated carbon domains in the polymer chains. For vulcanized NR, the thermal and ozone resistance of NR could be improved by using HPIP as filler.

Department: Chemical Technology Student's Signature .....

Field of Study: Chemical Technology Advisor's Signature .....

Academic Year: 2013 Co-advisor's Signature .....

ACKNOWLEDGEMENTS

The author would like to express heartfelt gratitude and sincere appreciation to his advisor, Prof. Dr. Pattarapan Prasassarakich and co-advisor, Prof. Garry L. Rempel for the helpful discussion, encouraging guidance, supervision and support throughout his research. The author also would like to acknowledge Assoc. Prof. Dr. Kejvalee Pruksathorn, Asst. Prof. Dr. Napida Hinchiranan, Asst. Prof. Dr. Sirilux Poompradub and Dr. Suwadee Kongparakul for serving as the dissertation chairman and members of thesis committee, respectively, and for their worthy comments and suggestions.

The author gratefully acknowledge the funding support from the Thailand Research Fund (through the Royal Golden Jubilee Project), Graduate School, Chulalongkorn University, the Natural Sciences and Engineering Research Council of Canada (NSERC), the Thai Government Stimulus Package 2 (TKK2555) under the Project for Establishment of Comprehensive Center for Innovative Food, Health Products and Agriculture and the National Research University Project of CHE and Ratchadaphiseksomphot Endowment Fund (AM1024I).

Many thanks also go to the Department of Chemical Technology, Faculty of Science, Chulalongkorn University and Department of Chemical Engineering, University of Waterloo, Canada for providing research facilities throughout this research work.

Finally, the author would also express his deep sense of gratitude to his family for their love, support and encouragement throughout graduate study. Special thanks are also extended to his friends for friendship, support and encouragement.

CONTENTS

Page

Page

Page

Page

LIST OF TABLES

Table PAGE

LIST OF FIGURES

Figure PAGE

Figure PAGE

LIST OF ABBREVIATIONS

ASTM	: American Society for Testing and Materials
D_n	: Number-average diameter
HD	: Hydrogenation Degree
HNR	: Hydrogenated Natural Rubber
HPIP	: Nanosized Hydrogenated Polyisoprene
ISO	: International Standardization for Organization
NR	: Natural Rubber
PIP	: Nanosized Polyisoprene
PPh_3	: Triphenylphosphine
SDS	: Sodium Dodecylsulfate
SPS	: Soduim Persulfate
T_g	: Glass Transition Temperature
TGA	: Thermal Gravimetric Analysis
T_{id}	: Initial Decomposition Temperature
T_{max}	: Maximum Decomposition Temperature
TPPMS	: Monosulfonated Triphenylphosphine
TPPTS	: Trisulfonated Triphenylphosphine
ZDEC	: Zincdiethyl Dithiocarbamate
ZnO	: Zinc Oxide

CHAPTER I

INTRODUCTION

1.1 Motivation

Currently, the increasing concern of environmental consciousness and the concept of green chemistry has approached significant attention globally due to the increase of hazardous substances, waste and energy consumption. The concept of green chemistry concentrates on finding a friendly process for the environment and human health. For polymer processes, some of the most important commercial polymers are diene based polymers e.g., polyisoprene, polybutadiene, styrene butadiene rubber (SBR) and acrylonitrile butadiene rubber (NBR) containing olefinic groups within the polymer which are the basis for a variety of chemical modification reactions. One green (biodegradable and renewable) diene polymer is natural rubber. Due to its ability to crystallize under stretching with high impact resilience and tear strength, NR has outstanding mechanical and dynamic properties. It also exhibits low heat build-up with good formability[1]. However, it is deteriorated by thermal and oxidative degradation due to its unsaturated carbon–carbon double bonds in the polyisoprene backbone, which limits NR for outdoor applications. To improve the thermal properties, hydrogenation is a simple chemical modification which involves the reduction of the unsaturated carbon-carbon double bonds (C=C) to enhance stability against thermal and oxidative degradation of the diene-based elastomer. Most hydrogenation processes are carried out in the presence of an organic solvent which are usually toxic and cause damage to the environment. So, using aqueous media instead of organic solvents becomes more attractive since water is non-toxic, non-flammable, inexpensive, and is an environmentally friendly solvent. Thus, organic solvent-free hydrogenation would be a “green process” which may be an alternative approach in the future for the realization of a commercial process for green latex hydrogenation.

1.2 Green Process: Aqueous Media

Although a term only coined over the past decade, “Green Chemistry” is not a new concept or an approach. This concept can be applied throughout chemistry and chemical engineering because it can be applied to processes or procedures that may involve one or more of a number of issues: reduce or eliminate the use and generation of hazardous substances, reduce waste, reduce energy consumption, and utilize renewable resources [2]. These ideals are elegantly defined in Paul Anastas’ principles of green chemistry which can be summarized in that all materials and energy inputs and outputs should be as inherently nonhazardous as possible and should be renewable rather than depleting resources and should prevent waste instead of having to clean up waste after it is formed. Moreover, material diversity in multicomponent products should be minimized to promote disassembly and value retention. In addition, the design of products, processes, and systems must include integration and interconnectivity with available energy and materials flows and should be designed to maximize overall efficiency and minimize energy consumption and materials used [3]. These concepts have not just been created; but indeed, the chemist and chemical engineer should always try to find better reaction selectivity and activity, better catalysts, and improved process conditions, without damaging human well-being and the environment. Therefore, developments in green chemistry, whether they involve improved syntheses, catalysis, new environmentally friendly solvents, alternative energy sources, renewable resources, or new technologies are important [4].

Focusing on organic solvents, a survey of past and present knowledge of toxic solvents reveals outstanding features and continuous development to preserve the health of people who are exposed to toxic solvents. People dealing with organic solvents have exhibited recognizable symptoms of ill-health, or have even died without accurate diagnosis of their cause. When solvents are judged to be toxic, measures should be instituted to prevent as far as possible the entry of the toxic substances into the body [5]. It is now possible to forecast through animal experiments whether a solvent is likely to be toxic to human beings and even to determine the probable nature and site of action of its toxic effect. Although much

deeper research may be needed to translate the effects of such animal experiments into human experience, preventing people from toxicity of organic solvents should be a first priority.

An aqueous solution is a solution in which the solvent is water. The word aqueous means pertaining to, related to, similar to, or dissolved in water. As water is an excellent solvent and is also naturally abundant, it is an ubiquitous solvent in chemistry. Substances which are hydrophobic ('water fearing') often do not dissolve well in water whereas those that are hydrophilic ('water-loving') do. Water is a natural solvent. Molecular interactions and biochemical transformations in living systems mostly occur in an aqueous environment. Nevertheless, the use of water as a solvent in modern synthetic chemistry practically disappeared when the role of highly polar organic solvents endowed with solvation properties was recognized. The lack of water-solubility of organic compounds, along with the water-sensitivity of some reagents or reactive intermediates, prevented chemists from thinking about water as a solvent for organic synthesis. However, using aqueous media was rediscovered in the 1980s in cycloaddition of cyclopentadiene with methyl vinyl ketone [6]. The rate of the cycloaddition of cyclopentadiene in water was enhanced by a factor of more than 700 compared with the reaction in isooctane

The green credentials of water as a solvent are that it is nonflammable, not combustible, and nontoxic. In addition, its polarity and density make it easy to separate from most organic compounds, and it has favorable thermal properties. Hydrophobic effects and hydrogen bonding can each contribute to the rate enhancement of some reactions in water [4]. In addition, the low solubility of oxygen in water can facilitate the use of air sensitive transition metal catalysts in air. The use of water as a solvent implies that there is no need for protection-deprotection processes for acidic hydrogen-containing functional groups, thereby increasing synthetic efficiency. Similarly, laborious derivatization processes are not necessary for water-soluble compounds such as carbohydrates. Potential drawbacks include the low solubility of organic substrates and reactions involving water sensitive compounds, though it is noteworthy that larger rate increases are sometimes found for insoluble substrates.

1.3 Natural Rubber

Natural rubber (NR) is used as a general propose elastomer and is often irreplaceable by other synthetic rubbers due to its unique mechanical properties such as high tensile strength with high flexibility and low heat build-up. Thus, NR is normally applied in various industries such as the tire industry, medical equipment and for engineering thermoplastic materials. NR latex is obtained from the milky secretion which is largely produced from tapping the para rubber tree or "*Hevea Brasiliensis*", which is an original native of the tropical rain forest in the Amazon Basin in Brazil. Nowadays, most NR in the world is supplied from Southeast Asia, mainly Thailand, Malaysia and Indonesia. The statistics for NR gross exportation is shown in Figure 1.1.

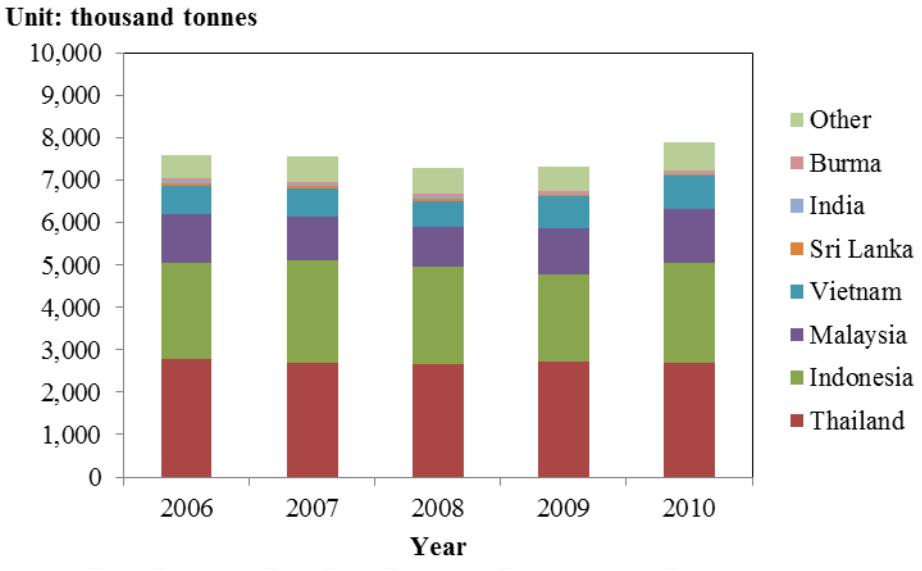

Figure 1.1 Gross Exports of Natural Rubber 2002-2010 (Thai rubber statistic, The Thai Rubber Association) [7].

NR latex contains rubber particles suspended in an aqueous serum phase. The latex exuded from cutting is called fresh NR latex or fresh latex. The chemical structure of NR latex mainly consists of *cis*-1,4 polyisoprene higher than 94%, initiating-ends (ω-terminal group) and terminating-ends (α-terminal group) (Figure 1.2)

with a molecular weight of 100,000 to 1,000,000 [8]. The fresh latex is composed of approximately 30 – 40% dry rubber content (DRC) and 5 – 10% of non-rubber components such as proteins, lipids, carbohydrates and inorganic salts. The composition depends on the clones and age of the rubber tree including the tapping method. A typical fresh latex composition is shown in Table 1.1

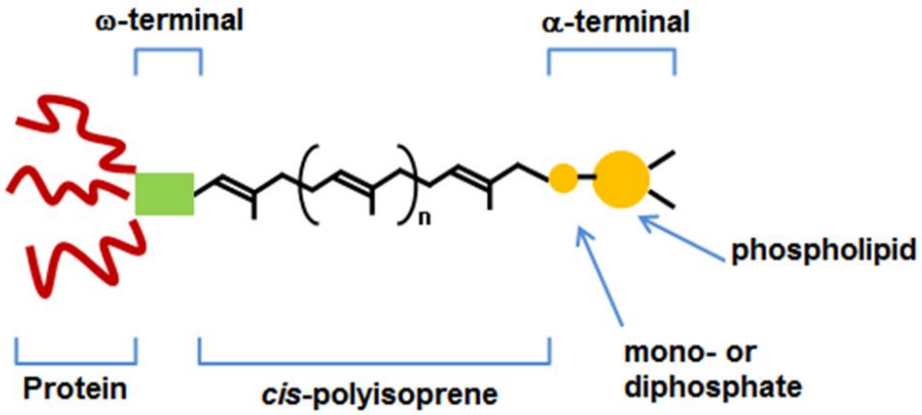

Figure 1.2 The chain structure of NR. [8].

Table 1.1 Composition of NR Latex [9].

Composition	wt.%
Water	55
Rubber hydrocarbon	35
Protein	4.5
Acetone extraction	3.9
Amino acid	0.2
Quebrachitol	1
Inorganic salts	0.4

Hevea rubber is a very high molecular weight polymer with a broad molecular weight distribution (MWD). The broad MWD of hevea rubber is presumed to be derived from the branching and crosslinking reactions by certain special functional groups in the rubber molecules. The NR in dry solid form consists of two components which are called “sol” and “gel” [10]. The sol phase is the rubber component which dissolves easily in solvents such as cyclohexane, toluene, tetrahydrofuran (THF), etc., while the gel phase is insoluble but swells in the same solvent. Commercially dry Hevea rubber contains 5-50% gel component, depending on the clonal origin of the rubber, processing conditions, time and the storage temperature. The true gel phase in NR is presumed to consist of small crosslink latex particles or “microgels” [11] as shown in Figure 2.5. The microgels are combined into a matrix with the sol fractions and form an apparent gel phase. Since the gel phase in NR comprises nitrogenous and mineral components higher than the sol phase, it can be postulated that the gel phase is linked up with the network of proteins via hydrogen bonding. The removal of gel content in the rubber can be performed by deproteinization, transesterification and saponification [12]. These treatments can decompose the branching and crosslinks that include protein and fatty acid ester groups, respectively. This can be attributed to the fact that the branching and crosslinks are composed of two types of branch-points. One is presumed to be formed by the intermolecular interaction of proteins and another by phosphoric ester groups and long chain fatty acid ester groups as shown in Figure 2.6. Moreover, the gel phase in Hevea rubber is sometimes classified as “loose gel” or “soft gel” and “tight gel” or “hard gel”. The soft gel is derived from the various non-rubber components, which can be decomposed by chemical reaction such as enzymatic deproteinization transesterification and saponification [12]. On the other hand, the hard gel is formed by crosslinking of unsaturated rubber chains, and cannot be decomposed by chemical reaction.

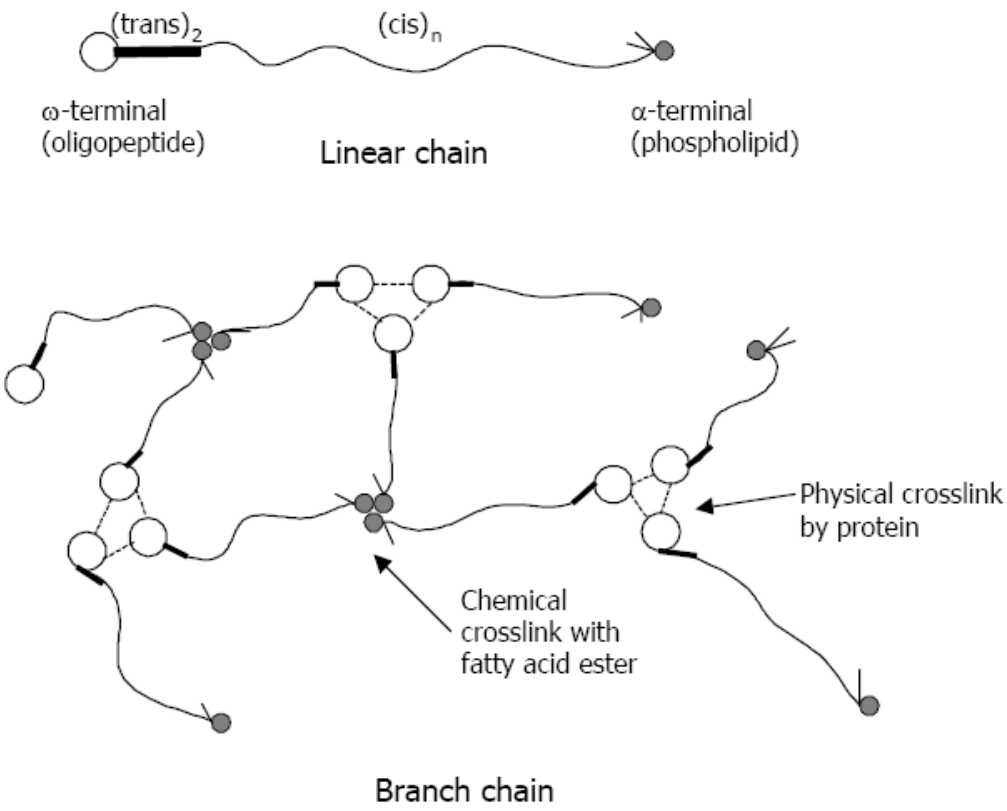

Figure 1.3 Presumed structure of branching and crosslinking of natural rubber [12].

1.4 Chemical Modification: Hydrogenation of Diene Polymers

Some of the most important commercial polymers are diene based polymers, e.g., polyisoprene, polybutadiene, styrene butadiene rubber (SBR) and acrylonitrile butadiene rubber (NBR). Their usefulness to scientists and engineers forms the basis for a variety of chemical modification reactions that are made possible because of the presence of the olefinic group within the polymer. Chemical modification of polymers is a post-polymerization process. In the broadest sense, chemical modification could include reactions such as crosslinking, grafting, degradation, oxidation, isomerization, and cyclization. Its main use is to produce polymers with desirable physical and chemical properties that are not accessible by standard polymerization techniques. In the past several years, considerable interest has been expressed in the modification of diene polymers by metal-catalyzed

reactions such as hydrosilylation, hydrocyanation, hydrocarboxylation, hydrofromylation, hydrooxymethylation, and hydrogenation. Among these, hydrogenation has been the most widely investigated. The subject has been reviewed previously; however, since the publication of these reviews there has been a surge of new research on this subject, and this current review will illustrate the progress made in the field over the last 15 or so years [13, 14].

Hydrogenation in itself simply reduces the degree of unsaturation in the diene polymer. Nevertheless, it leads to significant changes in the chemical and physical properties of the polymer. The reasons for carrying out this process are quite varied, and hydrogenated diene polymers are being used in an ever-growing number of applications, such as in research examining polymer structure and morphology. The major utilization has been in applications that require material with enhanced resistance to thermal and oxidative degradation. Possibly, the only factor that has prevented hydrogenated polymer from being used in a wide range of applications is the fact that they are relatively expensive to produce. Conversely, the ever-growing body of research on hydrogenated polymers suggests that this economic factor is becoming less important or that lower cost processes are becoming more feasible.

Hydrogenation of polymers can be achieved by both catalytic and noncatalytic methods. There are some recent citations of the use of noncatalytic hydrogenation of diene polymers. The main method of noncatalytic hydrogenation is by diimide reduction using hydrazide as the reagent. This method has one major advantage over others in that it circumvents the need for specialized hydrogenation apparatus. Despite this advantage, studies into the catalytic hydrogenation of diene polymers are by far more numerous.

Within the general heading of catalytic hydrogenation, there are examples of the use of both heterogeneous and homogeneous catalyst systems. The use of heterogeneous catalysts is still prevalent, however, the majority of new developments in the field of catalytic hydrogenation over the last few years have involved the use of homogeneous catalysis because it provides a better opportunity to realize quantitative and selective hydrogenation of carbon-carbon unsaturation [15].

1.4.1 Non-Catalytic Hydrogenation

The hydrogenation of rubber generally requires hydrogen, an organic solvent, and a metal catalyst; therefore, an alternative way of diimide reduction was developed [16]. The numerous sources of diimide mentioned below were discovered through the uncatalysed hydrogenation of olefins. Diimide hydrogenation is divided into two steps: (1) the reaction between hydrazine and hydrogen peroxide to produce the diimide and (2) the reaction between diimide and carbon–carbon double bonds to form the hydrogenated polymer, as given by the following equations:

$$N_2H_4 + H_2O_2 \longrightarrow N_2H_2 + 2H_2O \qquad (1.1)$$

$$N_2H_2 + R_1HC{=}CHR_2 \longrightarrow N_2 + R_1H_2C\text{-}CH_2R_2 \qquad (1.2)$$

The source for releasing diimide as an active species from the redox reaction of hydrazine hydrate (N_2H_4) with hydrogen peroxide (H_2O_2) as a strong oxidizing agent is energetically favorable due to the production of the final product in latex form and the absence of any organic solvent [17]. Furthermore, this technique could be operated without high hydrogen pressure equipment.

Diimide reduction has been applied for the hydrogenation of carbon-carbon double bonds within acrylonitrile-butadiene rubber (NBR) with a hydrogenation degree of 81% [18] and NR latex with a hydrogenation degree of 67% [19]. However, a low degree of hydrogenation of NR was obtained due to the larger size of the rubber particles (0.2-2 μm).

Wideman [16] studied the use of the diimide reduction method to hydrogenate NBR latex. The N_2H_4/H_2O_2 (or oxygen) redox system was used to generate an *in situ* diimide (N_2H_2). 80% hydrogenation was achieved when copper ion (or ferric sulfonate) was applied as a promoter.

Parker et al. [20] provided more refined results and a detailed process for the preparation of highly saturated NBR latex. The diimide hydrogenating agent was generated from the N_2H_4/H_2O_2 system at the surface of the polymer particles. Carboxylated surfactants, which were adsorbed at the latex particle surface, played an important role by forming hydrazinium carboxylates with hydrazine and copper ions. Then, the generated N_2H_2 intermediates were stabilized by copper ions (Cu^{2+}) to effectively reduce the carbon–carbon double bonds.

Simma et al. [21] reported on the diimide hydrogenation of skim natural rubber latex (SNRL) in a system of N_2H_4/H_2O_2 using cupric ion as promoter. Their results provided a degree of hydrogenation of 64.5% at a hydrazine: hydrogen peroxide ratio of 1.6:1 and a low copper sulfate concentration of 49.5 μM. The kinetic results of diimide hydrogenation of SNRL exhibited a first order behavior with respect to the carbon double bond concentration, and the apparent activation energy of the promoted (with cupric ion) and non-promoted hydrogenation (without cupric ion) of SNRL over the range of 60–80 °C was found to be 9.5 and 21.1 kJ/mol, respectively.

Xie et al. [22] reported on the hydrogenation of NBR latex via diimide reduction to produce HNBR by reduction of the gel content of the hydrogenation product to 15% while maintaining a high hydrogenation degree. The hydrogenated product exhibited good oil resistance, excellent thermo-oxidative resistance and good mechanical properties. The retention after thermal ageing in tensile strength and ultimate elongation was 98% and 96%, respectively.

Lin et al. [23] investigated the hydrogenation of NBR latex via utilization of diimide. It was found that the use of boric acid as a promoter could produce a hydrogenation efficiency of nearly 100% and the hydrogenation efficiency by using promoters of copper ion, silver ion or ferrous ion were lower than that of boric acid.

He et al. [24] studied the diimide hydrogenation of styrene-butadiene rubber (SBR) latex as a function of different particle sizes. It was found that the hydrogenation of carbon–carbon double bonds depended on the latex particle size and the extent of crosslinking in the particles. The SBR latex with a diameter of 50 nm could be hydrogenated to the extent of 91% using a N_2H_4/H_2O_2 mole ratio of 1 per mole of carbon-carbon double bonds. For the SBR latex with a diameter of 230 nm, the hydrogenation degree was only 42%. The effect of particle size on the %

hydrogenation could be explained according to a “layer model”. The copper ion promoter was postulated as staying at the surface of the latex particles. By modulating the concentration of copper ions at the particle surface, a higher degree of hydrogenation could be attained. However, the gel fraction of SBR latex was increased after the hydrogenation.

1.4.2 Catalytic Hydrogenation in Organic Solvents

Homogeneous catalysts are favoured for catalytic hydrogenation of unsaturated polymers because they have higher selectivity and do not have a macroscopic diffusion problem. In addition, the performance of homogeneous catalysts can be explained and understood at the molecular level [25]. There is much research reported on hydrogenation of synthetic diene-based polymers such as polybutadiene [26-28], styrene-butadiene copolymers (SBR) [29-31], acrylonitrile-butadiene copolymers (NBR) [32-36], NR [37-39] and grafted NR [40, 41] using homogeneous catalysts composed of transition metal complexes of Rh, Ir, Ru, Os and metallocenes including Ziegler-Natta type catalysts. For hydrogenation of latex rubber, there are three possible methods for hydrogenation in the latex phase [42]; hydrogenation of the latex using oil soluble catalysts with an organic co-solvent, hydrogenation of latex using water soluble catalysts, hydrogenation of latex using hydrazine and hydrogen peroxide.

For hydrogenation of diene based copymers containing potentially reducible functional groups such as –CN, Wilkinson’s catalyst, $RhCl(PPh_3)_3$, has been well known to be the effective catalyst with high selectivity for reduction of the carbon-carbon unsaturation. This catalyst can be produced in high yield and it is easy to handle because it has excellent stability in air. For the kinetics of polybutadiene hydrogenation catalyzed by $RhCl(PPh_3)_3$, the kinetic data for the hydrogenation were collected using a gas-uptake apparatus [43]. The polybutadiene hydrogenation was found to exhibit a first-order dependence on the carbon-carbon double bond, catalyst and hydrogen concentration. For the kinetics of hydrogenation of NBR catalyzed by $RhCl(PPh_3)_3$ and $RhH(PPh_3)_4$, the results indicated that the hydrogenation reaction had an inverse first-order dependence with respect to nitrile

concentration [34]. From the kinetic results, the reaction mechanism was proposed as shown in Figure 1.4. Moreover, another advantage of these Rh complexes for NBR hydrogenation is that the relative viscosity of hydrogenated product was constant when the polymer and catalyst loading was increased [44]. This implies that these complexes did not promote cross-linking or gel formation of NBR.

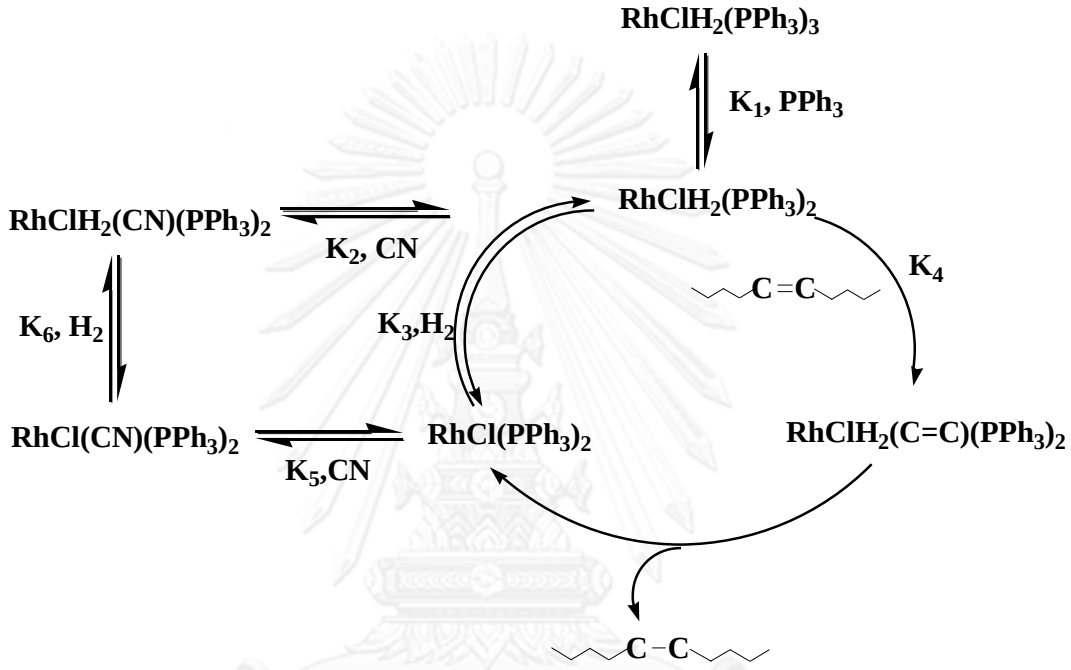

Figure 1.4 Proposed reaction mechanism for NBR hydrogenation catalyzed by $RhCl(PPh_3)_3$ [34].

Homogeneous catalysts have been reported to increase the rate of rubber hydrogenation. High degrees of hydrogenation (≥97%) of *cis*-1,4 polyisoprene were achieved with a $Ru(CH=CH(Ph))Cl(CO)(PCy_3)_2$ concentration of 200 μM and 180 °C in monochlorobenzene [45]. For the hydrogenation of natural rubber using $Ru(CH=CH(Ph))Cl(CO)(PCy_3)_2$, a degree of hydrogenation of 99% was obtained. The hydrogenation of NR led to an increase in the thermal stability of HNR without affecting its glass transition temperature (T_g) [37].

Hinchiranan et al. [38] studied the hydrogenation of natural rubber by using the homogeneous catalyst $OsHCl(CO)(O_2)(PCy_3)_2$ for producing an alternating ethylene-propylene copolymer. The kinetic results showed that the NR

hydrogenation exhibited a first-order dependence on the carbon-carbon double bond and catalyst concentration. It was also found that the hydrogenation rate was first-order and shifted to a zero-order depending on hydrogen pressure at lower to moderate hydrogen pressure which then decreased toward an inverse behavior at pressures higher than 41.4 bar.

Mahittikul et al. [39] studied the use of $OsHClCO(O_2)(PCy_3)_2$ as an effective catalyst for hydrogenation of NR latex in chlorobenzene; however, impurities in NR latex such as protein and lypolipids reduce the catalytic activity. However, the presence of a sulfonic acid in the hydrogenation process could prevent to a considerable extent the poisoning of the osmium catalyst by impurities.

Mohammadi et al. [46] reported a useful method for the hydrogenation of acrylonitrile-butadiene rubber using Wilkinson's catalyst under mild conditions. The process is selective to terminal or internal double bonds in the rubber backbone without any hydrogenation of the nitrile groups. Moreover, the Wilkinson's catalyst could be used for hydrogenation of chloroprene rubber [47]. The hydrogenated chloroprene rubber exhibited improvement in properties such as oxidative resistance, thermal degradation resistance and oil resistance.

Escobar Barrios et al. [30] studied the hydrogenation of styrene-butadiene rubber (SBR) by using n-butyllithium in cyclohexane as the solvent and a catalyst promoter. The dissolved SBR in cyclohexane was homogeneously hydrogenated using a Ziegler-Natta catalyst, prepared from nickel acetylacetonate and n-butyllithium. The Ziegler-Natta catalyst demonstrated an increase in selectivity towards the saturation of the 1,2- vinyl double bonds, as compared with the 1,4-*trans* double bonds.

Kongparakul et al [41] studied the catalytic hydrogenation of styrene-g-natural rubber (ST-g-NR) in the presence of $OsHCl(CO)(O_2)(PCy_3)_2$. ST-*g*-NR was synthesized via emulsion polymerization using CHPO/TEPA as initiator. $OsHCl(CO)(O_2)(PCy_3)_2$ was found to be an effective catalyst for hydrogenation of ST-*g*-NR in monochlorobenzene. From kinetic results, the hydrogenation of ST-g-NR exhibited a first-order dependence on [C=C]. The addition of acid could promote the hydrogenation rate of the ST-*g*-NR. The apparent activation energy over the range of 120–160 °C was found to be 83.3 kJ/mol. The hydrogenation improved the thermal stability of grafted NR without affecting its glass transition temperature.

Similarly, the hydrogenation of methyl methacrylate-g-natural rubber (MMA-*g*-NR) using $OsHCl(CO)(O_2)(PCy_3)_2$ as a catalyst was also studied [40]. Hydrogenation of grafted NR exhibited a first-order dependence on catalyst concentration, implying that the active complex is mononuclear. The addition of a small amount of acid provided a positive effect on the hydrogenation of grafted NR. The hydrogenation rate was dependent on the reaction temperature and H_2 pressure. The apparent activation energy was found to be 70.3 kJ/mol.

1.4.3 Catalytic Hydrogenation in Aqueous Media

Due to the toxicity of organic solvents, catalytic hydrogenation in aqueous media has become more attractive. Sulfonated triphenylphosphine derivatives as catalysts for hydrogenation are very interesting because they are easily synthesized [48]. There are some research reports on the hydrogenation of diene based polymers using sulfonated triphenylphosphine as a ligand. $(RhCl(HEXNa)_2]_2$ (HEXNa = $Ph_2P(CH_2)_5CO_2Na$) and $RhCl(TPPMS)_3$ (TPPMS = $PPh_2(C_6H_4$-m-$SO_3Na)$) are efficient catalyst complexes for biphasic hydrogenation of polybutadiene-based elastomers, especially for low molecular weight polymers. In addition, the Rh/TPPTS complex (TPPTS = $P(C_6H_4$-*m*-$SO_3Na)_3$) is one such water-soluble catalyst complex which has found various applications in the biphasic hydrogenation of polymers. The structures of rhodium with different water-soluble ligands are shown in Figure 1.5.

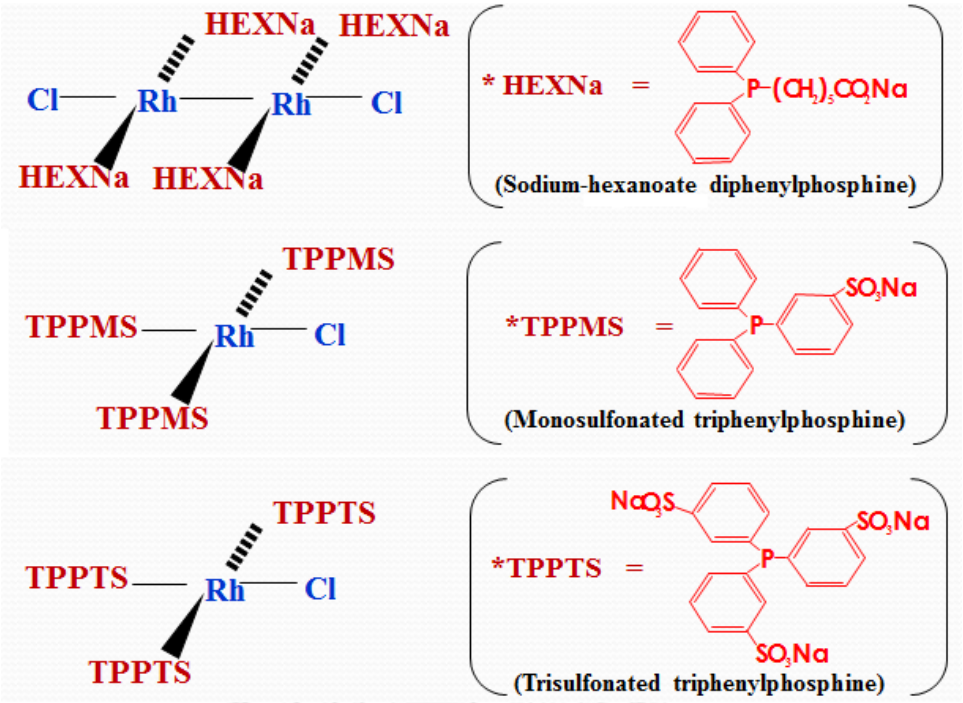

Figure 1.5 Water-soluble rhodium complexes.

Use of a biphasic catalyst is one alternative for hydrogenation of rubber latex. A biphasic catalyst is a type of organometallic catalyst that can react in aqueous media. It has become an alternative and emerging approach in modern homogenous catalytic reactions. Due to the fact that they can operate without organic solvent, this type of catalyst has been successful employed for the hydroformylation of olefins. However this method has a problem with mass transfer limitation between the organic phase and aqueous phase. The only one report was the hydrogenation of NBR latex by using water-soluble catalysts, such as $RhCl(DPM)_3$ (DPM = diphenyl phosphino benzene m- sulphonate) [49]. The hydrogenation of NBR latex was carried out at various pressures (1–50 kg/cm^2), temperatures (50-90 °C) and catalyst concentrations (0.335-1.608 mmol). 63% hydrogenation was achieved at 75 °C at atmospheric pressure for 12 h.

Mudalige et al. [50] reported that the water-soluble complexes $[RhCl(HEXNa)_2]_2$ (HEXNa = Ph_2P-$(CH_2)_5$ –CO_2Na) and $RhCl(TPPMS)_3$ (TPPMS = monosulphonated triphenylphosphine) are effective catalysts for hydrogenation of polybutadiene (PB) and PB-based elastomers in aqueous/organic biphasic media. The % hydrogenation of rubber and extraction behavior of the catalyst in a solvent and the aqueous phase was considered. $[RhCl(HEXNa)_2]_2$ exhibited a reasonable activity

for polymer hydrogenation, especially for low molecular weight polymers, however, it did not satisfy the requirement for a hydrogenation of a 1,4 addition unit under the present experimental conditions.

Kotzabasakis et al. [51] studied the hydrogenation of polybutadiene-1,4-*block* poly(ethylene oxide) (PB-*b*-PEO) catalyzed by Rh/TPPTS [TPPTS = $P(C_6H_4$-*m*-$SO_3Na)_3$] in a mixed micellar system. Effects of the surfactant, dodecyltrimethylammonium chloride (DTAC), addition and n-hexane addition were investigated. It was found that high catalytic activities (TOF>840 h^{-1}) with 94 % hydrogenated C=C conversion were achieved in a micellar nanoreactor formed by DTAC when n-hexane was added to this system. It could be explained by model of a spherical Hartley ionic micelle as shown in Figure 1.6. The position of Rh in the micelle is dependent on the "Hydrophilic-Lipophilic Balance value"– or HLB value of the micelle system. N-hexane and the DTAC surfactant were solubilized in the micelle core and stabilized the HLB value; therefore the rhodium can move to micelle core.

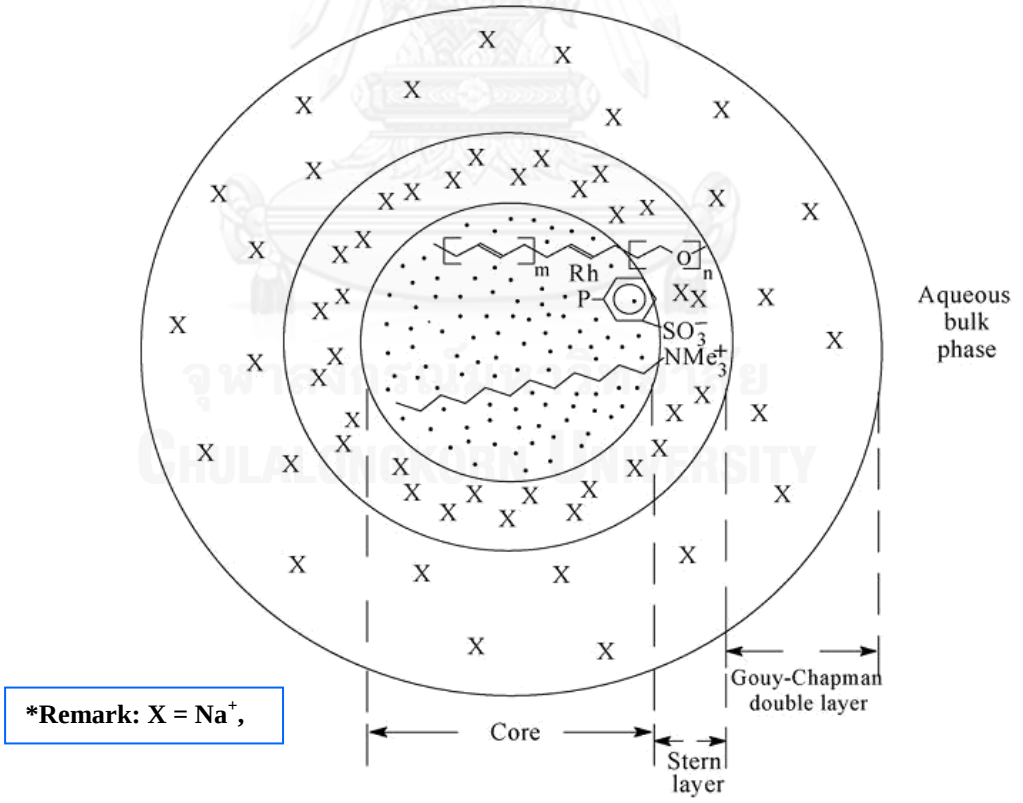

Figure 1.6 Model of a spherical Hartley ionic mixed micellar containing Rh/TPPTS catalyst, PE-*b*-PEO and DTAC [51].

Similar work was also carried out for hydrogenation of polybutadiene (PB) using Rh/TPPTS complex [52]. For PB hydrogenation, effects of temperature, the molar ratio of TPPTS/Rh and the polymer microstructure were investigated. Activity of the catalyst was high (TOF>900 h^{-1}) for the biphasic hydrogenation of the completely water-insoluble heavy PB with a hydrogenated C=C conversion of 84 % at a temperature of 100 °C and TPPTS/Rh molar ratio of 3. For PB with high 1,4-unit content, the catalyst activity was high in mixed micelles created by DTAC and Brij-35 surfactants. For PB with a high 1,2 unit content, the catalyst activity was high in single micelles created by DTAC.

Wei et al. [53] reported on a new approach for hydrogenation of acrylonitrile-butadiene rubber (NBR) in latex form using $RhCl(PPh_3)_3$ as a homogeneous catalyst. A degree of hydrogenation greater than 95% was achieved in the absence of any organic solvent. Although the reaction rate for the direct hydrogenation of the NBR latex was slower than that of NBR in an organic solution, this process did not show any problems of cross-linking in the resulting product and could hydrogenate only the carbon-carbon double bonds.

Wang et al. [54] studied the organic solvent-free hydrogenation of synthetic nitrile butadiene rubber nanoparticles emulsion using $RhCl(PPh_3)_3$ and the required additive triphenylphosphine. This plays a vital role in a ‘‘green’’ latex hydrogenation process. The reaction has reached about 95 mol % conversion and no cross-linking was found. The kinetic study shows that the reaction is chemically controlled with an apparent activation energy of 100–110 kJ/mol. The latex hydrogenation of diene-based polymers is performed in a three-phase reaction system, solid (polymer)–liquid (water)–gas (hydrogen), as descripted in Figure 1.7.

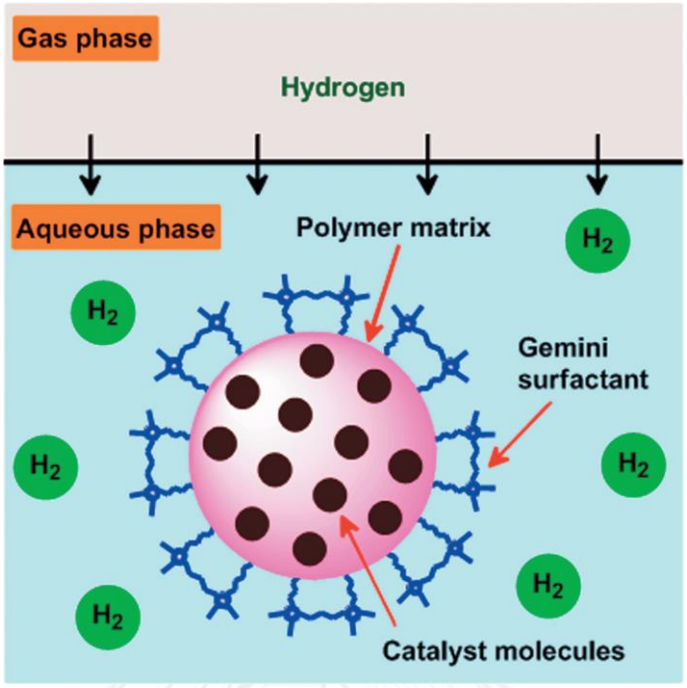

Figure 1.7 Illustrative diagram of three-phase latex hydrogenation of unsaturated polymer [54].

1.5 Objectives and Scope of Dissertation

The principle objective of this research is to investigate the aqueous hydrogenation of nanosized polyisoprene (PIP) emulsion and NR latex using rhodium complex catalysts ($RhCl_3/PPh_3$, $RhCl_3$/TPPTS and $RhCl_3$/TPPMS). One approach is to improve the mechanical properties and thermal stability of the rubber. The focus on mechanical properties, thermal and ozone resistance of NR filled with hydrogenated nanosized polyisoprene (HPIP) is also included.

In Chapter I, the concepts of green chemistry for chemical processes are reviewed. The fundamentals of catalytic hydrogenation of diene-based rubber in organic solvents and aqueous media are also described.

In Chapter II, the experimental procedures for the aqueous-phase hydrogenation of PIP and NR latex as well as the preparation of PIP filled NR and HPIP filled NR are presented. The various techniques used for the characterization of hydrogenated rubber product are also given.

In Chapter III, the results of the influence of process variables on the hydrogenation of PIP emulsions in the absence of an organic solvent are presented. The kinetics of the aqueous-phase hydrogenation, as well as a reasonable mechanism for the hydrogenation of polyisoprene is discussed. The thermal stability of HPIP is also reported.

In Chapter IV, the results for the organic solvent-free hydrogenation of natural rubber latex are reported. The effect of process variables on the hydrogenation level was investigated. The thermal stability of hydrogenated natural rubber (HNR) compared with HPIP is also presented.

In Chapter V, for utilization of hydrogenated rubber in various applications, the mechanical properties, thermal resistance by ageing and ozone resistance of rubber blends are presented. PIP filled NR and HPIP filled NR were prepared. A discussion of the stress-strain behavior and surface morphology was included in order to compare the improved properties of the rubber composites with unfilled NR.

In Chapter VI, the conclusions resulting from this study and recommendations for future work are summarized

CHAPTER II

EXPERIMENTAL

2.1 Materials

2.1.1 Synthesis of Nanosized Polyisoprene Emulsion

Isoprene (IP) (Aldrich), sodium bicarbonate ($NaHCO_3$) (Aldrich), sodium dodecyl sulphonate (SDS) (Sigma), sodium persulfate (SPS) (Fisher Scientific) and nitrogen gas (99.99%) (Praxair Inc.) were used as received for synthesis of the nanosized polyisoprene (PIP) emulsion. Methyl ethyl ketone (MEK) was obtained from Fisher Scientific for rubber precipitation, and d-chloroform ($CDCl_3$, 99.8%) was purchased from Aldrich for NMR analysis. Distilled water was also used as the reaction media for all experiments.

2.1.2 Aqueous-Phase Hydrogenation of Nanosized Polyisoprene Emulsion Using Rhodium Catalysts

PIP emulsions were used for aqueous-phase hydrogenation. Catalyst precursors including rhodium trichloride ($RhCl_3.3H_2O$), triphenylphosphine (PPh_3), trisulfonated triphenylphosphine (TPPTS) and monosulfonated triphenylphosphine (TPPMS) were purchased from Aldrich. Hydrogen gas (99.99%) was supplied by Praxair Inc. Methyl ethyl ketone (MEK) was obtained from Fisher Scientific for rubber precipitation, and d-chloroform ($CDCl_3$, 99.8%) was purchased from Aldrich for NMR analysis. Distilled water was used as the reaction media for all experiments.

2.1.3 Aqueous-Phase Hydrogenation of Natural Rubber Latex Using Rhodium Catalysts

Natural rubber latex with high ammonia content was provided by Thai Rubber Latex Corporation (Thailand) Public Company. Rhodium trichloride ($RhCl_3.3H_2O$) (Aldrich), triphenylphosphine (PPh_3) (Aldrich), trisulfonated triphenylphosphine (TPPTS) (Aldrich) and monosulfonated triphenylphosphine (TPPMS) (Aldrich) were used as catalyst precursors for aqueous-phase hydrogenation. Hydrogen gas (99.99%) was supplied by Praxair Inc. Methyl ethyl ketone (MEK) was obtained from Fisher Scientific for rubber precipitation, and d-chloroform ($CDCl_3$, 99.8%) was purchased from Aldrich for NMR analysis. Distillated water was used as the reaction media for all experiments.

2.1.4 Pre-vulcanization

For rubber sheet preparation, PIP and HPIP emulsion were used as nanofillers in NR. For the preparation of prevulcanized NR nanocomposites, high ammonia NR latex with 60% dry rubber content, with sulfur as the vulcanizing agent, zinc oxide (ZnO) and zincdiethyl dithiocarbamate (ZDEC) as vulcanization accelerators were obtained from the Rubber Research Institute of Thailand.

2.2 Synthesis of Nanosized Polyisoprene Emulsion

A differential microemulsion polymerization technique was used for synthesizing PIP nanoparticles [55]. In a typical synthesis, 0.3 wt% of SPS initiator, 0.2 wt% of SDS surfactant, 0.6 wt% of $NaHCO_3$, and 90 mL of distilled water were charged into the 300-mL Parr reactor as shown in Figure 2.1. The solution was stirred at 300 rpm under a nitrogen atmosphere, heated to the reaction temperature of 70°C, and then condensed isoprene monomer (IP/H_2O=0.4 w/w) was continuously fed into the reactor at a feeding rate of 0.8 mL/min. After the monomer addition was completed, the polymerization system was aged for 18 h to reach a maximum conversion.

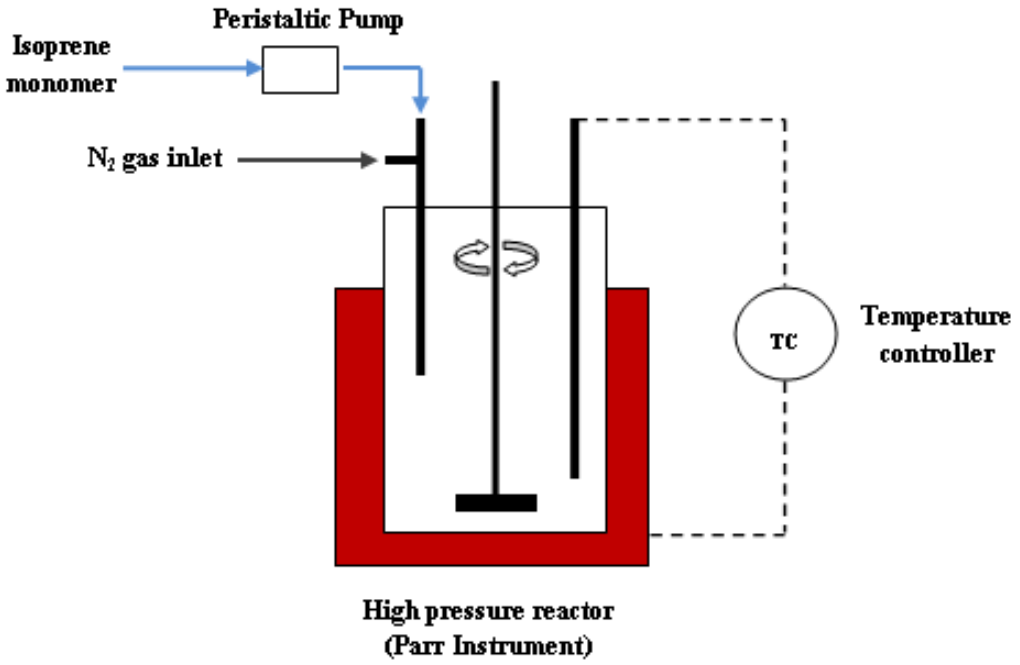

Figure 2.1 Apparatus for nanosized polyisoprene synthesis.

After the polymerization of PIP was stopped, the monomer conversion and solid content of the PIP emulsion were determined by a gravimetric method and calculated from Eq. (2.1) and (2.2), respectively:

$$\text{Conversion (\%)} = \frac{\text{Weight of monomer reacted}}{\text{Weight of monomer charged}} \times 100 \qquad (2.1)$$

$$\text{Solid content (\%)} = \frac{\text{Weight of dry polymer}}{\text{Weight of polymer emulsion}} \times 100 \qquad (2.2)$$

2.3 Aqueous-Phase Hydrogenation of Nanosized Polyisoprene Emulsion Using Rhodium Catalysts

All the hydrogenation reactions were carried out in a 300-mL Parr reactor with a catalyst addition and sampling device. The schematic diagram for the aqueous-phase hydrogenation of the PIP emulsion is shown in Figure 2.2. In a typical run, 6 g of PIP emulsion was added to distilled water to give a 120 mL mixture ([C=C] = 125 mM). The catalyst was weighed into a glass bucket and placed in the catalyst addition device, and the reactor was assembled. After flushing with hydrogen three times, the mixture was degassed by bubbling hydrogen gas for 30 min. The reaction system was then heated to the required temperature with agitation under 13.8 bar hydrogen. After temperature equilibrium was reached, the bucket containing the catalyst was dropped into the solution by pressurizing the catalyst addition device to the reaction pressure. Hydrogen gas was introduced into the reactor when required to maintain a constant reaction pressure throughout the reaction. After the reaction, the reactor was cooled to room temperature, vented of hydrogen and the reaction mixture was removed. The mixture was precipitated in MEK, The hydrogenation degree of HPIP was determined using ^{1}H NMR spectroscopic analysis.

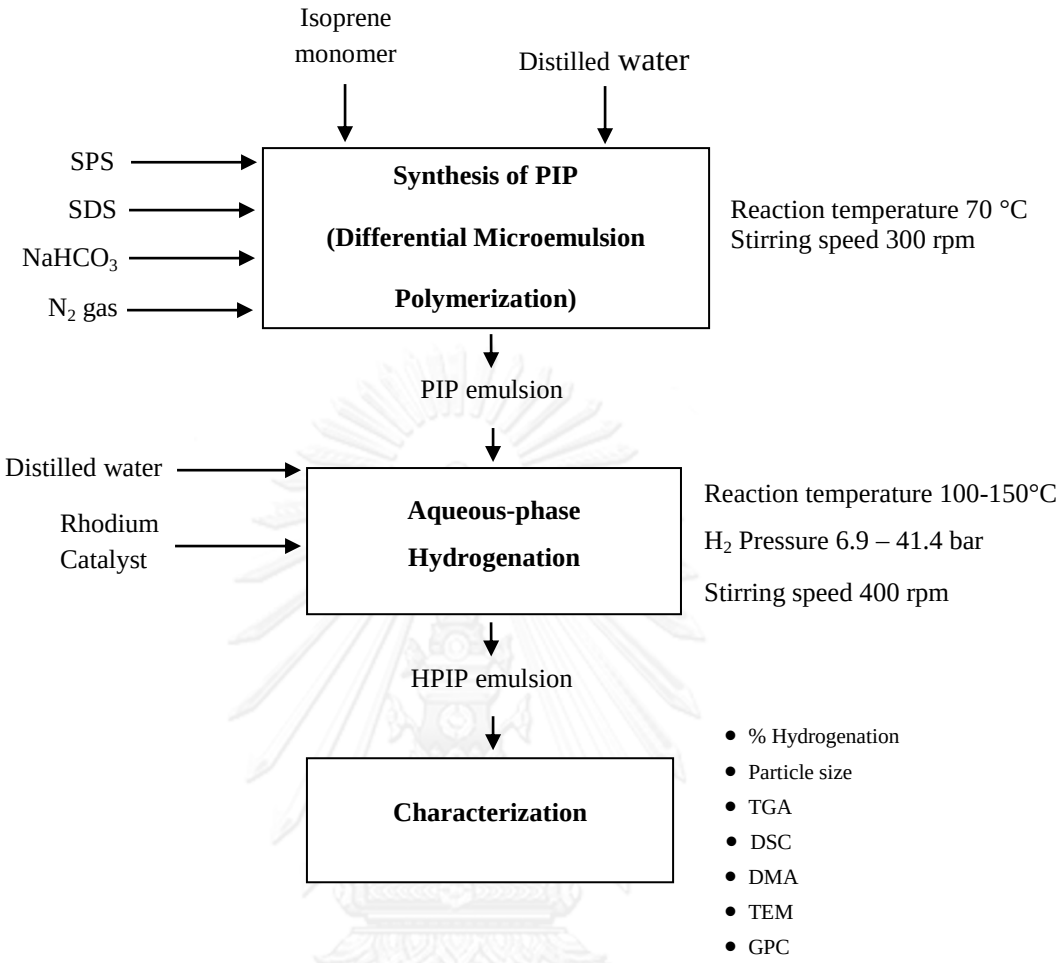

Figure 2.2 Schematic diagram for aqueous-phase hydrogenation of PIP emulsion.

2.4 Aqueous-Phase Hydrogenation of Natural Rubber Latex Using Rhodium Catalysts

All the hydrogenation reactions were performed in a 300-mL Parr Reactor. The schematic diagram for the aqueous-phase hydrogenation of NR latex is shown in Figure 2.3. 1.5 g of NR latex (60% dry rubber content) was added to distilled water to give a 120 mL mixture ([C=C] = 125 mM). The catalyst was weighed into a glass bucket and placed in the catalyst addition device in the reactor. After the reactor was assembled, the mixture was flushed three times with hydrogen gas and degassed by bubbling hydrogen gas at 13.8 bar for 30 min. The reaction system was then heated to the required temperature at a stirring rate of 400 rpm. After the

desired temperature was reached, the bucket containing the catalyst was dropped into the reaction mixture by pressurizing the reaction system to the reaction pressure. The reaction temperature and hydrogen pressure were maintained constant throughout the reaction period of 6 h. After completion of the reaction, the reactor was cooled, and depressurized. The hydrogenated solid rubber was obtained by precipitation with MEK

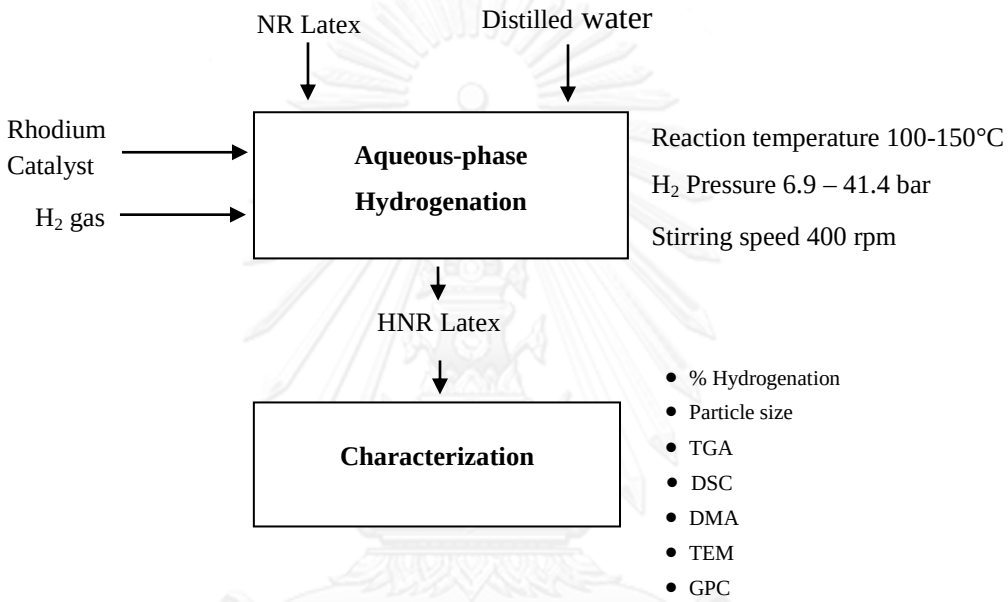

Figure 2.3 Schematic diagram for the aqueous-phase hydrogenation of NR latex.

2.5 Preparation of NR/PIP and NR/HPIP Blends

(i) Preparation of NR/PIP blends

For the preparation of pre-vulcanized NR/PIP blends, NR latex with a total solid content of 60% was selected to blend with PIP. The PIP emulsion was dropped into NR latex at various weight ratios (NR:PIP = 100:0, 90:10, 80:20, 70:30, 60:40) under a stirring rate of 300 rpm for 30 min to form a good dispersion of the NR/PIP composite. Then, surfur (1.5 phr) as vulcanizing agent, ZnO (2 phr) and ZDEC (1 phr) as accelerators were added into the mixture and the temperature was raised to 60°C with constant stirring at 300 rpm for 2 h. After reaction, the NR/PIP latex was cooled

to room temperature and cast on a raised glass plate having dimensions of 13 cm×13 cm×3 mm. The cast sheet was dried at 70°C for 5 h.

For thermal ageing of the composites, tensile specimens were aged at 100°C for 24 h in an air circulating ageing oven and the mechanical properties of the samples before and after ageing were measured to estimate the ageing resistance.

ii) Preparation of NR/HPIP Blends

The preparation of pre-vulcanized NR/HPIP blends was carried out according to the procedure mentioned in section 2.5 (i).

2.6 Characterization

2.6.1 Nuclear magnetic resonance (NMR) spectroscopy

Proton nuclear magnetic resonance (^{1}H NMR) spectroscopy was used to confirm the actual final degree of hydrogenation of HNR and HPIP. The rubber sample was dissolved in $CDCl_3$ at room temperature, and the spectra were recorded using an Advance Bruker 300 MHz spectrometer. Integration of spectra was used to determine the amount of characteristic protons of each structural unit in the polymer. The integration peak area for the saturated protons (-CH_2- and –CH_3) in the range of 0.8-2.3 ppm and the unsaturated protons (=CH) peak area at 5.2 ppm were measured in order to calculate the hydrogenation degree (HD) by using Eq. (2.3):

$$\text{Hydrogenation degree (\%)} = \frac{A-7B}{A+3B} \times 100 \qquad (2.3)$$

where A and B are the peak areas of the saturated protons over the range 0.8-2.3 ppm and the unsaturated protons at 5.2 ppm, respectively. An example of the calculation of the hydrogenation level is presented in Appendix A. The structure identification of the hydrogenated rubber was also interpreted from carbon-13 nuclear magnetic resonance (^{13}C NMR) spectroscopy.

2.6.2 Particle Diameter Measurement

For the determination of particle size, the number-average diameter (D_n) and particle size distribution of the PIP emulsion, NR latex, HPIP emulsion and HNR latex were measured using a dynamic light scattering technique (DLS, Nanotrac Instrument).

2.6.3 Gel Permeation Chromatography (GPC)

The number average molecular weight (M_n) and the weight average molecular weight (M_w) were determined using a gel permeation chromatography system (GPCMALLS, Wyatt Technology). HPLC grade tetrahydrofuran (THF) was used as the mobile phase at a flow rate of 1.0 ml/min. Samples of 0.1% (w/v) rubber solution were filtered through a 0.45 mm pore size filter and then 100 mL of the filtered samples were injected into the GPC for analysis. The molecular weight distribution was also determined by the polydispersity index (PDI) which equal to M_w/ M_n.

2.6.4 Morphological Study

The morphology of NR, PIP and its hydrogenated samples were examined using a transmission electron microscope (TEM) (JEOL, 80 kV). The 20-times diluted samples were stained with OsO_4 and dropped on a copper grid.

2.6.5 Thermogravimatic Analysis (TGA)

Thermogravimetric analysis (TGA) of NR, PIP and the corresponding hydrogenated samples was performed on a Perkin–Elmer Pyris Diamond TG/DTA. A sample weight of 10 mg was placed on a platinum pan, and heated from room temperature to 800 °C at a constant heating rate of 10 °C/min with a flow rate of nitrogen gas of 50 mL/min. The initial decomposition temperature (T_{id}) was determined from the intersection of two tangents at the onset of the decomposition

temperature; and the temperature at the maximum of mass loss rate (T_{max}) was obtained from the peak maxima of the derivative of the TG curves.

2.6.6 Differential Scanning Calorimetry (DSC)

Differential scanning calorimetry (DSC) of the samples was performed using a Mettler–Toledo DSC 822 instrument. The instrument signal was derived from the temperature difference. The sample in a crimped aluminum pan was cooled to -100 °C using liquid nitrogen and then heated up to 25 °C with a temperature scan rate of 20 °C/min. The midpoint of the transition region from the glassy to rubbery state was taken as the glass-transition temperature (T_g).

2.6.7 Dynamic Mechanical Analysis (DMA)

Dynamic mechanical analysis (METTLER) in a shear mode was used to measure the dynamic mechanical properties of the PIP, NR, HPIP, HNR, NR/PIP and NR/HPIP blends samples. All samples were prepared as strips with dimensions of 5x5x2 mm^3, and analyzed with a strain of 20-μm peak to peak displacement. The temperature was raised over range of -80 °C to 25 °C with a heating rate of 5 °C/min at an oscillation frequency of 10 Hz. The storage modulus (E') was determined from the elastic energy storage of the polymer. The loss tangent (tan δ) was determined to obtain the glass transition temperature (T_g).

2.6.8 Mechanical Properties of Vulcanized Rubber

Mechanical properties of vulcanized rubber, in terms of tensile strength, % elongation at break and modulus, were measured using a Universal Testing Machine (LLOYD model LR5K), according to the ASTM-412 method at a cross-head speed of 500 mm/min. All samples were cut into dumbbell-type specimens using a Wallance die cutter. The data points were averaged from three measurements of the four specimens, and stress-strain curves were also recorded.

2.6.9 Ozone Resistance of Vulcanized Rubber

Ozone resistance of NR/PIP and NR/HPIP blends were studied using an ozone test chamber (HAMPDEN, Northampton, England) according to ISO 1431-1:2004. Before exposure to ozone, all rubber specimens were stretched by 20% elongation for 48 h in the absence of light under an ozone-free atmosphere. Then, the specimens were placed into an ozone test chamber for 72 h. The ozone concentration used was 50 parts per hundred million (pphm) under a temperature of 40 °C. Photographs of the samples after testing were taken to investigate the cracks on the rubber surface.

CHAPTER III

AQUEOUS-PHASE HYDROGENATION OF NANOSIZED POLYISOPRENE EMULSION USING RHODIUM CATALYSTS

3.1 Introduction

Polydiene-based polymers are widely used as rubber products, binders, and adhesives due to their high strength and good elastic properties. However, one disadvantage of these materials is their poor ageing behavior, which is caused by the oxidation of residual double bonds in the polydienes. Chemical modification of polydiene-based polymers by hydrogenation is one of the important methods for improving and changing the properties of unsaturated elastomers toward greater stability against thermal and oxidative degradation. Polyisoprene and NR have been used extensively in the automobile and adhesive industries. It is preferably used in blends with other rubbers, such as polybutadiene or styrene-butadiene rubber, to improve their processibility. Thus, hydrogenation of polyisoprene improves the heat and oxygen resistance of the rubber.

With the recovery and recycling of the catalyst and eliminating the need for organic toxic solvents, latex hydrogenation provides substantial environmental and economical benefits [56]. Moreover, water is a non-toxic, non-flammable, inexpensive, and an environmentally friendly solvent. Therefore, catalysis in aqueous media fully implements the principles of “Sustainable/Green Chemistry” [57].

The propose of the present work was to study the aqueous - phase hydrogenation of PIP emulsions using water-soluble rhodium catalyst complexes. The influence of catalyst precursors and concentration, reaction temperature and hydrogen pressure on the hydrogenation degree (HD) and rate constant of the reaction were investigated. The thermal and dynamic mechanical properties of HPIP were also investigated.

3.2 Synthesis of nanosized Polyisoprene

The influence of SDS concentration on the particle size of the PIP emulsion is presented in Table 3.1. The particle size of PIP decreased with increasing surfactant concentration. The results implied that the nanosized PIP particle size could be controlled by the amount of surfactant. This behavior had a similar trend with that of the synthesis of nanosized poly(vinyl acetate) via microemulsion polymerization (41.5-89.2 nm) [58] and polystyrene via emulsion polymerization (62.5-94.0 nm) [59].

From Table 3.1, the monomer conversion slightly increased with increasing surfactant concentration and reached a maximum of around 85% at a SDS concentration of 2.18 wt%. Increasing the amount of SDS did not affect the solid content of PIP (13.5-16.1%). The synthesis of nanosized PIP, initiated by an oil-soluble initiator, is believed to occur in the micelles. Consequently, the micelle number increased with increasing SDS concentration, as each micelle became smaller [60]. The small micelles resulted in a decrease in diffusion resistance resulting in a fast polymerization rate. In this work, PIP with a particle size of 22.3 nm, 43.9 nm and 49.3 nm was selected for further hydrogenation.

Table 3.1 Effect of SDS concentration on the particle size, monomer conversion and solid content of PIP synthesis.

[SDS] (wt%)	D_n (nm)	Conversion (%)	Solid Content (%)	PDI
0.25	49.3±1.0	69.3±2.3	13.4±0.3	0.010
0.35	43.9±0.3	82.2±3.3	15.8±0.6	0.011
0.69	32.8±0.6	83.6±3.0	15.9±0.6	0.007
2.18	22.3±0.4	85.3±2.2	16.1±0.4	0.006

Condition: [SPS] = 0.3 wt%; IP/H_2O= 0.4 w/w; [$NaHCO_3$] = 0.6 wt%; temperature=75°C; stirring speed=300 rpm; reaction time = 18 h.

3.3 Characterization of PIP and HPIP

(i) Nuclear magnetic resonance (NMR) spectroscopy

The ^{1}H NMR spectra of PIP and HPIP are shown in Figure 3.1. From Figure 3.1a-c, the characteristic ^{1}H NMR signal attributed to olefinic protons (5.15 ppm), -CH_2- (1.91 ppm) and -CH_3 (1.67 ppm) were decreased; and the new signals, saturated -CH_3 (0.8 ppm) and -CH_2- (1.2 ppm), were observed after the hydrogenation process. The % HD was calculated from the change in the integral area of peaks representing protons for HPIP as presented in Appendix A.

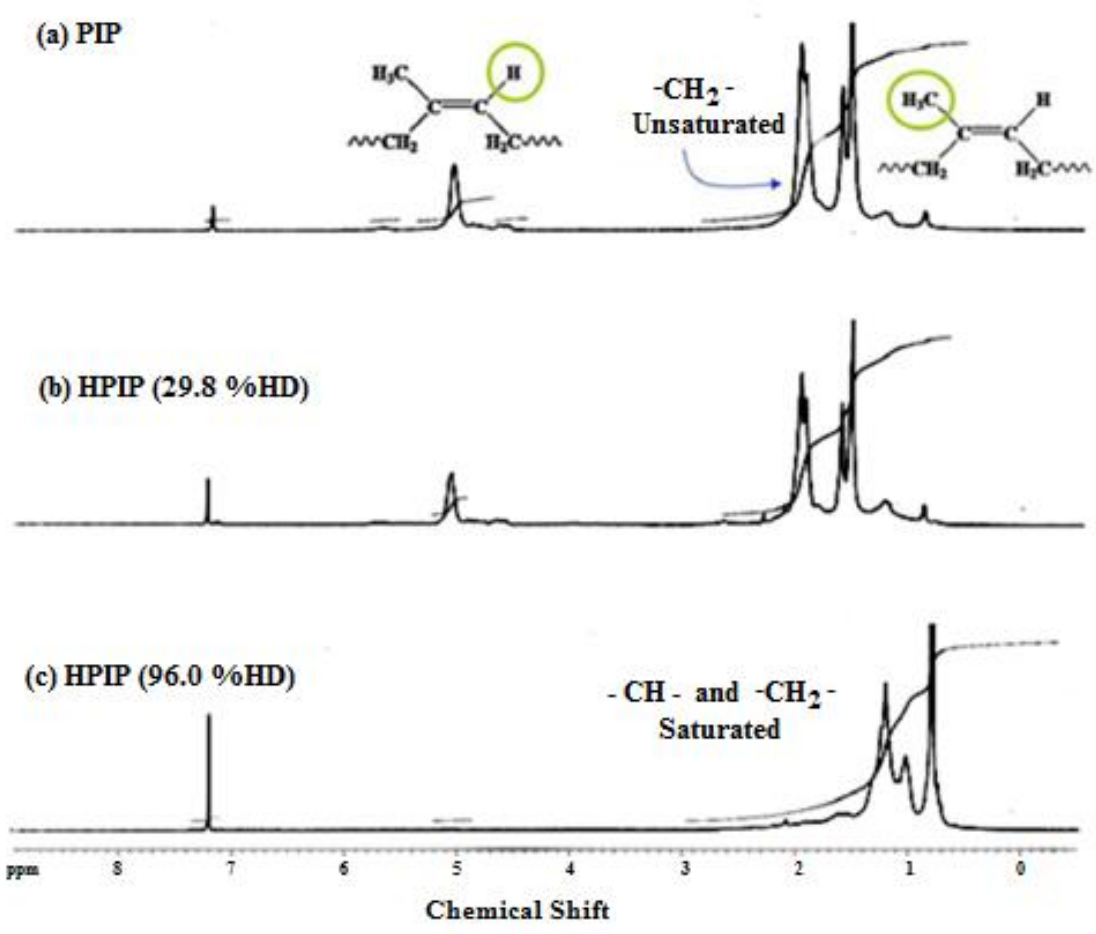

Figure 3.1 ^{1}H NMR spectra of samples: (a) PIP, (b) HPIP (29.8 % HD), and (c) HPIP (96.0 % HD).

The HPIP structure was confirmed by ^{13}C NMR spectra as shown in Figure 3.2. For the PIP structure in Figure 3.2a, the peaks at 139.3 ppm were attributed to the unsaturated carbon of *cis*-polyisoprene and *trans*-polyisoprene, and the signals at 125.7 and 125.9 ppm were attributed to the -CH of the unsaturated carbon of the *cis*- and *trans*-polyisoprene, respectively. The peaks at 26.8 and 28.0 ppm belonged to the $-CH_2$ of *cis*-polyisoprene while the peaks at 39.8 and 40.0 ppm corresponded to the $-CH_2$ of *trans*-polyisoprene. The peak of methyl groups of *cis*- and *trans*-polyisoprene appeared at 23.4 ppm, and the peak of $-CH_3$ of vinyl-polyisoprene peak was at 17.0 ppm. After hydrogenation, the peak in the region of 124–135 ppm corresponding to unsaturated carbon disappeared (Figure 3.2b). In addition, the new peaks appearing at 19.6 and 32.7 ppm were attributed to $-CH_3$ and CH, respectively, and the peaks at 32.7 and 24.4 ppm were attributed to CH_2 of the saturated unit. It can be concluded that the C=C units in the PIP backbone were hydrogenated.

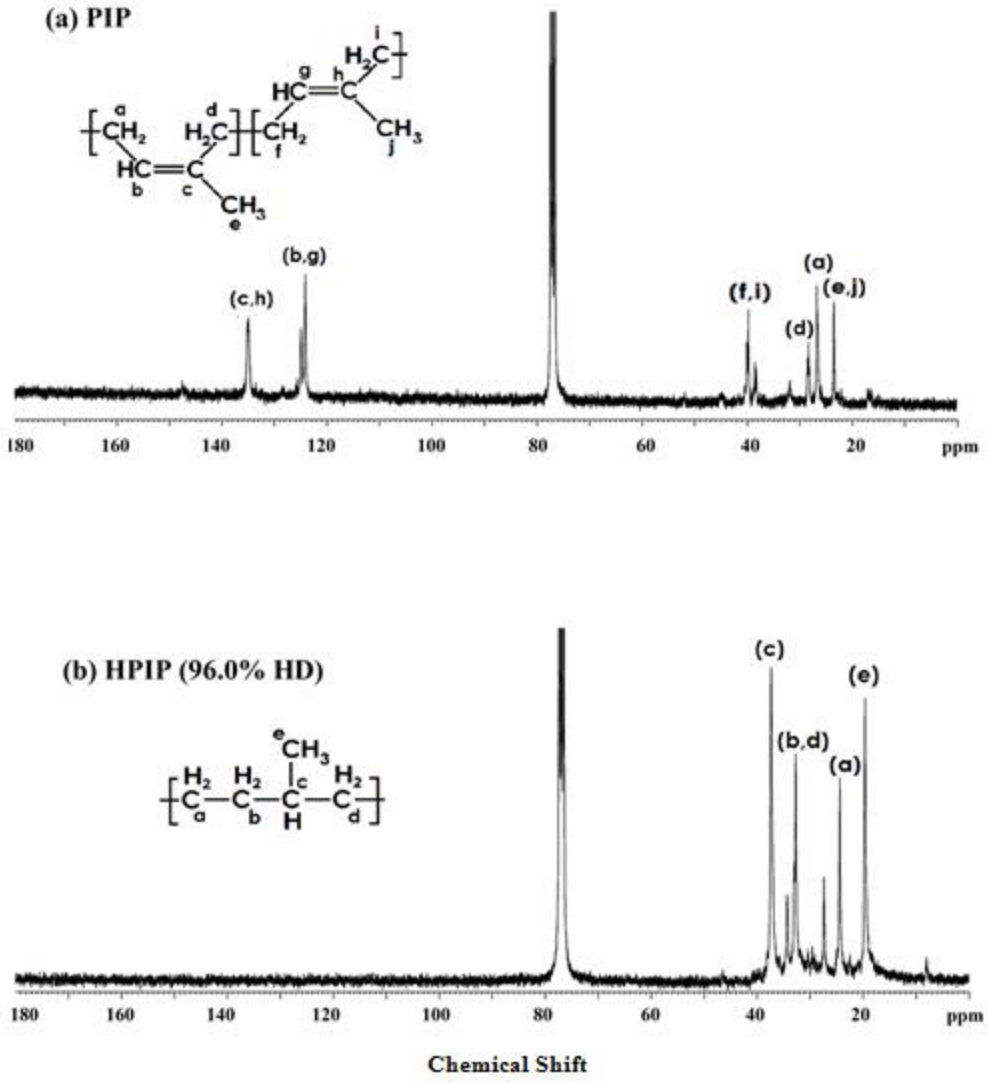

Figure 3.2 ^{13}C NMR spectra of samples: (a) PIP, (b) HPIP (96.0 % HD).

(ii) Particle Diameter Measurement

The particle size distributions of PIP and HPIP latex were analyzed by a dynamic light scattering technique (DLS), as shown in Figure 3.3. After hydrogenation, the particle sizes of HPIP (28.5 nm) increased by about 27.8%

from the initial PIP (22.3 nm) with the same distribution pattern. This confirmed that the PIP particles did not agglomerate during the hydrogenation process

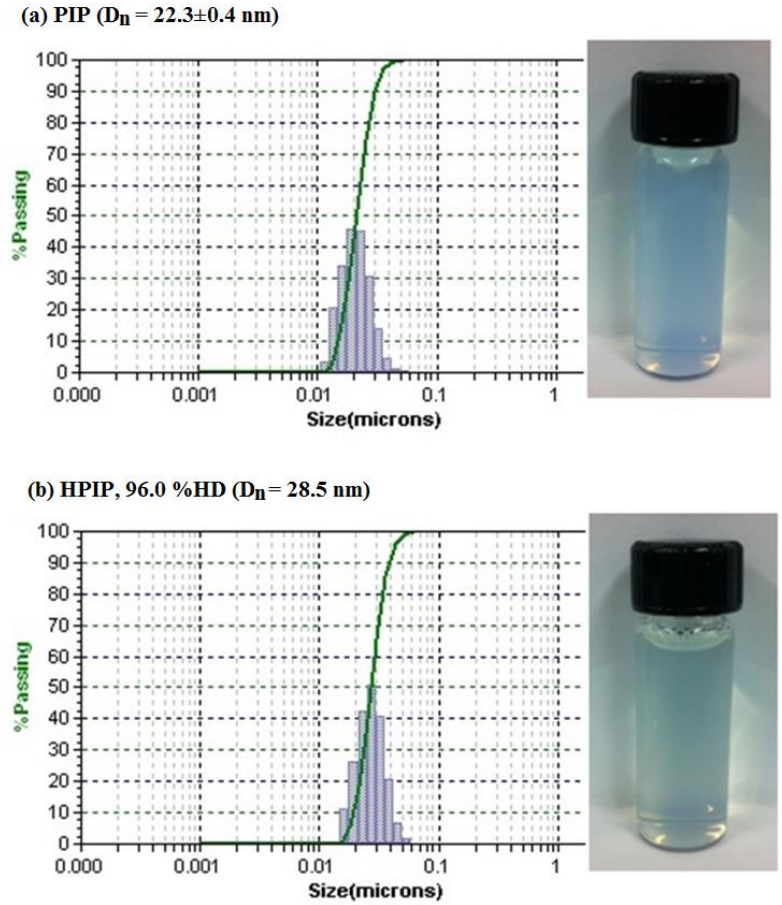

Figure 3.3 Polymer particle size distribution histograms: (a) PIP (22.3 nm) and (b) HPIP, 96.0 % HD (28.5 nm).

3.4 Hydrogenation of PIP: Effect of Catalyst Ligands

The influence of catalyst precursors on the hydrogenation degree of PIP is presented in Table 3.2. At a phosphorus/rhodium (P/Rh) molar ratio of 3, the degree of hydrogenation (HD) of PIP increased in the order: $RhCl_3/PPh_3$ < $RhCl_3$/TPPTS < $RhCl_3$/ TPPMS. Using $RhCl_3/PPh_3$ as catalyst, a low hydrogenation level was achieved due to the lipophilic behavior of the PPh_3 ligand. This implied

that the $RhCl_3/PPh_3$ catalyst complex was formed as an individual droplet in aqueous media; and therefore, some carbon double bonds of PIP were hydrogenated in this system.

Table 3.2 Effects of catalyst precursors on aqueous-phase hydrogenation of PIP.

Entry	Catalyst precursor	P/Rh Molar ratio	D_n (HPIP) (nm)	% HD
1	-	-	27.2	2.6
2	$RhCl_3/PPh_3$	3	28.3	25.3
3	$RhCl_3/PPh_3$	9	28.3	22.5
4	$RhCl_3$/TPPTS	3	26.6	38.0
5	$RhCl_3$/TPPTS	4	26.4	29.8
6	$RhCl_3$/TPPMS	3	28.5	96.0

Conditions: initial D_n= 22.3 nm; [C=C] = 125 mM; time = 6 h; [Rh] = 250 μM; temperature = 140 °C; H_2 Pressure = 41.4 bar.

To explain the catalytic activity for the aqueous-phase hydrogenation of PIP, catalyzed by the Rh/TPPTS and Rh/TPPMS complexes, a Hartley ionic spherical micelle model [51, 52, 61-63] was proposed as shown in Figure 3.4. The micelle core is composed of the hydrophobic chain of the surfactant SDS where the PIP with the C=C unsaturation units are located. Surrounding the core is the Stern layer where the charged head groups (SO_3^- of SDS and ligands) are located together, along with the counter ions (Na^+ of SDS and the ligand) of the ionic micelle. The Gouy–Chapman double layer is the outer layer where the counter ions of Na^+ are located. The rhodium atom is probably located on the polarity gradient between the Stern layer and the micelle core. The high polarity of TPPTS caused the rhodium atom to be located more at the Stern layer instead of the core of the micelle. 38.0 % HD occurred under this condition. In contrast, the polarity of the TPPMS is lower than that of TPPTS since there is one charged head group SO_3^- in its structure. The rhodium atom of the Rh/TPPMS complex was more driven towards the micelle core. So, a high conversion (96.0 % HD) was achieved for hydrogenation using TPPMS as the catalyst ligand.

The degree of hydrogenation of PIP decreased with an increase in the P/Rh molar ratio. At the higher TPPTS/Rh molar ratio of 4 and PPh_3/Rh molar ratio of 9, the hydrogenation degree was decreased to 29.8% and 22.5%, respectively. Decreasing olefin conversion at a higher P/Rh molar ratio could be explained by a competition for a coordination site on rhodium between the C=C units of PIP and the added free ligand which tends to retard the rate of hydrogenation.

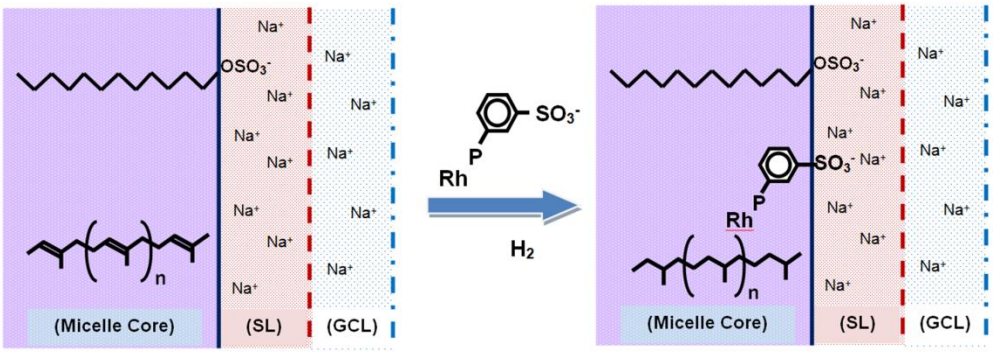

Figure 3.4 Representation of structures of PIP and HPIP catalyzed by a rhodium complex in a model of a Hartley ionic micelle, including micelle core, the Stern layer (SL), and the Gouy–Chapman double layer (GCL).

3.5 Hydrogenation of PIP using $RhCl_3$/TPPTS

For the aqueous-phase hydrogenation of PIP using $RhCl_3$/TPPTS as catalyst, the effects of catalyst amount, reaction temperature, hydrogen pressure, and catalyst precursor ratio (P/Rh molar ratio) on hydrogenation are presented in Table 3.3. The results show that less than 50.0% hydrogenation of PIP was obtained when using Rh/TPPTS as catalyst for hydrogenation. Increasing the catalyst amount (125-375 μM) and reaction temperature (110-150 °C) enhanced the conversion. However, only a slight increase in the degree of hydrogenation was observed with increasing rhodium concentrations up to 375 μM reaching a degree of hydrogenation of 39.0% (Entry 7-9). Similarly, the degree of hydrogenation increased with increasing reaction temperature up to 150 °C approaching 40.1% hydrogenation (Entry 10-13). However, a low hydrogenation level was obtained when the hydrogen pressure (13.8-41.4 bar) and TPPTS/Rh

molar ratio (3-4) were varied (Entry 14-16). Previous work reported that using water-soluble transition metal Rh/TPPTS complexes for catalytic hydrogenation of an unsaturated polymer in aqueous media are efficient when the organic solvent, n-hexane, was added (water/n-hexane = 82/18 w/w) [51, 52]. In our work, all of experiments were carried out with no addition of organic solvent. Therefore, Rh/TPPTS was not effective for PIP hydrogenation in aqueous media for all of the conditions investigated.

Table 3.3 Effects of process variables on hydrogenation of PIP using $RhCl_3$/TPPTS as catalyst precursor.

Entry	[Rh] (μM)	T (°C)	P (bar)	P/Rh Molar ratio	D_n (HPIP) (nm)	%HD
7	125	130	41.4	3	26.3	28.9
8	250	130	41.4	3	26.9	30.1
9	375	130	41.4	3	26.2	39.0
10	250	110	41.4	3	24.3	13.2
11	250	120	41.4	3	26.4	18.6
12	250	140	41.4	3	26.6	38.0
13	250	150	41.4	3	27.4	40.1
14	250	150	27.6	3	25.3	38.8
15	250	150	13.8	3	26.6	24.2
16	250	140	41.4	4	26.4	29.8

Conditions: initial D_n= 22.3 nm, [C=C] = 125 mM; catalyst precursor = $RhCl_3$/TPPTS time = 6 h.

3.6 Hydrogenation of PIP using $RhCl_3$/TPPMS

The influence of process variables on aqueous-phase hydrogenation of PIP in the presence of $RhCl_3$/TPPMS was studied by varying the rhodium catalyst amount, reaction temperature and hydrogen pressure. The effects of all parameters on particle size and %HD are presented in Figure 3.5 – Figure 3.7 and discussed in detail as follows.

3.6.1 Effect of Catalyst Concentration

The effects of catalyst amount on the hydrogenation level and particle size after hydrogenation of PIP catalyzed by water- soluble Rh/TPPMS at 41.4 bar and 140 °C are shown in Figure 3.5. The C=C conversion dramatically increased with increasing catalyst amount approaching 96.0% at rhodium concentrations over the range of 125- 250 μM with the same trend for both particle sizes of PIP. In addition, the higher hydrogenation degree was achieved when the particle size of PIP was small (22.3 nm) compared to the large size PIP (43.9 nm). A similar behavior regarding the dependence of the degrees of hydrogenation on catalytic concentration has been reported for hydrogenation reactions in aqueous media using Rh/TPPTS precursors [64]. In addition, the influence of catalyst concentration on particle size after hydrogenation of PIP using the Rh/TPPMS complex is shown in Figure 3.5. The particle size slightly increased 11.6 – 30.3% (25.0 - 28.1 nm from the initial particle size of 22.3 nm, and 49.0 – 57.2 nm from the initial particle size of 43.9 nm) with increasing catalyst amount (50 – 250 μM) It could be concluded that an increase in the catalyst amount had no effect on the increase in PIP particle size after hydrogenation.

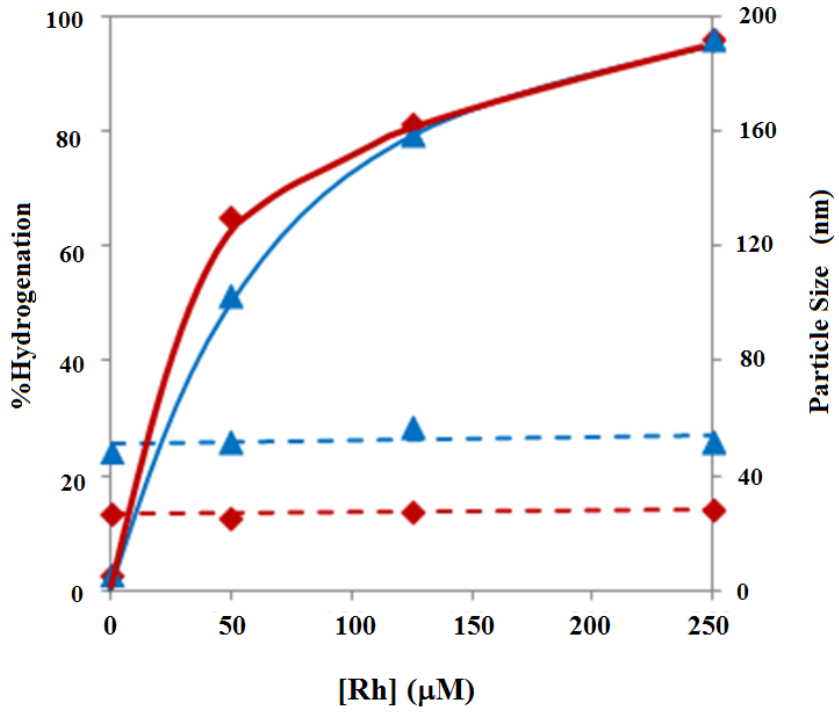

Figure 3.5 Effect of catalyst concentration on hydrogenation (——) and particle size (-----) of PIP. Condition: initial particle size, ◆ 22.3 nm, ▲ 43.9 nm; [C=C] = 125 mM; time = 6 h; temperature = 140 °C; H_2 pressure = 41.4 bar; catalyst precursor = $RhCl_3$/TPPMS (P/Rh molar ratio = 3)

3.6.2 Effect of Temperature

The hydrogenation degree as a function of temperature for PIP hydrogenation using Rh/TPPMS catalyst in aqueous-phase systems is illustrated in Figure 3.6. The hydrogenation degree slightly increased with increasing temperature over the range of 100 - 120 °C for both sizes of PIP. After increasing the reaction temperature above 120 °C, a hydrogenation degree of 95.8% and 96.0% was achieved at 130 and 140 °C, respectively. For the influence of particle size, however, the high level of hydrogenation for the small size of PIP was achieved compared to the large PIP size. This can be explained in that high temperature could increase the probability of collisions between the reactant

with the polymer chain and accelerate the catalyst mobility to coordinate with the carbon-carbon double bond [18]. For the particle size after hydrogenation of PIP as shown in Figure 3.6, the reaction temperature does affect the HPIP particle size. The particle size increased 5.2 – 30.3% (25.0 - 28.6 nm from the initial particle size of 22.3 nm, and 46.2 – 56.0 nm from the initial particle size of 43.9 nm) with increasing reaction temperature (120 – 140 °C).

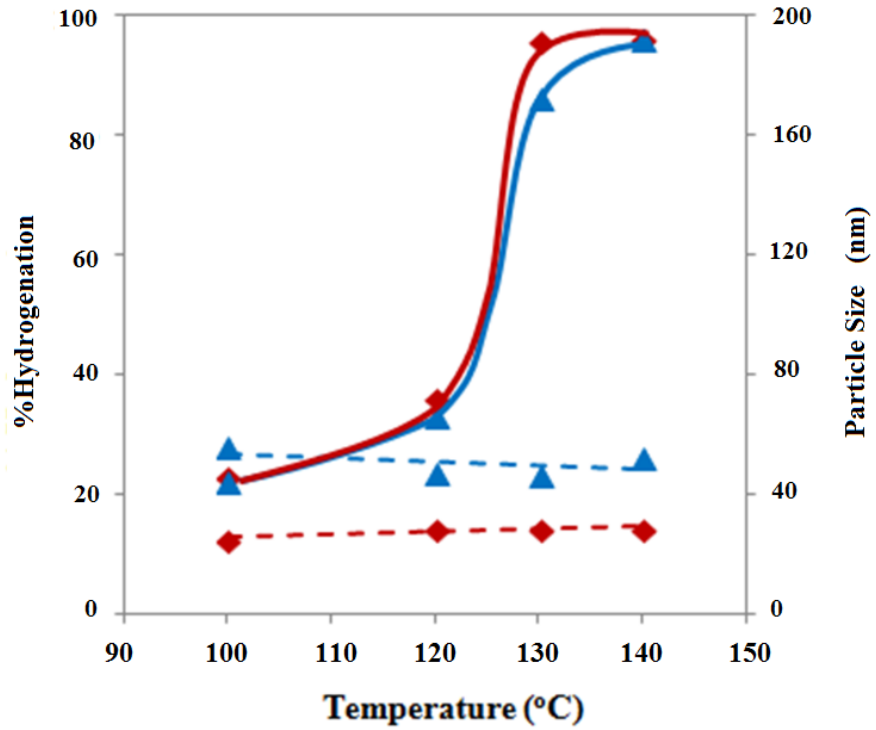

Figure 3. 6 Effect of temperature on hydrogenation (———) and particle size (-----) of PIP. Condition: initial particle size, ◆ 22.3 nm, ▲ 43.9 nm; [C=C] = 125 mM; time = 6 h; H_2 pressure = 41.4 bar; catalyst precursor = $RhCl_3$/TPPMS (P/Rh molar ratio = 3); [Rh] = 250 μM.

3.6.3 Effect of Hydrogen Pressure

The dependence of the % HD on hydrogen pressure was studied over the range 6.9– 41.4 bar at 140 °C and a rhodium concentration of 250 μM. The results presented in Figure 6 indicated that the extent of hydrogenation increased with

an increase in hydrogen pressure up to 14 bar, and a high hydrogenation level for the small particle size PIP (22.3 nm) was achieved compared with the larger particle size PIP (43.9 nm). For hydrogen pressures above 14 bar, the hydrogenation level tended to slightly increase to 96.0% with increasing hydrogen pressure (27.6 - 41.4 bar) for both particle sizes of PIP used. In addition, the PIP tended to have the same hydrogenation level independent of the initial particle size of PIP. Previous work reported a similar behavior regarding the effect of hydrogen pressure on catalytic hydrogenation of polyisoprene and NR using ruthenium [37, 45] and osmium complexes [38, 65]. In addition, the influence of hydrogen pressure on HPIP particle size is shown in Figure 3.7. The particle size increased by 8.4 – 32.7% (25.3 – 29.6 nm from the initial particle size of 22.3 nm, and 47.6 – 56.0 nm from the initial particle size of 43.9 nm) with increasing hydrogen pressure (6.9 – 41.4 bar).

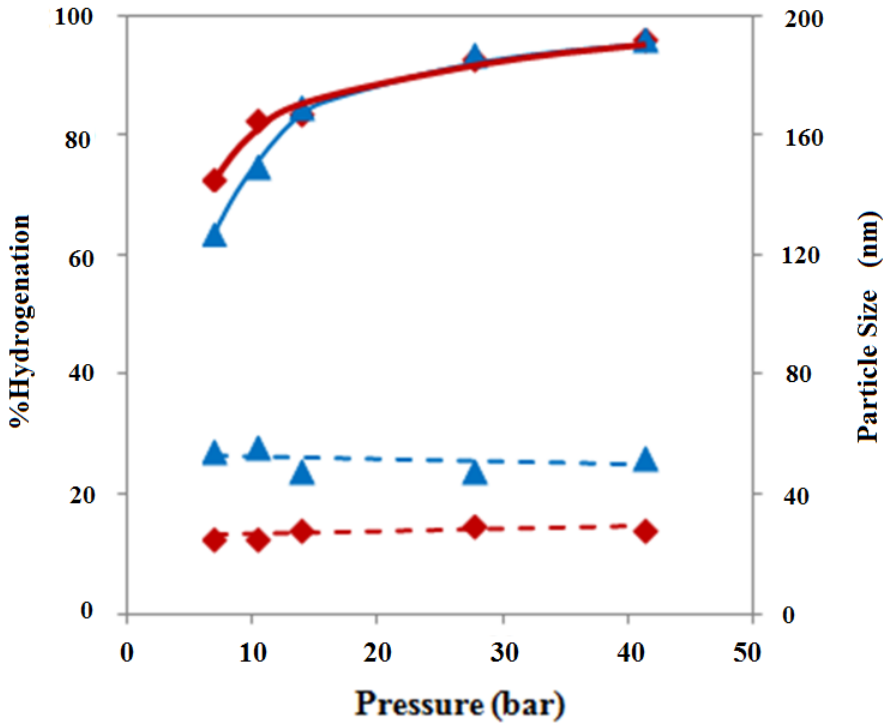

Figure 3. 7 Effect of hydrogen pressure on %hydrogenation (——) and particle size (-----) of PIP. Condition: initial particle size, ◆ 22.3 nm, ▲ 43.9 nm; [C=C] = 125 mM; time = 6 h; temperature = 140 °C; catalyst precursor = $RhCl_3$/TPPMS (P/Rh molar ratio = 3); [Rh] = 250 μM.

3.7 Conversion Profile for PIP Hydrogenation

A detailed kinetic study of the aqueous-phase hydrogenation of PIP in the presence of $RhCl_3$/TPPMS has been conducted in an attempt to gain a better understanding of the reaction mechanism. The hydrogenation degree versus reaction time profiles for various process variables are shown in Figure 3.8a and 3.9a. The conversion of double bonds was dramatically increased with time initially, and then leveled off. The hydrogenation rate exhibits an apparent first-order rate law dependence on the carbon-carbon double bond concentration, as described by Eq. (3.1).

$$\frac{-d\,[C{=}C]}{dt} = k'[C{=}C] \qquad (3.1)$$

The fractional hydrogenation conversion, x is defined as

$$x = 1 - [C{=}C]_t / [C{=}C]_0 \qquad (3.2)$$

where $[C{=}C]_t$ is the double bond concentration at reaction time t and $[C{=}C]_0$ is the initial double bond concentration. Eq. (3.1) and (3.2) can further be expressed in terms of Eq.(3.3)

$$\ln(1 - x) = -k't \qquad (3.3)$$

Plots of ln(1 - x) versus time fit a first-order rate expression very well, and thus, the rate constant (k′) at various reaction conditions can be obtained from straight-line first-order plots of ln(1 - x) versus time, as shown in Figure 3.8b and 3.9b. A summary of the results showing the effect of the reaction variables on the rate constant is provided in Table 3.4.

The rate constants for hydrogenation of various initial particle sizes of PIP and catalyst concentrations (at 140 °C and 41.4 bar of hydrogen pressure) are presented in Table 3.4 (entry 17-20). The rate constants for PIP particle sizes of 22.3, 38.1 and

49.3 nm were 10.48×10^{-5}, 5.80×10^{-5} and 2.90×10^{-5} (s^{-1}), respectively. Thus, the hydrogenation rate decreased as expected with increasing initial particle size over the range of 22.3 – 49.3 nm. A higher double bond reduction rate for a small particle can be explained in that the aqueous-phase hydrogenation using Rh/TPPMS occurred at the outer surface of the particle and transferred to the inner part of the particles of PIP. The rhodium catalyst diffused through the smaller particles at a higher rate than through the larger particles resulting in an increase in the degree of hydrogenation. Related work reported a similar behavior regarding the effect of particle size on diimide hydrogenation of polyisoprene [66]. The effect of catalyst concentration on the rate constant of hydrogenation in aqueous media (140 °C under 41.4 bar of hydrogen pressure) (entry 17 and 20) showed that rate constant increased with increasing rhodium concentration (125 and 250 μM).

The rate constants of hydrogenation at various hydrogen pressures and reaction temperatures (22.3 nm PIP particle size and 250 μM of catalyst concentration) are presented in Table 4 (entry 17, 23-24). The rate constants of PIP hydrogenation at 13.8, 27.6 and 41.4 bar were 6.27×10^{-5}, 8.40×10^{-5} and 10.48×10^{-5} (s^{-1}), respectively. Therefore, the rate constant was linearly proportional to the hydrogen pressure. This first-order behavior implied that a single mechanistic pathway is probably involved in the reaction of the polymer with hydrogen. Previous work reported a similar behavior regarding the effect of hydrogen pressure on the hydrogenation of polyisoprene using a ruthenium catalyst [45].

With respect to the influence of reaction temperature (120 - 140 °C) on the aqueous-phase hydrogenation (22.3 nm of initial PIP particle size, 250 μM of catalyst concentration, and 41.4 bar of hydrogen pressure) (entry 17, 21-22), the rate constants of PIP hydrogenation at 120, 130 and 140 °C were 1.85×10^{-5}, 4.56×10^{-5} and 10.48×10^{-5} (s^{-1}), respectively. The hydrogenation rate increased with increasing reaction temperature because the activity of the rhodium catalyst was limited at lower temperature [42, 45]. The effect of temperature on the rate constant can be represented by a good linear Arrhenius plot and yielded a correlation coefficient (R^2) of 0.99. The activation energy calculated from a least squares regression analysis of a plot of ln(k') versus 1/T was 117.0 kJ/mol. This further provides evidence that the kinetic data were obtained without severe mass transfer limitations and the diffusion of the reactants was not the main rate-determining factor under these conditions.

For hydrogenation of polybutadiene using $RhCl(PPh_3)_3$ in toluene, an activation energy value of 102 kJ/mol was reported [26].

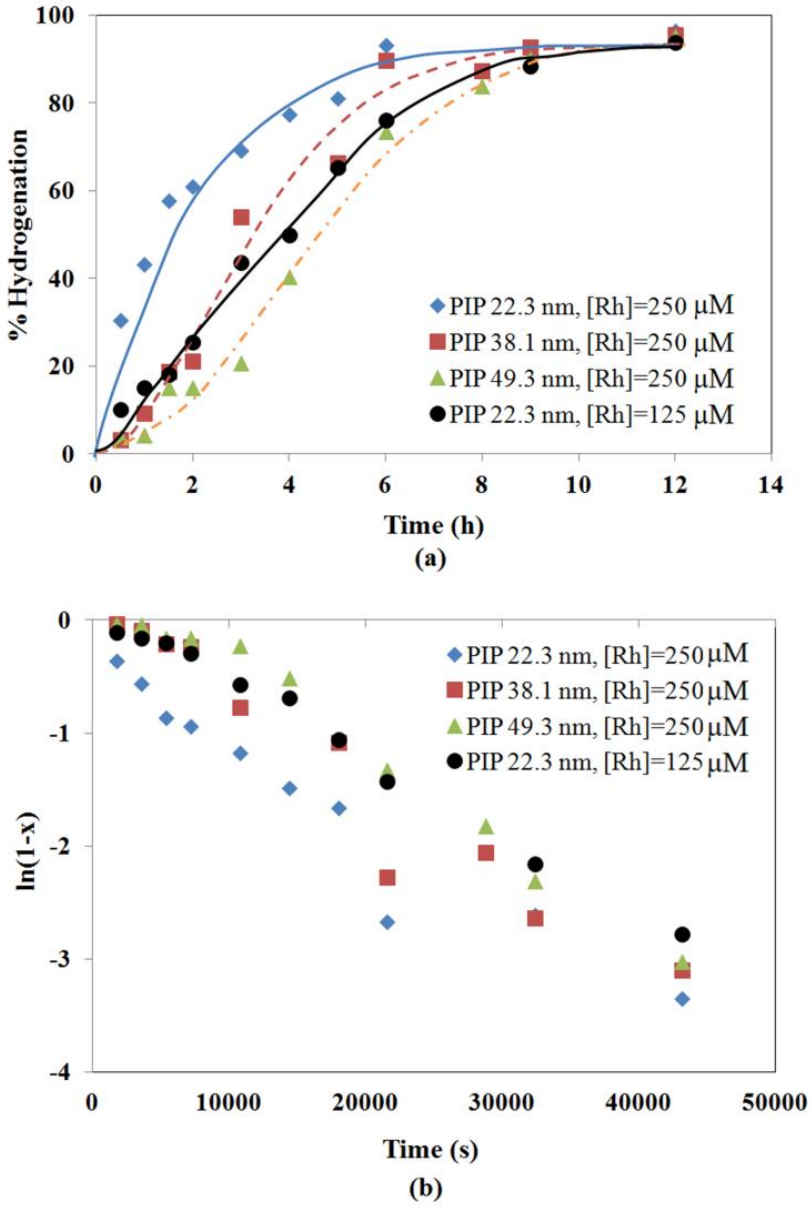

Figure 3.8 (a) Conversion profile and (b) first order ln plot of PIP hydrogenation at various initial D_n. and catalyst concentration. Condition: [C=C] = 125 mM; temperature = 140 °C; H_2 pressure = 41.4 bar; catalyst precursor = $RhCl_3$/TPPMS (P/Rh molar ratio = 3).

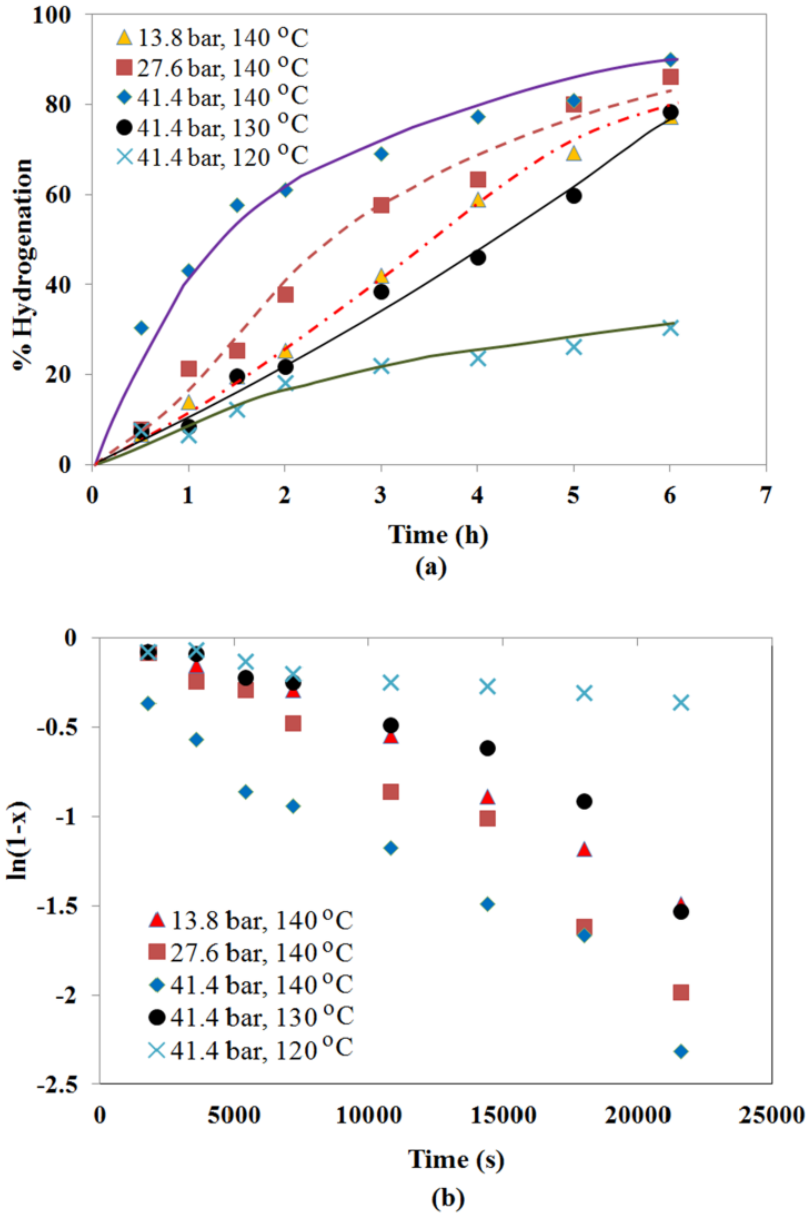

Figure 3.9 (a) Conversion profile and (b) first order ln plot of PIP hydrogenation at various hydrogen pressures and temperatures. Condition: [C=C] = 125 mM; catalyst precursor = $RhCl_3$/TPPMS (P/Rh molar ratio = 3); [Rh] = 250 μM.

Table 3.4 Rate constant of hydrogenation of PIP using $RhCl_3$/TPPMS as catalyst precursor.

Entry	Initial D_n (nm)	[Rh] (μM)	T (°C)	P (bar)	k'x10^5 (s^{-1})
17	22.3	250	140	41.4	10.48
18	38.1	250	140	41.4	5.80
19	49.3	250	140	41.4	2.90
20	22.3	125	140	41.4	5.26
21	22.3	250	130	41.4	4.56
22	22.3	250	120	41.4	1.85
23	22.3	250	140	27.6	8.40
24	22.3	250	140	13.8	6.27

Conditions: [C=C] = 125 mM; catalyst precursor = $RhCl_3$/TPPMS (P/Rh molar ratio = 3).

3.8 Proposed Reaction Mechanism of Aqueous-Phase Hydrogenation

A reaction mechanism for the aqueous-phase hydrogenation using the catalyst $RhCl_3$/TPPMS is proposed as shown in Appendix B. According to its coordinative unsaturation, TPPMS in $RhCl(TPPMS)_3$ subsequently is dissociated, and active species $RhCl(TPPMS)_2$ is formed, as shown in Eq. (3.4).

$$RhCl(TPPMS)_3 \rightleftharpoons RhCl(TPPMS)_2 + TPPMS \quad (3.4)$$

Hence, a molecule of H_2 coordinates to $RhCl(TPPMS)_2$ by η^2 coordination, and then the insertion of the carbon–carbon double bond of PIP occurs with $H_2RhCl(TPPMS)_2$ to generate the hydrogenated polymer, as shown in Eq. (3.5) - (3.7), respectively.

$$RhCl(TPPMS)_2 + H_2 \rightleftharpoons H_2RhCl(TPPMS)_2 \quad (3.5)$$

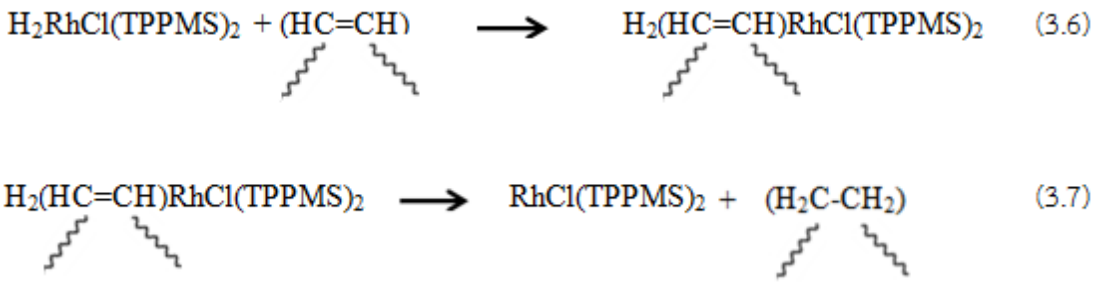

The rate expression for hydrogenation of unsaturated units is assumed from the coordination of olefin onto a Rh-H bond or by a reductive elimination of an rhodium-alkyl to produce the hydrogenated product, as shown in Eq. (3.8).

$$-\frac{d[C=C]}{dt} = k_{rds}[H_2RhCl(TPPMS)_2][C=C] \quad (3.8)$$

A material balance on the rhodium complex charged into the system given by Eq. (3.9) is a function of the total amount of rhodium ($[Rh]_T$).

$$[Rh]_T = [H_2RhCl(TPPMS)_2] + [RhCl(TPPMS)_2] + [RhCl(TPPMS)_3] \quad (3.9)$$

All of the rhodium complex species concentration terms in Eq. (3.9) can be converted in terms of $H_2RhCl(TPPMS)_2$ using the equilibria condition, and then can be substituted into Eq. (3.8) to provide the resulting rate law, as shown in Eq. (3.10).

$$-\frac{d[C=C]}{dt} = \frac{k_{rds}K_1K_2K_{H_2}P_{H_2}[Rh]_T[C=C]}{K_1K_2K_{H_2}P_{H_2} + K_1 + [TPPMS]} \quad (3.10)$$

The rate law equation of PIP hydrogenation catalyzed by the rhodium complex indicates that the reaction exhibits a first-order dependence on C=C concentration and rhodium concentration. According to the observed kinetic data in Figure 3.8-3.9 and Table 3.4, the rate of PIP hydrogenation exhibited a first-order dependence on C=C concentration. From the reaction mechanism, it can be concluded that the PIP hydrogenation rate also depends on catalyst concentration, reaction temperature and hydrogen pressure.

3.9 Morphology of PIP and HPIP

Morphologies of PIP and HPIP at hydrogenation levels of 96% are presented by TEM micrographs as shown in Figure 3.10. It is seen that the polyisoprene nanoparticles with uniform size were spherical with smooth surface, and the average particle size was about 38-49 nm (Figure 3.10a). The surface morphology of all rubber samples was stained with OsO_4 to increase the contrast and gradation of the particles. From Figure 3.10b, when the degree of hydrogenation increased to 96%, a lightly colored domain at the outer layer of the nanoparticles appeared. This can be explained in that the OsO_4 agent could stain only the carbon-carbon double bonds in the polymer chain, the dark color domain indicated a high double bond concentration while the lightly colored domain indicated a region of low C=C amount. This observation could confirm that C=C in the isoprene backbone of PIP was hydrogenated to saturated units during aqueous-phase hydrogenation.

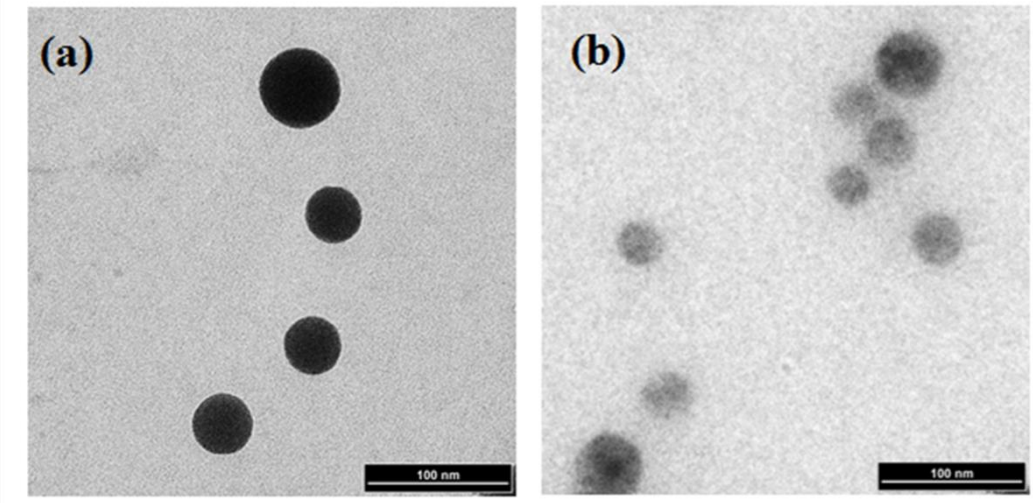

Figure 3.10 TEM micrographs of (a) PIP and (b) HPIP at 96 % HD.

3.10 Thermal Analysis of PIP and HPIP

Thermogravimetric analysis (TGA) is used to investigate the physical properties of substrates as a function of temperature. The TGA thermogram for PIP and HPIP samples at various degrees of hydrogenation are shown in Figure 3.11. It can be seen that polymer degradation occurred via an overall one-step reaction since the TG curve of the samples exhibited one-step smooth weight loss curves. From the TGA thermograms, HPIP began to lose weight starting at around 150 °C. This can be explained in that the residual C=C bonds of HPIP (12.1 – 96.0 %HD) are present in a random manner in the molecular chain resulting in degradation in the first place, while the saturated unit obtained could resist the high temperature applied for a longer time. A similar behavior has been reported for hydrogenated natural rubber latex by diimide reduction [67].

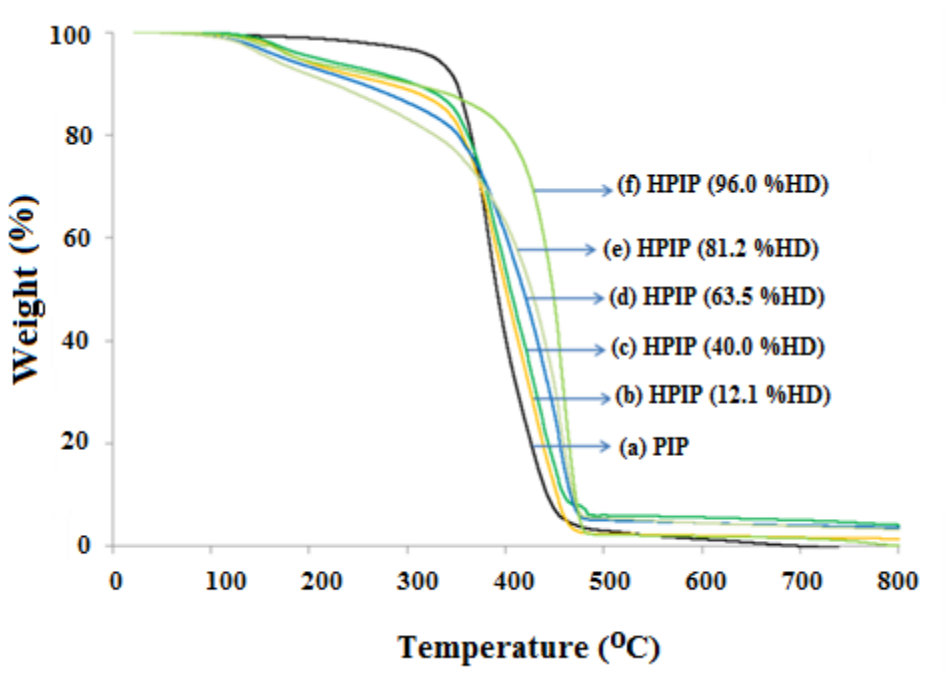

Figure 3.11 TGA thermograms of (a) PIP, (b) HPIP (12.1 % HD), (c) HPIP (40.0 % HD), (d) HPIP (63.5 % HD), (e) HPIP (81.2 % HD), and (f) HPIP (96.0 % HD).

The initial decomposition temperature (T_{id}) and the temperature at the maximum of mass loss rate (T_{max}) of HPIP at various hydrogenation levels are presented in Table 3.5. T_{id} of HPIP samples increased from 355.0 to 429.6 °C with an increase in the reduction of carbon–carbon double bonds in PIP (% HD) from 0 to 96.0%. In addition, T_{max} of HPIP samples increased from 386.0 to 461.5 °C with an increase in the hydrogenation degree from 0 to 96.0%. This can be explained in that the C=C bonds in PIP consist of a strong σ-bond and a weak π-bond and the hydrogenation reaction involves the breakage of the weak π-bond by the hydrogen molecule to form a stronger C-H σ-bond, which leads to higher thermal stability; therefore, the hydrogenation can improve the thermal stability of PIP.

Differential scanning calorimetry (DSC) experiments were performed to determine the glass transition temperatures (T_g). The DSC thermogram for PIP and HPIP samples at various degrees of hydrogenation are shown in Figure 3.12. The DSC thermogram of the HPIP sample indicates a one-step base-line shift at -55 °C. This implies that the HPIP sample has a single glass transition temperature. The T_g values of HPIP at various degrees of hydrogenation are presented in Table 5. The T_g of HPIP increased from -58.3 to -49.4 °C with an increase in the degree of hydrogenation from 0 to 96.0%. This can be explained in that the amorphous segments in PIP are replaced by crystalline ethylene segments. A similar shift in T_g from -55.5 to -52.6 °C was observed for hydrogenated *cis*-1,4-polyisoprene [68].

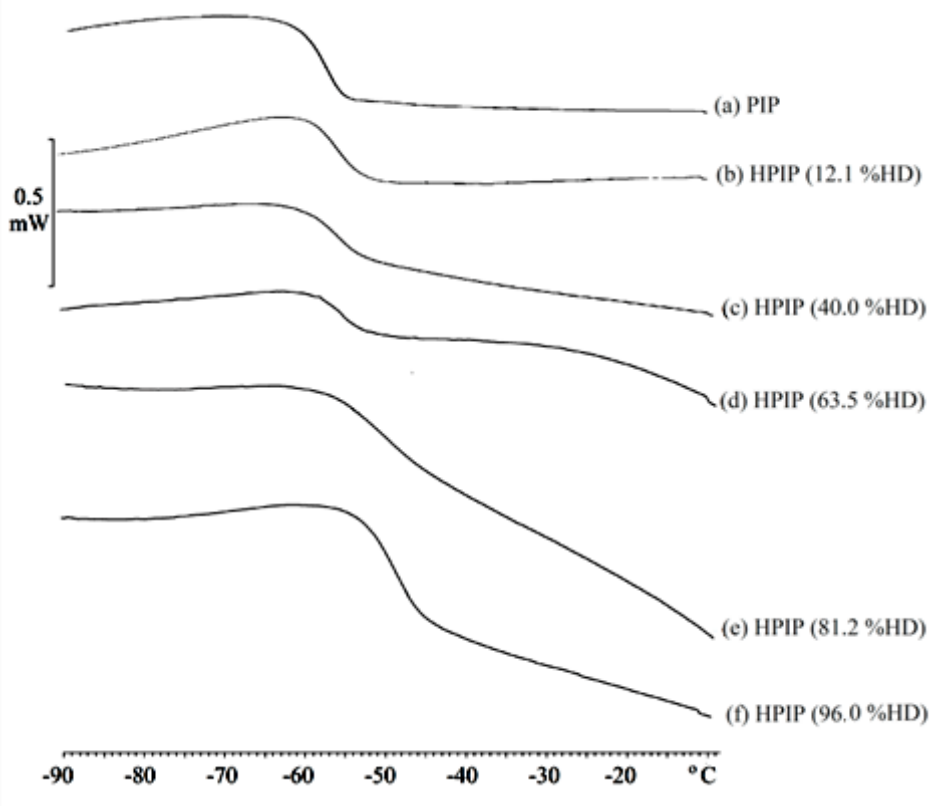

Figure 3.12 DSC thermograms of (a) PIP, (b) HPIP (12.1 %HD), (c) HPIP (40.0 % HD), (d) HPIP (63.5 % HD), (e) HPIP (81.2 % HD), and (f) HPIP (96.9 % HD).

Table 3.5 Analysis of glass transition temperature and decomposition temperature of hydrogenated samples.

Polymer	%HD	T_g (°C)	T_{id} (°C)	T_{max} (°C)
PIP	-	-58.3	355.0	386.0
HPIP	12.1	-56.7	356.0	389.8
	40.0	-55.6	371.9	423.6
	63.5	-55.2	384.4	448.8
	81.3	-54.3	404.0	455.0
	96.0	-49.4	429.6	461.5

3.11 Dynamic Mechanical Properties of HPIP

The elastic modulus of a rubber and its mechanical damping or energy dissipation characteristics as a function of frequency and temperature can be determined by dynamic mechanical analysis. The storage modulus (E′) for all PIP and HPIP samples, shown in Figure 3.13a, was dramatically decreased in the transition region because the mobility and deformation of the polymer chains increased with increasing temperature. Therefore, this showed that the samples have some elastic properties at temperatures above the glass transition temperature (T_g). In addition, the storage modulus of HPIP at 12.1, 63.5, and 96.0% hydrogenation were 190, 215, and 231 MPa, respectively; and the E′of all HPIP samples was higher than that of PIP (177 MPa). The improvement of the storage modulus properties can be explained in that the free volume and mobility are decreased by the replacement of the ethylene-propylene units via hydrogenation of the isoprene unit in the polymer chain, resulting in high stiffness of the hydrogenated samples.

The tan δ determined from the ratio of the dynamic loss modulus (E′′) to the storage modulus (E') is shown in Figure 3.13b. HPIP at 96.0 % HD showed a lower tan δ than pure PIP which indicated that HPIP had low dynamic loss due to a high interaction of the ethylene–propylene unit in the polymer chain. The T_g could also be determined from the center of the peak of the tan δ curves shown in Figure 3.13b. T_g of HPIP increased from -31.3 to -22.9 °C with an increase in hydrogenation level from 0 to 96.0%. This result was due to the replacement of isoprene units of PIP by crystalline ethylene-propylene segments in the structure of HPIP.

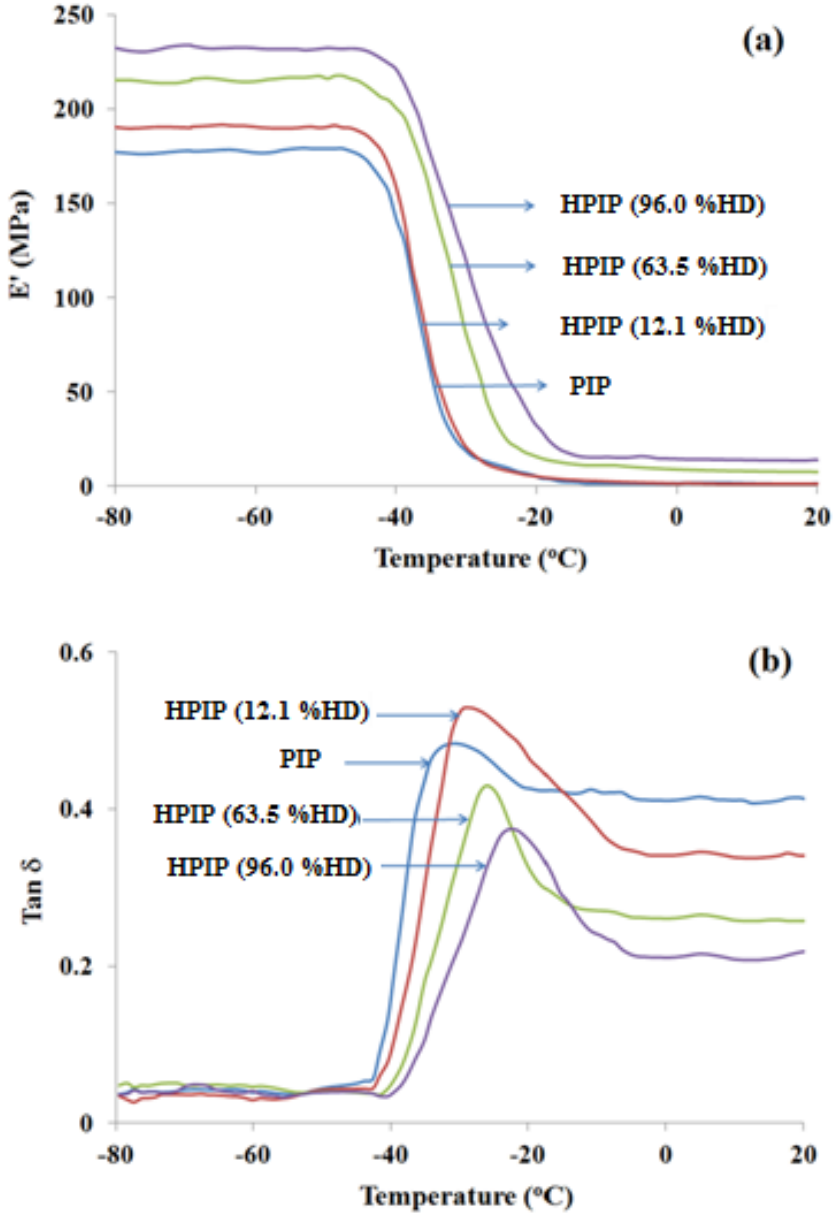

Figure 3.13 Temperature dependence of (a) storage modulus (E′) and (b) loss tangent (tan δ) for PIP and HPIP.

CHAPTER IV

AQUEOUS-PHASE HYDROGENATION OF NATURAL RUBBER LATEX USING RHODIUM CATALYSTS

4.1 Introduction

Natural rubber (NR) is an elastomer that is originally derived from a milky colloidal suspension, ie., latex, found in the sap of the Para rubber tree, *Hevea brasiliensis*. The purified form of NR contains more than 98% of the double bonds in the *cis*- configuration. NR also contains non-rubber components such as proteins and phospholipids. The chain structure of NR is presumed to be composed of initiating-ends (ω-terminal group) and terminating-ends (α-terminal group) as shown in Figure 1.2 [8]. Due to the unsaturation of carbon-carbon double bond of the isoprene backbone, NR can be degraded when exposed to sunlight, ozone and oxygen.

Hydrogenation, one type of chemical modification of unsaturated polymers, is an important method to reduce the amount of unsaturation and produce a saturated structure, which is resistant to oxidation and degradation. For latex hydrogenation, the use of aqueous media facilitates the process by eliminating toxic organic solvents; providing substantial environmental and economical benefits. Water is an environmentally friendly solvent which is non-toxic, non-flammable, and inexpensive. Therefore, water, as a substitution for organic solvents, can be identified as a "green solvent" and catalysis in aqueous media fully implements the principles of "Sustainable/Green Chemistry" [57].

In line with the above, we attempted to investigate the hydrogenation of NR and synthetic polyisoprene (PIP) catalyzed by rhodium complexes in the absence of organic solvent and the effects of catalyst precursors and concentration, reaction temperature and hydrogen pressure on hydrogenation level. The thermal properties and dynamic mechanical properties of HNR and HPIP were also investigated.

4.2 Characterization of NR and HNR

(i) Nuclear magnetic resonance (NMR) spectroscopy

The ^{1}H NMR spectra of NR, HNR are shown in Figure 4.1. For NR (Figure 4.1a and 4.1b), the hydrogenation led to the reduction in the intensity of the unsaturated peaks at 1.7, 2.1, and 5.2 ppm attributed to $-CH_3$, $-CH_2$, and olefinic protons, respectively. The appearance of the new signals including the peak of saturated $-CH_3$ and $-CH_2-$ at 0.8 ppm and 1.2 ppm, respectively, were observed after the hydrogenation process. The % HD was calculated from the change in the integral area of peaks representing protons for HNR as presented in Appendix A.

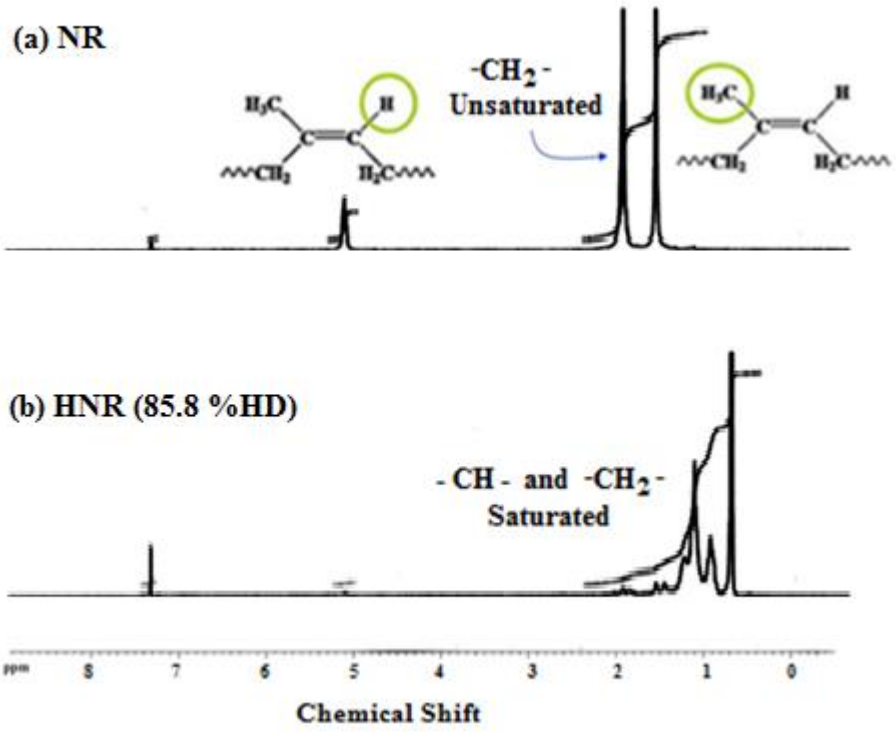

Figure 4.1 ^{1}H NMR spectra of (a) NR and (b) HNR, 85.8 % HD.

Hydrogenation of the samples was also confirmed by ^{13}C NMR as shown in Figure 4.2. For the NR structure (Figure 4.2a), the peak at 135.1 ppm was assigned to the unsaturated carbon of polyisoprene and the signal at 124.9 ppm was attributed to the -CH of the unsaturated carbon of the polyisoprene. The peaks at 26.2 and 32.0 ppm were attributed to $-CH_2$. After hydrogenation of NR, the peak areas in the region of 124–135 ppm decreased (Figure 4.2b), which indicates the reduction of the olefinic carbon bonds. The new peaks at 32.7 and 19.6 ppm were attributed to -CH and $-CH_3$ carbons, respectively, and the peaks at 37.4 and 24.4 ppm were attributed to $-CH_2$ of the saturated unit. Thus, it can be concluded that the C=C bonds in NR and in the synthetic polyisoprene backbone were converted to a saturated structure.

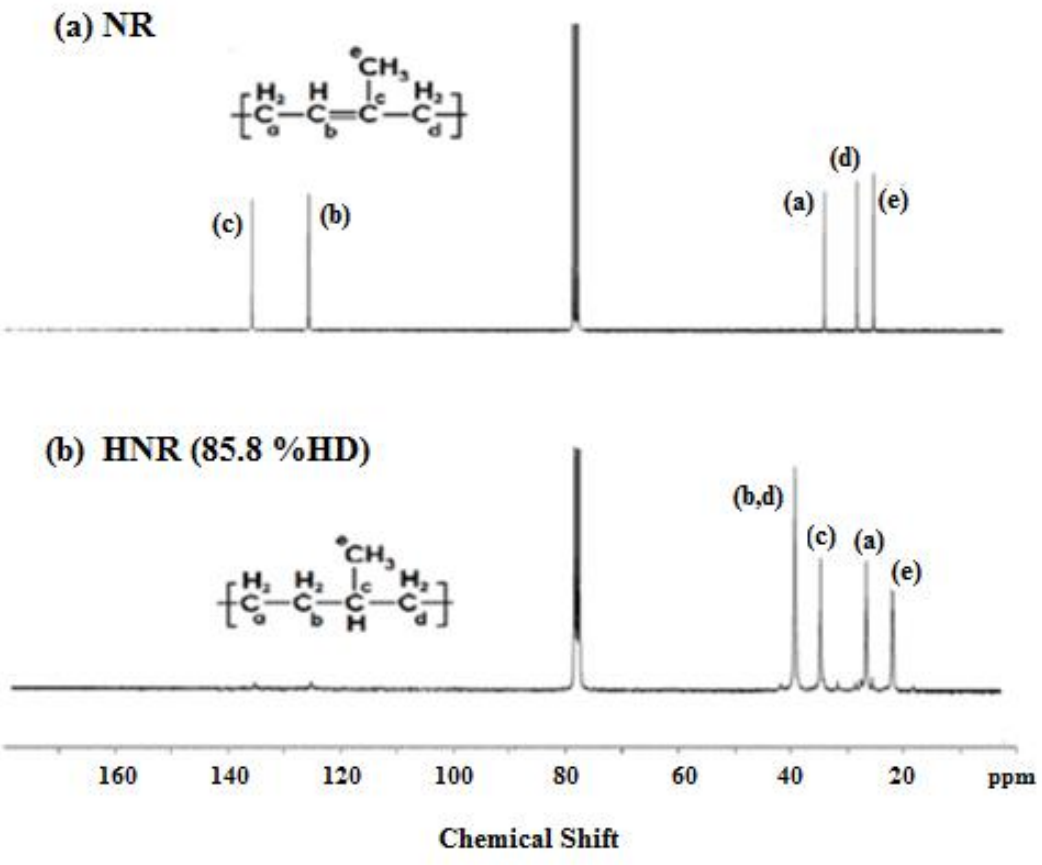

Figure 4.2 ^{13}C NMR spectra of (a) NR and (b) HNR, 85.8 % HD.

(ii) Particle Diameter Measurement

The particle size distributions of NR, HNR, PIP and HPIP were analyzed using a Dynamic light scattering (DLS) technique. From Figure 4.3, the particle sizes of HNR (172.6 nm) and HPIP (51.8 nm) had the same distribution pattern and slightly increased about 2.1% and 5.1% from that of the initial NR (169.1 nm) and PIP emulsion (49.3 nm), respectively. Thus, the hydrogenation process did not affect the particle size distribution of NR and PIP, and particle agglomeration was not observed.

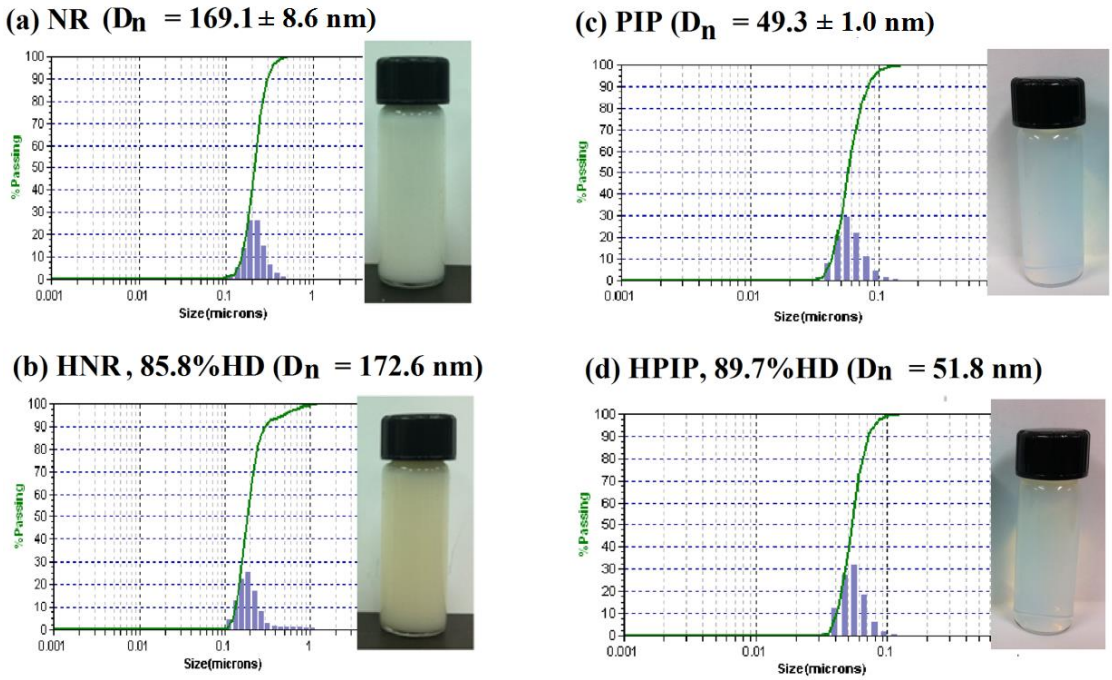

Figure 4.3 Polymer particle size distribution histograms of (a) NR (169.1 nm), (b) HNR, 85.8 % HD (172.6 nm), (c) PIP (49.3 nm), (d) HPIP, 89.7 % HD (51.8 nm).

(iii) Gel Permeation Chromatography (GPC)

Table 4.1 shows the polymer chain length of NR and PIP before and after hydrogenation. For NR hydrogenation, the number-average molecular weight (M_n = 260,000- 270,000) and weight-average molecular weight (M_w = 790,000–830,000) of HNR (% HD = 35.3-85.8 %) is substantially lower than that of the NR (M_n = 480,000 and M_w = 1,490,000). Similarly, for PIP hydrogenation, the number-average molecular weight (M_n = 660,000- 680,000) and weight-average molecular weight (M_w = 2,390,000–2,440,000) of HPIP (% HD = 39.2-89.7 %) is substantially lower than that of the starting polymer PIP (M_n = 1,590,000 and M_w = 3,380,000). This suggests that the high temperature and pressure used during the reaction caused some molecular chain scission of the polymer.

Table 4.1 Summary of Molecular Weight Data for NR, HNR, PIP and HPIP.

Polymer	%HD	M_w ($\times 10^{-6}$)	M_n ($\times 10^{-6}$)	PDI (M_w/M_n)
NR	-	1.49	0.48	3.10
HNR	35.3	0.83	0.26	3.19
	85.8	0.79	0.27	2.91
PIP	-	3.38	1.59	2.13
HPIP	39.2	2.39	0.68	3.50
	89.7	2.44	0.66	3.67

4.3 Hydrogenation of NR: Effect of Catalyst Ligands

The results of the effect of catalyst precursors ($RhCl_3/PPh_3$, $RhCl_3$/TPPTS and $RhCl_3$/TPPMS) and phosphorus/rhodium (P/Rh) molar ratio on hydrogenation of NR and PIP in aqueous media is presented in Table 4.2. At the same phosphorus/rhodium (P/Rh) molar ratio of 3 for NR (entries 2, 4, 6) and PIP (entries 8, 10, 12), the order of increasing hydrogenation degree (HD) and turnover frequency (TOF) using the three types of catalyst precursor is $RhCl_3/PPh_3$ <

$RhCl_3$/TPPTS < $RhCl_3$/TPPMS. In addition, the HPIP tended to have a higher HD compared to HNR. Using $RhCl_3/PPh_3$ as a catalyst precursor, a low HD (6.6% for NR, and 20.3% for PIP) was obtained due to the hydrophobic behavior of the PPh_3 ligand, and small droplets of the $RhCl_3/PPh_3$ catalyst complex were formed in aqueous media.

Table 4.2 Effects of catalyst precursors on hydrogenation of NR and PIP.

Entry	Polymer	Catalyst Precursor	P/Rh Molar ratio	D_n (nm)	%HD	TOF * (h^{-1})
1	NR	-	-	209.5	5.8	-
2	NR	$RhCl_3/PPh_3$	3	159.6	6.6	5.5
3	NR	$RhCl_3/PPh_3$	6	163.5	7.3	6.1
4	NR	$RhCl_3$/TPPTS	3	215.6	16.3	13.6
5	NR	$RhCl_3$/TPPTS	4	182.3	13.3	11.1
6	NR	$RhCl_3$/TPPMS	3	172.6	85.8	71.5
7	PIP	-	-	55.7	3.8	-
8	PIP	$RhCl_3/PPh_3$	3	53.4	20.3	16.9
9	PIP	$RhCl_3/PPh_3$	6	52.0	15.4	12.8
10	PIP	$RhCl_3$/TPPTS	3	55.8	39.2	32.7
11	PIP	$RhCl_3$/TPPTS	4	54.8	23.5	19.6
12	PIP	$RhCl_3$/TPPMS	3	54.9	88.9	74.1

Conditions: initial D_n of NR= 169.1 nm, PIP = 49.3 nm ; time = 6 h; [Rh] = 250 μM; temperature = 130 ºC; H_2 Pressure = 41.4 bar.

* TOF was defined as mole of hydrogenated C=C units in the polymer per mole of rhodium per hour.

The catalytic activity of the hydrogenation, when using $RhCl_3$/TPPTS and $RhCl_3$/TPPMS complexes, in the absence of organic solvent has been elucidated using the Hartley ionic spherical micelle model as shown in Figure 4.4 [51, 52, 61-63]. There are three layers in this micelle model: micelle core, Stern layer, and

the Gouy–Chapman layer. The backbone of the NR with the C=C unsaturated units are located in the micelle core. Surrounding the core is the Stern layer containing the hydrophilic groups SO_3^- (in the TPPMS and TPPTS ligands), and where protein at the ω-terminal position and phospholipid at α-terminal position is located in NR. The Gouy–Chapman layer is the outer layer where the counter ions Na^+ are located. The rhodium complex can be either hydrophilic or hydrophobic depending on the ligands surrounding the metal [69]. The rhodium location between the Stern layer and the micelle core was dependent on the polarity of the catalyst complex. Using $RhCl_3$/TPPTS as the catalyst precursor, low HD (16.3% for NR, and 39.2% for PIP) was obtained. This can be explained in that the high polarity of TPPTS ligand caused more rhodium atoms to locate in the hydrophilic layer instead of moving through the micelle core. In contrast, the polarity of the TPPMS ligand is lower than the TPPTS ligand due to only one charged head group of SO_3^- in its structure. The rhodium atom of $RhCl_3$/TPPMS complex is more driven to the micelle core. So, high conversion of NR (85.8 % HD) and PIP (88.9 % HD) was achieved for hydrogenation using TPPMS as a catalyst ligand.

For both catalyst precursors, $RhCl_3/PPh_3$ and $RhCl_3$/TPPTS, increasing the P/Rh molar ratio did not enhance the catalyst activity for the hydrogenation of NR and PIP. At a higher PPh_3/rhodium molar ratio of 6 (Table 4.2, entry 3) and with a TPPTS/rhodium molar ratio of 4 (entry 5), the TOF for NR hydrogenation was 6.1 h^{-1} and 12.8 h^{-1}, respectively. For PIP hydrogenation using $RhCl_3/PPh_3$ and $RhCl_3$/TPPTS at a molar ratio of 3 (entries 8, 10), a TOF of 16.9 h^{-1} and 32.7 h^{-1} were observed, respectively. Similarly, increasing the P/Rh molar ratio had a negative effect on catalyst activity for PIP hydrogenation (entries 9, 11). The decrease in catalyst activity at a higher P/Rh molar ratio for hydrogenation of both polymers could be explained by a competition between the added free ligand and the C=C units of the rubbers for a coordination site on rhodium tending to decrease the catalyst activity for the hydrogenation reaction.

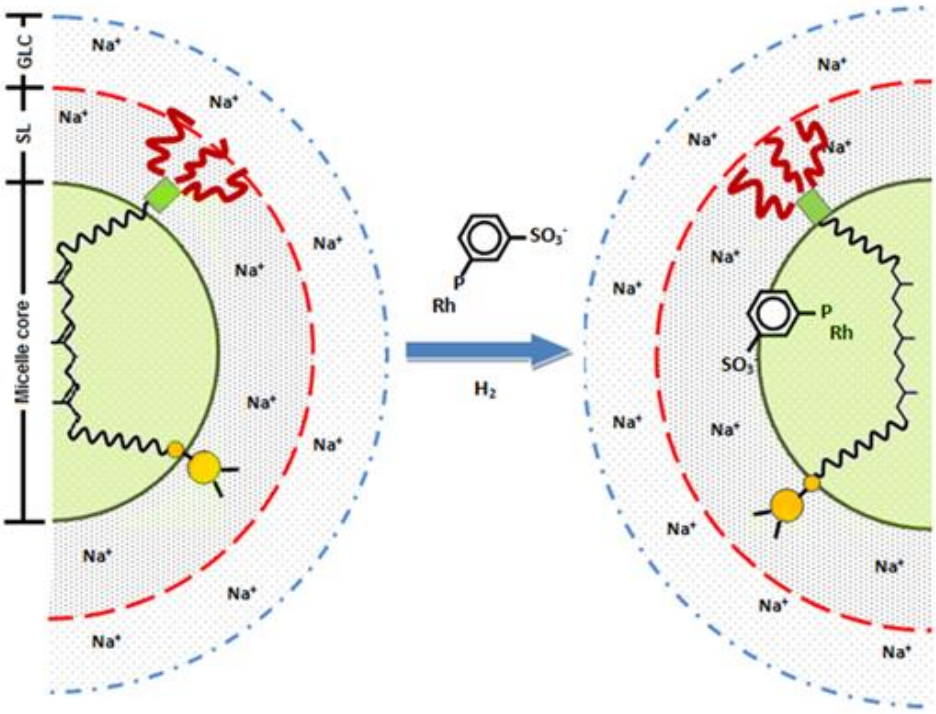

Figure 4.4 Representation of NR and HNR catalyzed by rhodium complex in a model of a Hartley ionic micelle, including micelle core, the Stern layer (SL), and the Gouy–Chapman double layer (GCL).

On comparing the NR and PIP hydrogenation, the catalyst activity of $RhCl_3/PPh_3$, $RhCl_3$/TPPTS and $RhCl_3$/TPPTS in PIP hydrogenation was higher than that in NR hydrogenation. This can be explained in that the impurities such as protein, ammonia, or other nitrogen content in the NR might affect the efficiency of hydrogenation. The impurities in the emulsion system, located in the Stern layer, were suspected to inhibit the catalyst activity. In addition, previous work reported that impurities decreased the catalytic hydrogenation rate of NR using an osmium complex in toluene, and *p*-toluenesulfonic acid was added to the solution for neutralizing the impurities in the rubber, and preventing the poisoning of the catalyst [38].

4.4 Hydrogenation of NR using RhCl3/TPPTS

The effects of process variables (catalyst amount, reaction temperature, hydrogen pressure, and P/Rh molar ratio) on organic solvent-free hydrogenation of NR and PIP using $RhCl_3$/TPPTS as a catalyst are given in Table 4.3. For the NR hydrogenation using Rh/TPPTS as catalyst, HD was less than 20%. The increase in catalyst amount tended to enhance the C=C conversion. However, the HD was slightly increased with increasing rhodium concentration up to 375 μM approaching a HD of 17.5% (entries 13-15). In addition, HD increased with increasing reaction temperature up to 130 °C approaching a HD of 16.3%, and decreased to 9.2% at a temperature of 150 °C (entries 14, 16, 17). Moreover, a low HD was still obtained when the hydrogen pressure and TPPTS/Rh molar ratio were varied (entries 14, 20 in Table 4.3).

Similarly, in the case of PIP hydrogenation using Rh/TPPTS, a low hydrogenation level (20.5-39.2%) was obtained when the catalyst amount (125-375 μM), reaction temperature (120-150 °C) and hydrogen pressure (13.8-41.4 bar) were varied (entries 21-28 in Table 4.3). Previous work has reported that Rh/TPPTS complexes are very efficient for the catalytic hydrogenation of unsaturated polymers in aqueous media when an organic solvent, such as n-hexane, was added (water/n-hexane = 82/18 w/w) [51, 52]. However, all of our experiments were performed in the absence of organic solvent. Thus, it can be concluded that Rh/TPPTS was not effective for organic solvent-free hydrogenation of NR and PIP.

Table 4.3 Effects of process variables on hydrogenation of NR and PIP using $RhCl_3$/TPPTS as catalyst precursor.

Entry	Polymer	[Rh] (μM)	T (°C)	P (bar)	P/Rh Molar ratio	D_n (nm)	% HD
13	NR	125	130	41.4	3	213.2	15.7
14	NR	250	130	41.4	3	215.6	16.3
15	NR	375	130	41.4	3	181.2	17.5
16	NR	250	110	41.4	3	201.5	11.0
17	NR	250	150	41.4	3	199.9	9.2
18	NR	250	130	27.6	3	181.6	16.7
19	NR	250	130	13.8	3	161.7	15.1
20	NR	250	130	41.4	4	182.3	13.3
21	PIP	125	130	41.4	3	55.1	24.3
22	PIP	250	130	41.4	3	55.8	39.2
23	PIP	375	130	41.4	3	54.2	31.4
24	PIP	250	120	41.4	3	54.2	32.4
25	PIP	250	140	41.4	3	53.3	29.6
26	PIP	250	150	27.6	3	53.2	33.9
27	PIP	250	150	13.8	3	54.2	20.5
28	PIP	250	140	41.4	4	54.9	23.5

Conditions: initial D_n of NR= 169.1 nm, PIP = 49.3 nm; time = 6 h; catalyst precursor = $RhCl_3$/TPPTS.

4.5 Hydrogenation of NR using RhCl3/TPPMS

The effect of process variables (rhodium catalyst amount, reaction temperature and hydrogen pressure) on NR and PIP hydrogenation using TPPMS as a catalyst ligand in absence of organic solvent are presented in Figure 4.5 – Figure 4.7 and discussed in detail as follows.

4.5.1 Effect of Catalyst Concentration

Figure 4.5 shows the effects of catalyst amount on the hydrogenation level and particle size after hydrogenation of NR and PIP at 41.4 bar and 130 °C. The HD of NR and PIP increased with increasing catalyst amount up to 250 μM approaching 85.8% and 88.9%, respectively. In addition, at low rhodium concentration of 50 μM, the low HD (35.3% for NR, and 44.5% for PIP) was observed at this condition. A similar behavior regarding the dependence of HD on catalyst concentration has been reported for hydrogenation of polybutadiene-1,4-*block*-poly(ethylene oxide) in aqueous media using a water-soluble rhodium complex [51]. On comparing NR and PIP hydrogenation, the results in Figure 4 show that the NR hydrogenation required higher catalyst loading to reach the same hydrogenation level as for PIP hydrogenation. It can be assumed that impurities in NR might reduce the catalytic activity. In addition, the influence of catalyst amount on the particle size after hydrogenation of NR and PIP using the Rh/TPPMS complex is shown in Figure 4.5. The particle size increased 3.9 – 14.6 % (175.7 – 191.2 nm from the initial particle size of 169.1 nm for NR, 54.7 – 56.5 nm and from an initial particle size of 49.3 nm for PIP) with increasing catalyst amount (0 – 250 μM).

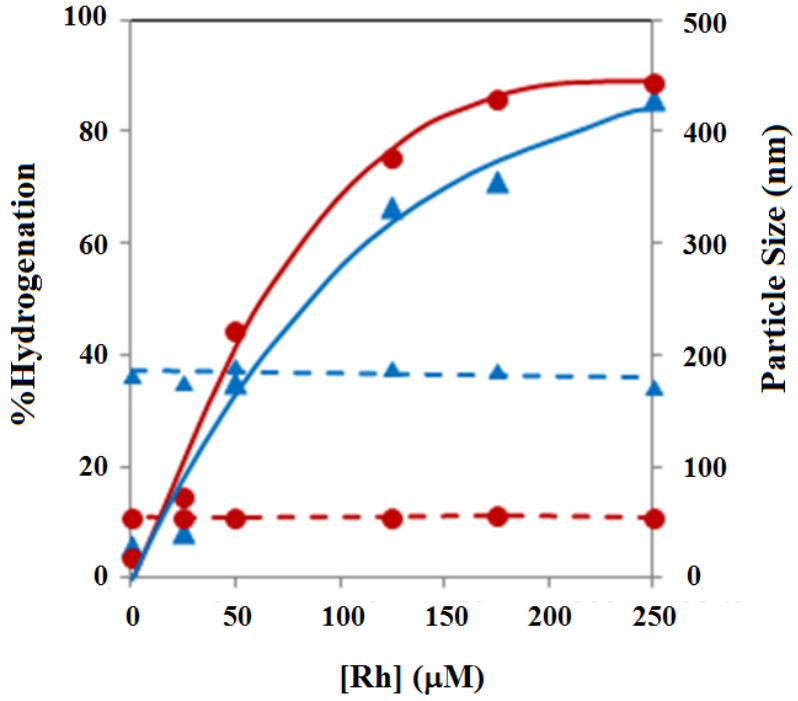

Figure 4.5 Effect of catalyst concentration on hydrogenation (——) and particle size (-----): polymer, ● PIP (initial D_n = 49.3 nm), ▲ NR (initial D_n = 169.1 nm); time = 6 h; temperature = 130 °C; H_2 pressure = 41.4 bar; catalyst precursor = $RhCl_3$/TPPMS (P/Rh molar ratio = 3).

4.5.2 Effect of Temperature

The effect of temperature on NR and PIP hydrogenation using $RhCl_3$/TPPMS as catalyst in aqueous-phase systems is represented in Figure 4.6. When the temperature was increased over the range of 100-120 °C, a low HD was obtained. For NR, the HD increased with increasing reaction temperature approaching 85.8% at a temperature of 130 °C. However, HD of NR decreased at temperatures above 130 °C. For PIP hydrogenation, the HD for PIP reached 88.9% at a temperature of 130 °C, and tended to level off with increasing temperature over the range of 140-150 °C. It can be explained that raising the reaction temperature above the optimum temperature had a negative effect on the

stability of the micelles resulting in a lower activity for the Rh/TPPMS catalyst complex [64]. For the HNR and HPIP particle size as shown in Figure 4.6, the particle size increased 2.1 – 14.6 % (172.6 – 179.0 nm from the initial particle size of 169.1 nm for NR, 51.8 – 56.5 nm and from an initial particle size of 49.3 nm for PIP) with increasing temperature (100 – 150 °C).

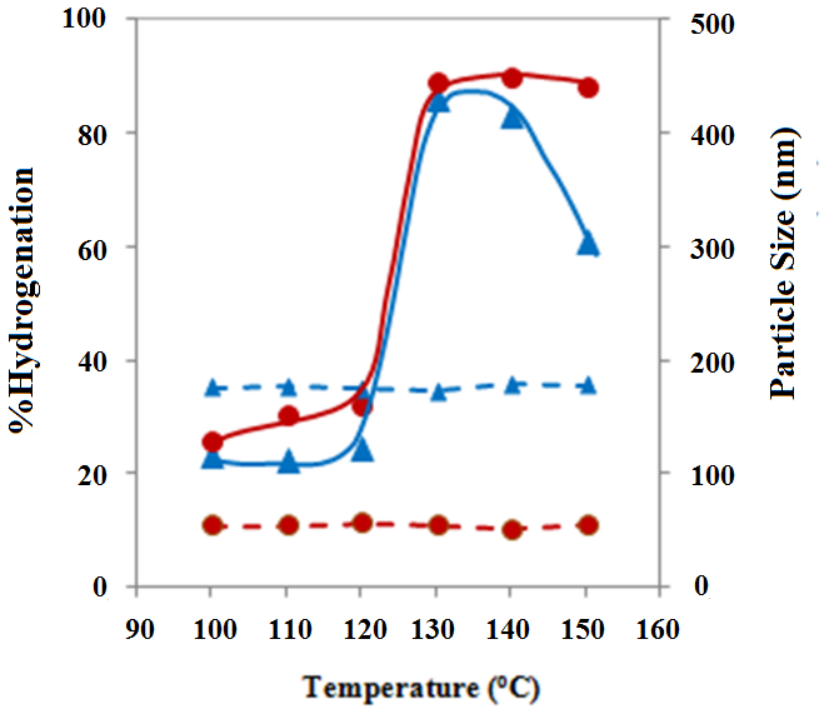

Figure 4.6 Effect of temperature on hydrogenation (——) and particle size (-----): polymer, ● PIP (initial D_n = 49.3 nm), ▲ NR (initial D_n = 169.1 nm); time = 6 h; H_2 pressure = 41.4 bar; catalyst precursor = $RhCl_3$/TPPMS (P/Rh molar ratio = 3); [Rh] = 250 μM.

4.5.3 Effect of Hydrogen Pressure

The dependence of C=C conversion on hydrogen pressure over the range 6.9– 41.4 bar (at 250 μM of [Rh] and 140 °C) is shown in Figure 4.7. The results indicated that the hydrogenation level dramatically increased with an increase in hydrogen pressure up to 13.8 bar, and HD of PIP (78.0 %) was slightly higher than that of NR (73.1%). For hydrogen pressures above 13.8 bar, the HD of NR and PIP

tended to only slightly increase with a further increase in hydrogen pressure approaching 85.8% and 88.9%, respectively, at a pressure of 41.4 bar. A similar behavior regarding the effect of hydrogen pressure on the hydrogenation of NR using a ruthenium complex [37] and an osmium complex [39] in monochlorobenzene has been reported. The influence of hydrogen pressure on the particle size after hydrogenation of NR and PIP using the Rh/TPPMS complex is shown in Figure 4.7. The particle size slightly increased 2.1 – 10.5 % (172.8 – 185.6 nm from the initial particle size of 169.1 nm for NR, 52.1 – 54.5 nm and from an initial particle size of 49.3 nm for PIP) with increasing hydrogen pressure (6.9 – 41.4 bar).

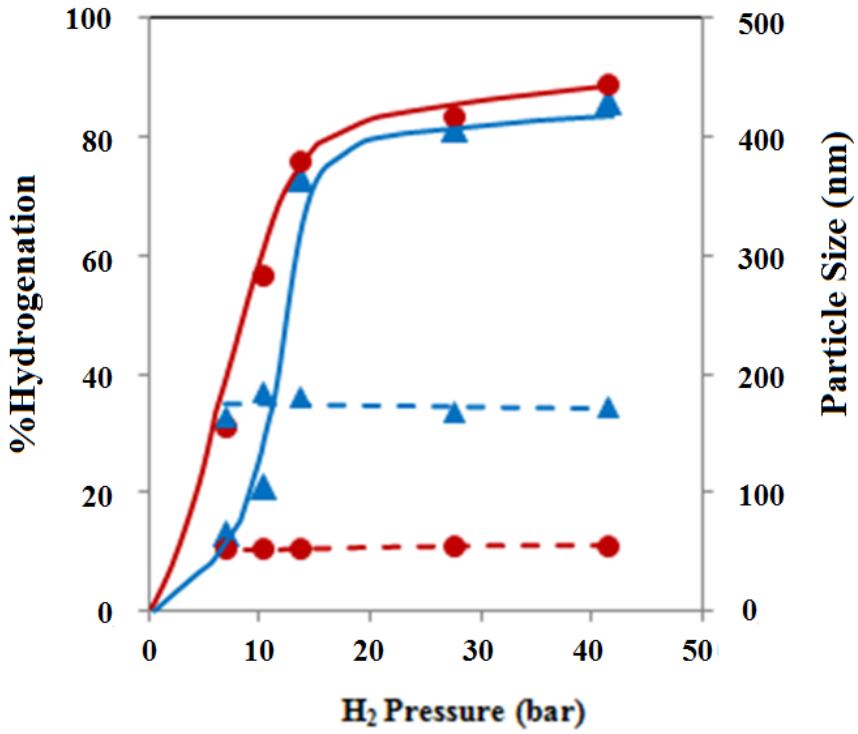

Figure 4.7 Effect of hydrogen pressure on hydrogenation (——) and particle size (-----): polymer, ● PIP (initial D_n = 49.3 nm), ▲ NR (initial D_n = 169.1 nm); time = 6 h; temperature = 130 °C; catalyst precursor = $RhCl_3$/TPPMS (P/Rh molar ratio = 3); [Rh] = 250 μM.

4.6 Morphology of NR and HNR

Morphologies of NR and HNR at hydrogenation levels of 86% are presented by TEM micrographs as shown in Figure 4.8. It is seen that the NR particle was partially agglomerated having a size of 200 nm (Figure 4.8a). In order to compare NR and HNR, the surface of the rubber sample was stained with OsO_4 to increase the contrast and gradation of the NR and HNR particles. The carbon-carbon double bonds in the polymer chain could be stained by the OsO_4 agent. Therefore, the dark colored domain indicated high C=C region in the polymer, and the region of low C=C amount was indicated by a lightly colored domain. For the HNR morphology shown in Figure 4.8b, a lightly colored domain in the particles appeared compared with NR (Figure 4.8a). This observation confirms that C=C in the isoprene backbone of NR was hydrogenated to saturated units during aqueous-phase hydrogenation.

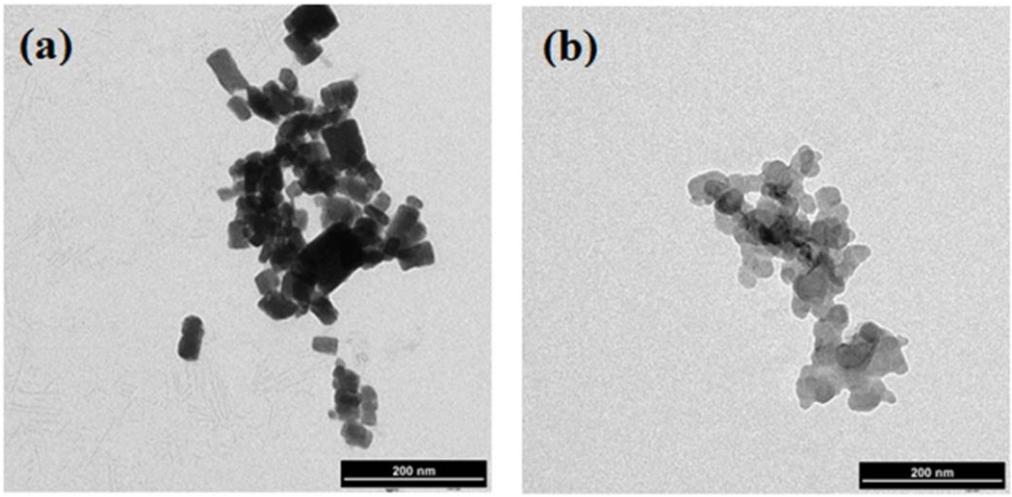

Figure 4.8 TEM micrographs of (a) NR and (b) HNR at 86 % HD.

4.7 Thermal Analysis of NR and HNR

Figure 4.9 illustrates the TGA thermograms for NR and HNR samples at various HD. The results indicate that decomposition of the rubbers is an overall one-step reaction because the decomposition curve of the samples show only one-step and provide smooth weight loss curves. The TGA thermograms of NR and HNR at 23.1 % HD have the same decomposition behavior, indicating that HNR at low %HD has a similar polymer chain structure to NR. For HNR at 35.5, 60.6, 73.1 and 85.8 %HD, the samples began to lose their weight starting at around 100 °C. This can be explained in that the residual C=C bonds of HNR (35.5 – 85.8 % HD) are present in a random manner in the molecular chain causing degradation in the first place, while the saturated unit obtained could resist high temperature applied for a longer time. The previous work reported a similar weight-loss behavior for hydrogenated natural rubber latex by diimide reduction [67].

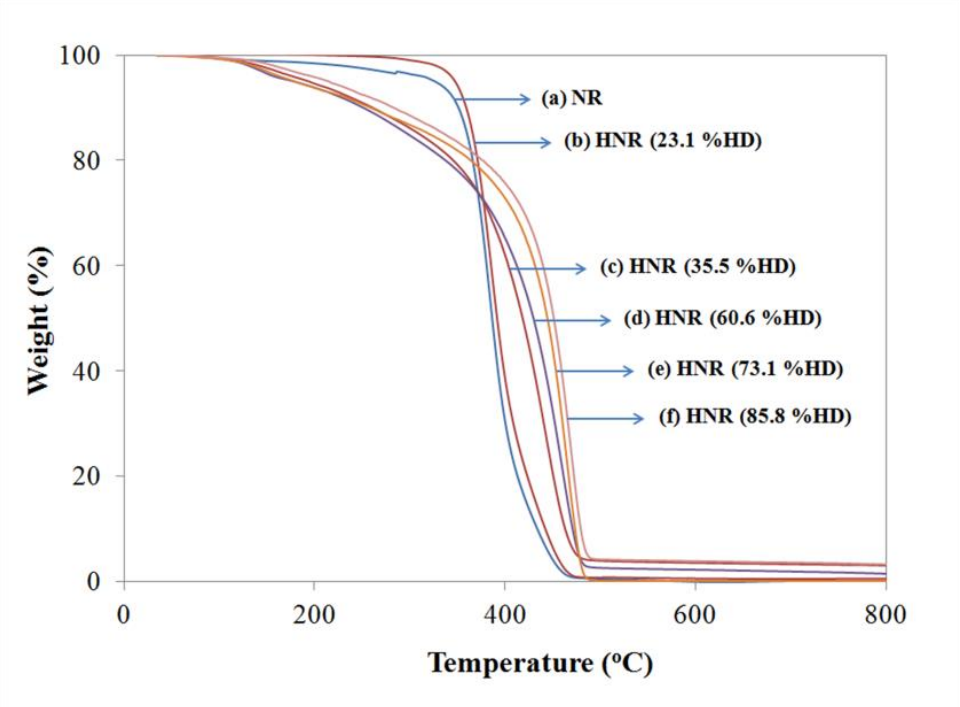

Figure 4.9 TGA thermograms of (a) NR, (b) HNR (23.1 % HD), (c) HNR (35.5 % HD), (d) HNR (60.6 % HD), (e) HNR (73.1 % HD), and (f) HNR (85.8 % HD).

The initial decomposition temperature (T_{id}) and maximum decomposition temperature (T_{max}) of the NR, PIP, HNR and HPIP at different HD, as evaluated from the TGA analysis, are summarized in Table 4.5. The T_{id} and T_{max} of HNR and HPIP samples increased with increasing HD. The T_{id} and T_{max} of HNR at the maximum hydrogenation level (85.8%) were higher than that of NR (ΔT_{id} = 77.3 °C and ΔT_{max} = 84.2 °C). Similarly, the T_{id} and T_{max} of HPIP at the maximum hydrogenation level (89.7%) were higher than that of PIP (ΔT_{id} = 74.7 °C and ΔT_{max} = 78.0 °C). This can be explained in that a weak π-bond within the rubbers was converted to a stronger C-H σ-bonds on the addition of a hydrogen molecule; thus, the hydrogenation improves the thermal stability of NR (T_{max} = 465.9 °C) and PIP (T_{max} = 464.0 °C).

The DSC thermogram of the HNR samples, shown in Figure 4.10, indicates a one-step base-line shift at -60 °C. Therefore, the HNR sample has a single glass transition temperature. The T_g values of HNR and HPIP at various HD are presented in Table 5. The T_g of HNR increased from -63.8 to -60.0 °C with an increase in HD from 0 to 85.8%; and the T_g of HPIP increased from -58.3 to -49.5 °C with an increase in HD from 0 to 89.7%. This can be explained by the replacement of amorphous segments of polyisoprene by crystalline ethylene-propylene units in the polymer structure. A similar shift in glass transition temperature was observed for hydrogenated *cis*-1,4-polyisoprene [68].

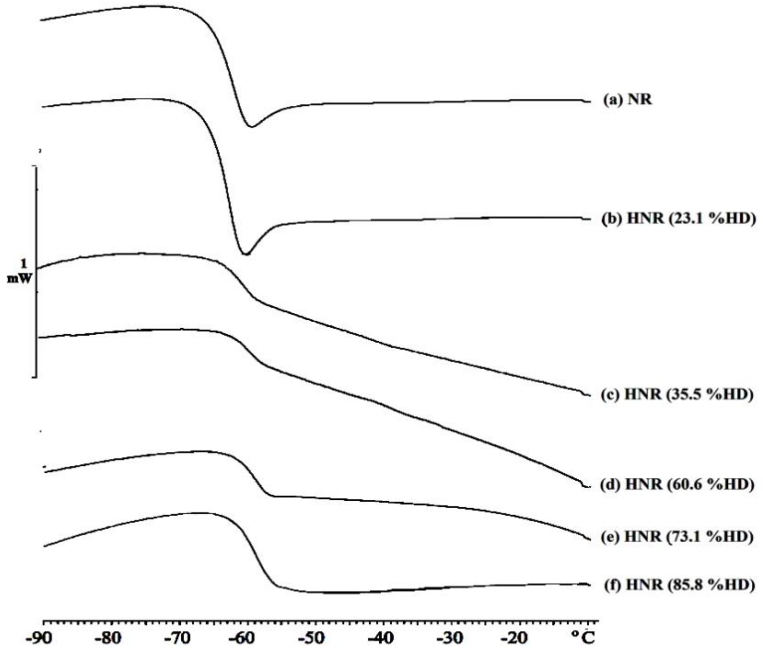

Figure 4.10 DSC thermograms of (a) NR, (b) HNR (23.1 % HD), (c) HNR (35.5 % HD), (d) HNR (60.6 % HD), (e) HNR (73.1 % HD), and (f) HNR (85.8 % HD).

Table 4.4 Analysis of glass transition temperature and decomposition temperature of HNR and HPIP.

Polymer	%HD	T_g (°C)	T_{id} (°C)	T_{max} (°C)
NR	-	-63.8	358.5	381.7
HNR	23.1	-64.7	359.8	384.7
	35.5	-61.6	392.9	441.5
	60.6	-60.9	413.8	459.0
	73.1	-59.6	429.5	462.2
	85.8	-60.0	435.8	465.9
PIP	-	-58.3	355.0	386.0
HPIP	14.6	-56.8	356.0	389.8
	39.2	-55.6	364.2	434.8
	56.8	-55.2	387.8	452.6
	79.8	-54.3	403.3	453.4
	89.7	-49.5	429.7	464.0

4.8 Dynamic Mechanical Properties of HNR

Dynamic mechanical analysis is used to measure the elastic modulus of a polymer and its mechanical damping characteristics as a function of frequency and temperature. The storage modulus (E′) indicating stiffness of rubbers as shown in Figure 4.11a decreased in the transition region due to the increase of mobility and deformation of the polymer chains with increasing temperature. Therefore, the samples have some elastic properties at temperatures above the glass transition temperature (T_g). The E′ of HNR at 21.0, 60.6, and 85.8 %HD were 227, 322, and 429 MPa, respectively, In addition, the E′ of all HNR samples was higher than that of NR (198 MPa). The higher E′ of HNR can be explained in that the replacement of the ethylene-propylene segments by hydrogenation of the isoprene unit in the polymer chain tends to decrease the mobility and the free volume of the polymer.

Figure 4.11b illustrates the tan δ determined from the ratio of the dynamic loss modulus (E″) to storage modulus (E′). The tan δ of HNR at the maximum HD (85.8%) was lower than that of NR. The results indicated that HNR had low dynamic loss due to the increasing ethylene–propylene unit in the polymer chain. The T_g could also be determined from the center of the peak of the tan δ curves shown in Figure 9b. While the HD of NR increased from 0 to 85.8%, the T_g of HNR increased from -41.6 to -36.8 ºC. This is due to the fact that the isoprene units in NR were substituted by crystalline units of ethylene-propylene in HNR.

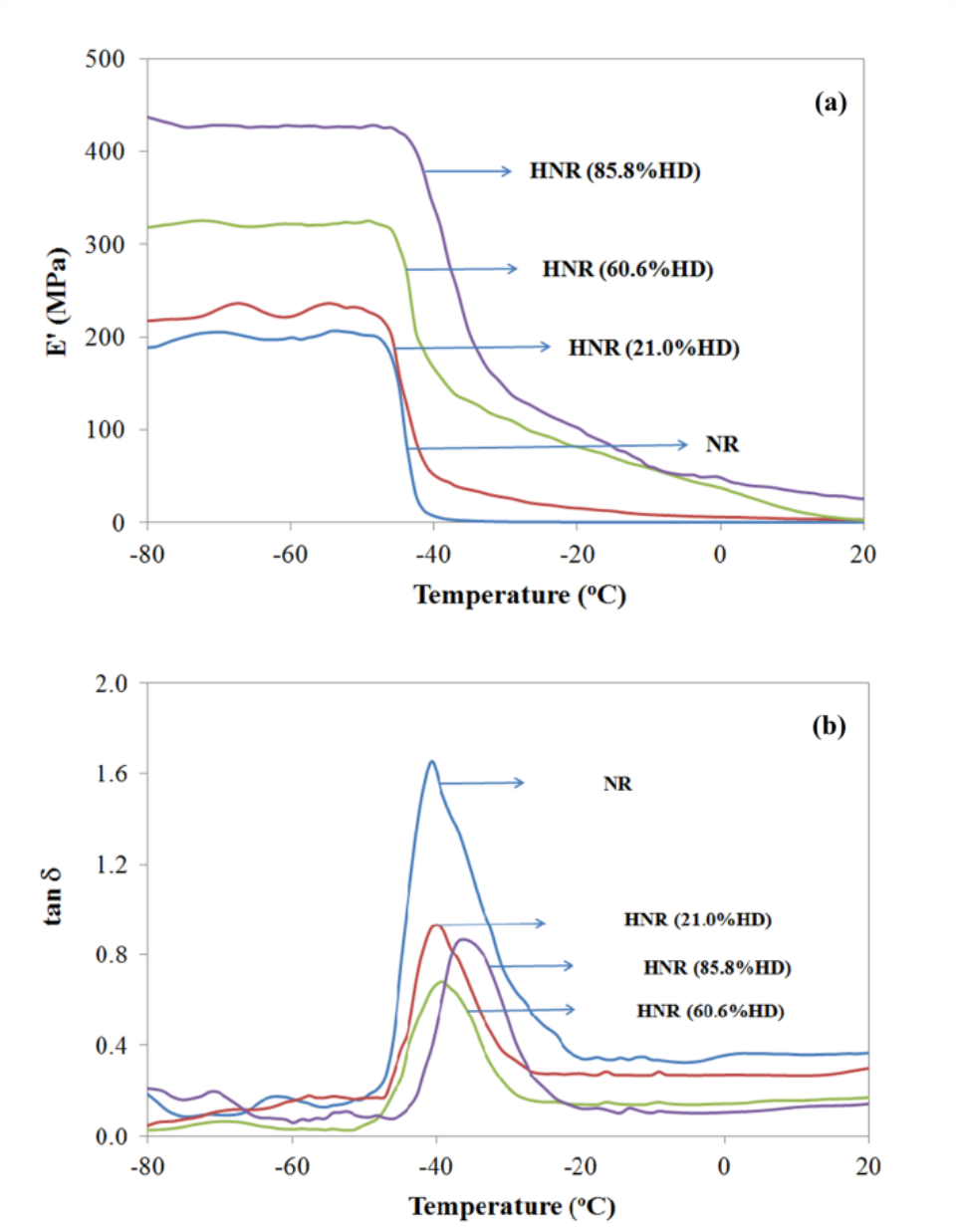

Figure 4.11 Temperature dependence of (a) storage modulus (E′) and (b) loss tangent (tan δ) for NR and HNR.

CHAPTER V

MECHANICAL PROPERTIES OF NR/PIP AND NR/HPIP BLENDS

5.1 Introduction

Polymer blending products are frequently formulated by blending two or more polymers. In generally, a miscible blend of two polymers exhibits combination properties obtained from those polymers. The rational for this development involves one or more of the following points: develop new properties, improve properties, reduce material costs, improve processibility, and the formation of modified polymeric materials. Nowadays, for commercial products, the rubber blends of NR and synthetic rubber have achieved some of these points. Technically, NR has a drawback in thermal and ozone stability due to the carbon-carbon double bonds present in polyisoprene backbone; therefore, the thermal and ozone degradation of NR could be prevented by blending with another polymer which acted as a thermal and ozone stabilizer.

One noteworthy polymer to blend with NR is the hydrogenated elastomer because of its thermal and ozone resistance. For the mechanical properties of blends consisting of HNR and NR blends using various cure systems: peroxide vulcanization, conventional vulcanization with peroxide, and efficient vulcanization with peroxide, the tensile strength of the blends decreased with increasing HNR content because of the higher incompatibility to cause a noncoherent behavior between NR and HNR [70]. This work was also extended to studies of the thermal and ozone stability of HNR/NR at various ratios vulcanized, and the highest retention of tensile strength after thermal aging was exhibited. Moreover, the increase in HNR content in the blends could retard the ozonolysis resulting in less surface cracking when attacked by ozone [71].

The purpose of this work was to study the dynamic mechanical properties and thermal properties of NR filled with PIP (NR/PIP blends) blends and NR filled with HPIP (NR/HPIP blends). The mechanical properties, thermal resistance and ozone resistance of NR/PIP and NR/HPIP blends were also investigated.

5.2 Dynamic Mechanical Properties of NR/PIP and NR/HPIP Blends

Dynamic mechanical analysis is a powerful technique for the determination of a rubber modulus as a function of temperature and frequency. PIP and HPIP, with 90% HD achieved by aqueous-phase hydrogenation using a water soluble rhodium catalyst, were selected to blend with NRL at the various blend ratios (100:0, 90:10, 80:20 70:30 and 60:40). Modulus data, in the form of the storage modulus (E'), and the mechanical damping behavior, in the form of loss tangent (tan δ), of NR, NR filled with PIP (NR/PIP) and NR filled with HPIP (NR/HPIP) as a function of temperature are shown in Figure 5.1.

The E' values of NR, NR/PIP and NRHPIP blends exhibited a plateau curve below the glass transition temperature (T_g) and decreased around the T_g. The storage modulus and loss tangent data of NR/PIP and NR/HPIP blends are presented in Table 5.1. For the E' of NR/PIP blends as shown in Figure 5.1a and Table 5.1, the E' decreased from 597 to 117 MPa with an increasing amount of PIP in the blends (100:0 - 60:40). Similarly, the E' of NR/HPIP blends decreased from 597 MPa to 117 MPa with an increasing amount of PIP in the blends (100:0 - 60:40), as shown in Figure 5.1b and Table 5.1. Comparing of NR and NR blends, unfilled NR has high storage modulus due to low mobility of NR chain, while the polymer chain in NR/PIP and NR/HPIP blends has high mobility resulting in decrease in storage modulus. In comparison with the blends at the same weight ratio, The storage modulus of the NR/HPIP blends were higher than that of the NR/PIP blends (19-39% increasing) for all blends ratios. This could be explained in that E′ of HPIP was higher than that of PIP, as reported in Chapter III, which can lead to an increase in the stiffness of the NR/HPIP blends. Therefore, the improvement of the storage modulus could be achieved by the addition of HPIP into the NR latex, resulting in enhancement of the strength and stiffness of NR.

Figure 5.1 c-d illustrates the loss tangent with respect to temperature for NR, NR/PIP and NR/HPIP blends. For NR and NR/PIP blends as shown in Figure 5.1c, the T_g was not changed when PIP at various amounts was blended with NR. However, T_g is shifted to a higher temperature with the addition of HPIP into the NR matrix. NR and its blends had a single glass transition temperature and the T_g was -40°C, -40°C and

-35°C for unfilled NR, NR filled with PIP and NR filled with HPIP, respectively. The addition of HPIP significantly affected the T_g value due to a lower mobility and flexibility of the polymer matrix by the saturated unit of ethylene-propylene. In addition, the tan δ of NR/HPIP was lower than that of NR/PIP blends (4-19% decreasing). The decrease in tan δ which is determined from the ratio of the loss modulus (E") to storage modulus (E') implies that the high storage modulus is due to an increase in the ethylene-propylene saturated structure of the composite materials.

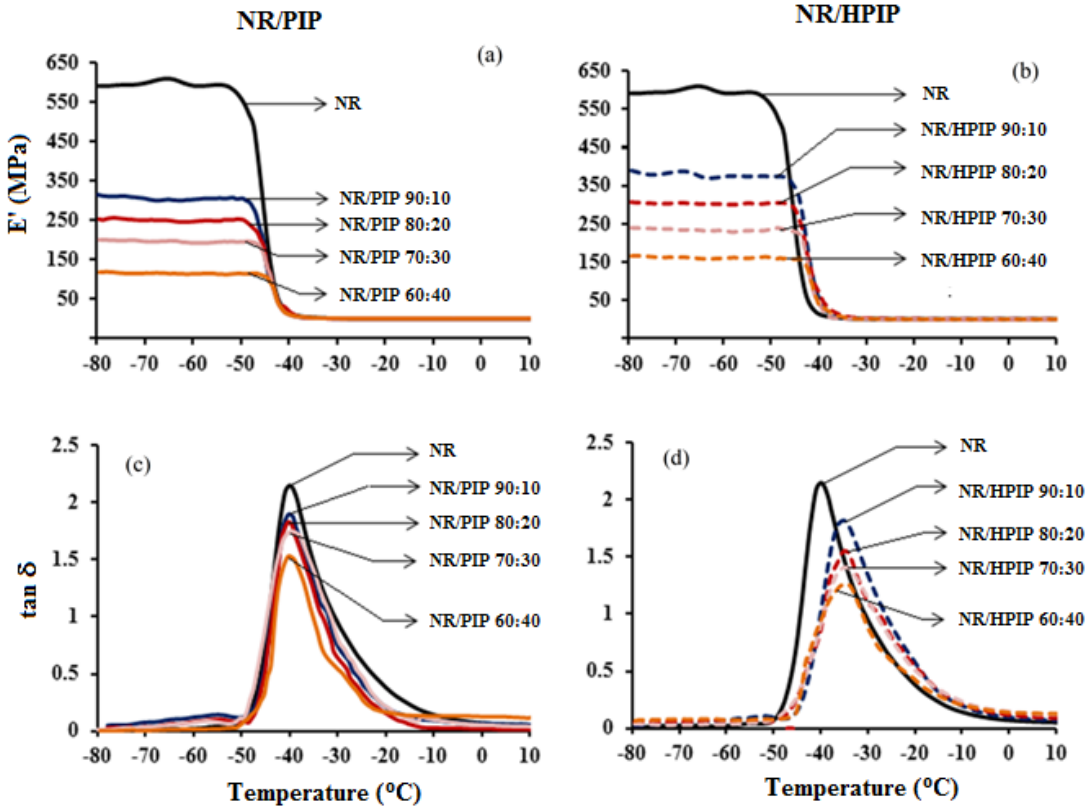

Figure 5. 1 Temperature dependence of (a) storage modulus, E', for NR/PIP blends, (b) E' for NR/HPIP blends, (c) loss tangent, tan δ for NR/PIP blends and (d) tan δ for NR/HPIP blends.

Table 5.1 Storage modulus and loss tangent of NR/PIP and NR/HPIP blends.

Rubber	NR/PIP or NR/HPIP [a]	E′ (MPa)	tan δ	T_g (°C)
NR		597.2	2.15	-39.8
NR/PIP	90/10	306.6	1.90	-40.2
	80/20	250.9	1.83	-40.3
	70/30	198.1	1.75	-39.3
	60/40	116.9	1.53	-40.2
NR/HPIP [b]	90/10	382.5	1.81	-35.9
	80/20	304.1	1.55	-35.3
	70/30	236.2	1.41	-34.3
	60/40	162.9	1.26	-34.4

[a] NR/PIP or HR/HPIP, ratio of NR to PIP or HPIP.

[b] HPIP at degree of hydrogenation 90%.

5.3 Thermal Properties of NR/PIP and NR/HPIP Blends

The TG and DTG curves for NR/PIP and NR/HPIP blends are illustrated in Figure 5.2. For unfilled NR and NR/PIP blends (Figure 5.2a and Figure5.2c), the results indicate that decomposition of the composite is an overall one-step reaction because the decomposition curve of the samples show only one-step and provide smooth weight loss curves. The DTG curve also showed one peak over the temperature range of 378-383 °C. However, for NR/HPIP blends (Figure 5.2b and Figure 5.2d), a 2-step decomposition of the composite occurred, and the DTG curve of the NR/HPIP blends showed two peaks at a temperature around 382 °C and 450 °C, respectively.

The initial decomposition temperature (T_{id}) and maximum decomposition temperature (T_{max}) of the unfilled NR, NR/PIP and NR/HPIP blends at different blend ratios are summarized in Table 5.2. The T_{id} of NR/PIP at blend ratios of 90:10, 80:20,

70:30 and 60:40 are 348.3 °C, 355.9 °C, 355.9 °C, and 355.8 °C, respectively. Similarly, the T_{id} of NR/HPIP blends at a blend ratio of 90:10, 80:20, 70:30 and 60:40 are 357.2 °C, 357.7 °C, 356.9 °C, and 356.3 °C, respectively. It is obvious that T_{id} of NR/PIP and NR/HPIP were not significantly changed compared with unfilled NR (358.0 °C). The T_{max} of NR/PIP blends (377.9-383.3 °C) and NR/HPIP blends (381.6-384.4 °C) was not significantly different from the T_{max} of unfilled NR (381.4 °C). However, according to the DTG curve, the NR/HPIP at a blend ratio of 80:20, 70:30 and 60:40 had another T_{max} of 449.5, 448.6 and 451.4 °C, respectively. This could be explained in that the second T_{max} was attributed to HPIP (Table 3.5) which had a higher maximum decomposition temperature than NR and PIP.

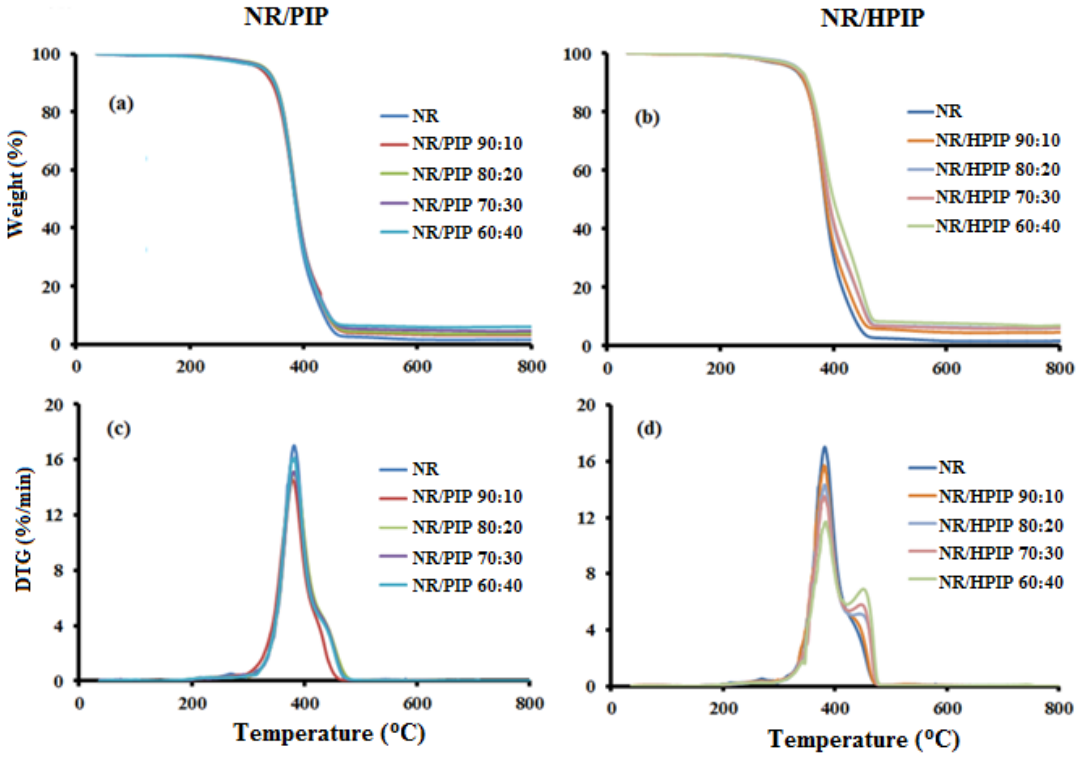

Figure 5.2 Temperature dependence of (a) weight loss for NR/PIP blends, (b) weight loss for NR/HPIP blends, (c) DTG for NR/PIP blends and (d) DTG for NR/HPIP blends.

Table 5.2 Analysis of decomposition temperature of NR/PIP and NR/HPIP blends.

Rubber	NR/PIP or NR/HPIP [a]	T_{id} (^{o}C)	T_{max1} (^{o}C)	T_{max2} (^{o}C)
NR		358.0	381.4	-
NR/PIP	90/10	348.3	377.9	-
	80/20	355.9	382.2	-
	70/30	355.9	382.2	-
	60/40	355.8	383.3	-
NR/HPIP [b]	90/10	357.2	382.6	-
	80/20	357.7	381.6	449.5
	70/30	356.9	382.0	448.6
	60/40	356.3	384.4	451.4

[a] NR/PIP or HR/HPIP, ratio of NR to PIP or HPIP.

[b] HPIP at degree of hydrogenation 90%.

5.4 Mechanical Properties of NR/PIP and NR/HPIP Blends

PIP and HPIP, by aqueous-phase hydrogenation using rhodium catalyst, were selected to blend with NRL for mechanical testing. Mechanical properties of PIP filled NR and HPIP filled NR were investigated in terms of tensile strength, modulus at 300% strain, and elongation at break. The influence of the amount of PIP and HPIP on the stress-strain behavior of NR composites was studied.

Figure 5.3(i) and Figure 5.4(i) shows the stress-strain curves before aging of PIP filled NR and HPIP filled NR (NR to PIP or NR to HPIP ratio of 100:0, 90:10, 80:20, 70:30 and 60:40), respectively. The tensile strength of NR/PIP and NR/HPIP blends decreased with an increase in PIP and HPIP ratios. The tensile strength of NR/PIP decreased by 19.4%, 28.4%, 42.2% and 60.2% from the tensile strength of unfilled NR on the addition of the PIP at a blend ratio of 90:10, 80:20, 70:30 and 60:40, respectively. In the same way, for the addition of the HPIP at a blend ratio of 90:10, 80:20, 70:30 and 60:40, the tensile strength of NR/HPIP was decreased by 26.1%,

38.9%, 59.7% and 75.8% of the tensile strength of unfilled NR, respectively. It is possible that the PIP and HPIP are incompatible with the NR due to the imbalance in the unsaturation level in the NR latex.

The modulus at 300% strain of PIP filled NR and HPIP filled NR at various blend ratios are presented in Table 5.3. The modulus at 300% strain of NR/PIP and NR/HPIP blends decreased with an increase in NR/PIP and NR/HPIP ratios. For the blend ratio of 60:40, the modulus at 300% strain of NR/PIP and NR/HPIP were found to decrease to 1.4 MPa and 0.9 MPa, respectively, compared with unfilled NR (1.7 MPa). This implied that the reduction in the modulus of NR composites was due to the low interaction between the PIP or HPIP and the NR matrix.

For the elongation at break for unfilled NR and filled NR as shown in Table 5.3, it can be seen that unfilled NR exhibited the highest elongation at break (828%). NR rich compounds possessed the highest elongation at break due to NR crystallization which resulted upon stretching. The % elongation at break decreased with an increase in PIP or HPIP amount due to the incompatibility of the filler and the NR. This phenomenon caused strain reduction of NR dominating the elongation.

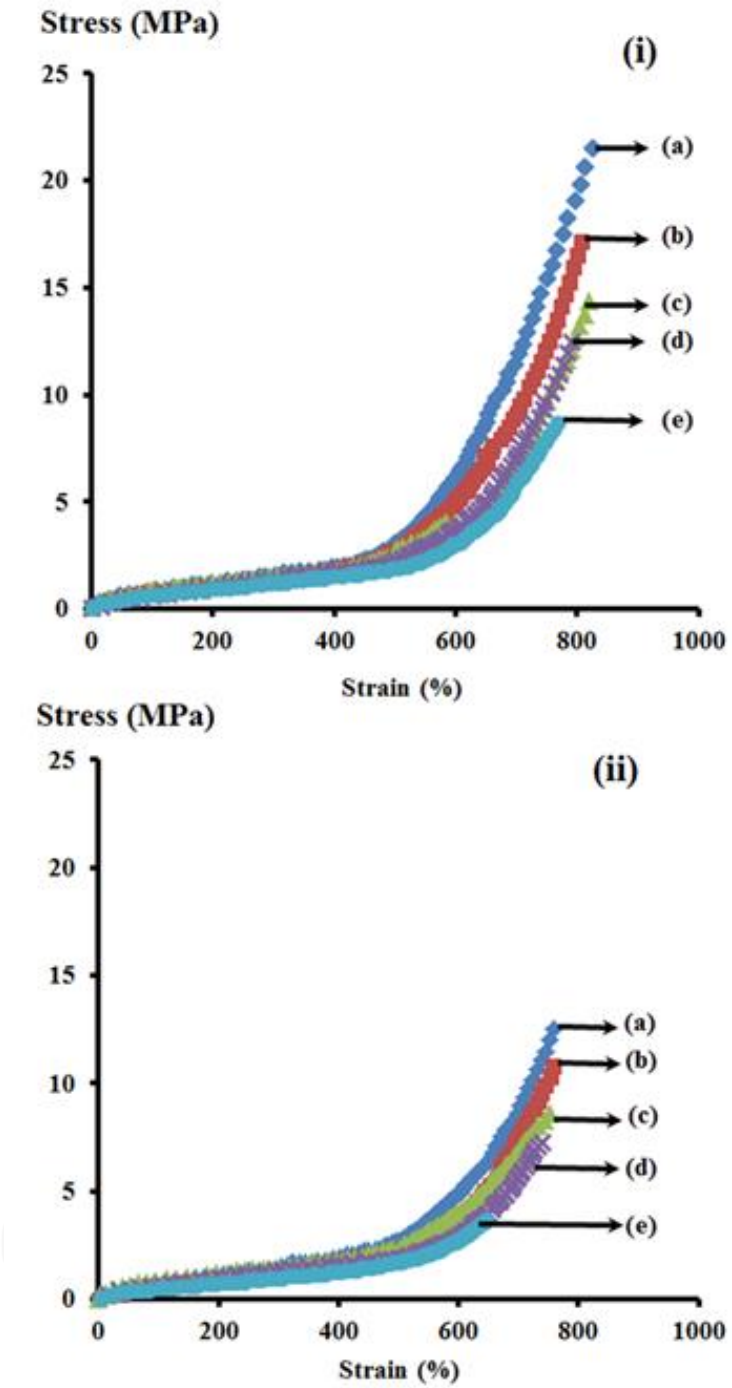

Figure 5.3 Stress-strain curve of (i) NR/PIP before ageing; (a) NR, (b) 90:10 of NR:PIP, (c) 80:20 of NR:PIP, (d) 70:30 of NR:PIP, (e) 60:40 of NR:PIP and (ii) NR/PIP after ageing.

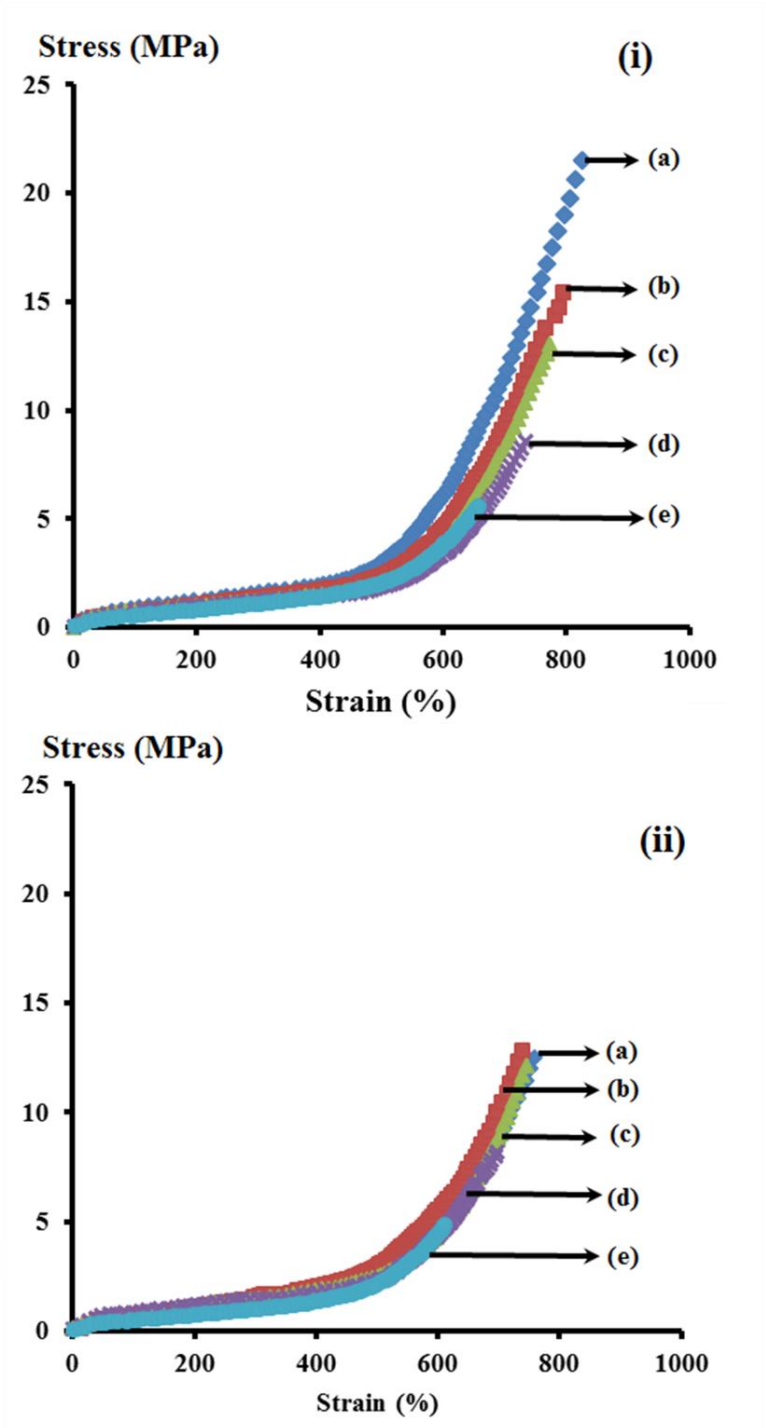

Figure 5.4 Stress-strain curve of (i) NR/HPIP before ageing; (a) NR, (b) 90:10 of NR:HPIP, (c) 80:20 of NR:HPIP, (d) 70:30 of NR:HPIP, (e) 60:40 of NR:HPIP and (ii) NR/HPIP after ageing.

5.5 Thermal Resistance of NR/PIP and NR/HPIP Blends

To investigate the thermal resistance of PIP filled NR and HPIP filled NR composites, the influence of heat ageing on the mechanical properties of NR filled with PIP and HPIP was studied as shown in Figure 5.3b and Figure 5.4b, respectively. The tensile strength of unfilled NR after heat ageing was greatly decreased from 21.1 MPa to 13.1 MPa (62.4 % retention) over the range of strain studied. Similarly, the tensile strength of NR/PIP blends, at all of blends ratios, after heat ageing were greatly decreased with a % retention of 55.7 – 61.9%. This indicated that the NR/PIP blends containing mainly the unsaturated carbon double bonds had poorer properties due to accelerated thermal ageing. For NR filled with HPIP, however, the properties did not change and retained high stress values after ageing. The % retention in tensile strength of NR/HPIP blend (82.1 – 96.5%) was much higher than that of unfilled NR (62.4%) and PIP filled NR (55.7 – 61.9%), respectively. This indicated that HPIP performed as a heat stabilizer and prevented polymer chain scission on high temperature treatment. The schematic of NR and NR/HPIP blends after thermal ageing can be described by Figure 5.5. When NR was exposed to high temperature (represented by red arrows), most polymer chain scission occurred and NR had been degraded due to low heat stability of C=C in the polymer backbone. On the other hand, for the NR/HPIP blends after heat ageing, some NR chain scission occurred but HPIP as heat stabilizer stopped the propagation of NR chain scission and retarded or stopped the degradation of the NR/HPIP blends.

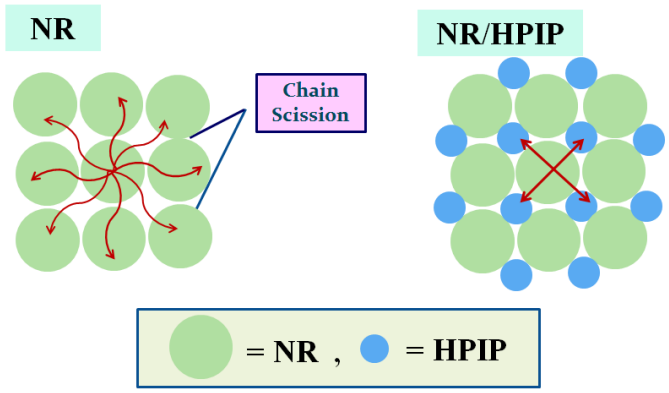

Figure 5.5 Schematic of NR and NR/HPIP blends after thermal ageing.

The percentage retention in modulus at 300% strain after ageing of PIP filled NR at various NR-to-PIP ratios remained constant (74-77%) as shown in Table 5.3. The lowest modulus retention of unfilled NR implied poor heat resistance. For NR/HPIP blends, however, the percentage retention in modulus increased up to 95% when the HPIP amount was increased up to 40 %wt. In addition, the elongation at break of HPIP filled NR after ageing slightly increased with an increase in NR/HPIP blend ratio. This can be seen in that the enhancement in ageing resistance was dominated by the addition of HPIP nanoparticles into the rubber matrix.

Table 5.3 Mechanical properties of NR/PIP and NR/HPIP blends before and after ageing.

Rubber	NR/PIP or HR/HPIP [a]	Tensile strength (MPa)			Modulus at 300% strain (MPa)			Elongation at Break (%)		
		Before ageing	After ageing	%Re [b]	Before ageing	After ageing	%Re [b]	Before ageing	After ageing	%Re [b]
NR	-	21.1 (0.8)	13.1 (0.3)	62.4	1.73 (0.06)	1.32 (0.03)	76.3	828 (11.4)	759 (11.0)	91.7
NR/PIP	90/10	17.0 (0.5)	10.5 (0.4)	61.9	1.65 (0.02)	1.25 (0.04)	75.6	810 (13.0)	758 (11.6)	93.6
	80/20	15.1 (0.3)	8.4 (0.6)	55.7	1.55 (0.07)	1.15 (0.06)	74.2	822 (14.6)	755 (10.5)	91.9
	70/30	12.2 (0.3)	7.2 (0.3)	59.1	1.58 (0.06)	1.22 (0.04)	76.8	793 (10.7)	741 (12.2)	93.4
	60/40	8.4 (0.4)	5.1 (0.5)	60.4	1.43 (0.05)	1.07 (0.13)	75.2	769 (11.9)	708 (12.5)	92.1
NR/HPIP [c]	90/10	15.6 (0.7)	12.8 (0.8)	82.1	1.51 (0.04)	1.22 (0.03)	80.8	796 (10.8)	739 (10.1)	92.8
	80/20	12.9 (0.7)	12.2 (0.3)	94.5	1.33 (0.08)	1.24 (0.08)	93.7	774 (11.1)	746 (11.6)	96.4
	70/30	8.5 (0.6)	8.2 (0.3)	96.5	1.11 (0.08)	1.07 (0.08)	96.4	734 (9.1)	698 (10.6)	95.1
	60/40	5.1 (0.4)	4.9 (0.4)	95.6	0.86 (0.12)	0.81 (0.13)	94.6	638 (11.5)	615 (15.6)	96.3

Ageing conditions: 100°C under air atmosphere for 24 h.

[a] NR/PIP or HR/HPIP, ratio of NR to PIP or HPIP.

[b] %Re, %Retention = (Properties after ageing/Properties before ageing) x 100.

[c] HPIP at degree of hydrogenation 90%.

5.6 Surface Morphology of NR/PIP and NR/HPIP Blends

The NR/PIP and NR/HPIP blends at higher blend ratio had a lower tensile strength. This could be explained in that the PIP and HPIP is incompatible with the NR. This result was also confirmed by SEM. The surface morphology of unfilled NR and filled NR before and after ageing was characterized by SEM as shown in Figure 5.6. It can be seen that the surface of the unfilled NR before and after ageing was smooth (Figure 5.6a and Figure 5.6b). For the effect of thermal ageing on surface morphology of NR/PIP and NR/HPIP blends (Figure 5.6 and Figure 5.7), the surface of all the rubber blends, at each blend ratio, after thermal ageing tended to be smoother than the surface before ageing.

For the addition of PIP into the NR matrix before ageing, SEM micrographs show that NR filled with PIP had a rough surface on the NR sample. Moreover, the roughness of the NR surface tended to increase with an increasing blend ratio (Figure 5.6c, e, g and i). For NR/PIP blends after ageing, the roughness of the surface also increased with an increasing NR/PIP blend ratio (Figure 5.6d, f, h and j). For NR/HPIP blends before ageing, similarly, SEM micrographs show that the roughness of NR filled with HPIP occurred on the NR surface, and tended to increase with increasing blend ratio (Figure 5.7c, e, g and i). For the NR/HPIP blends surface after ageing, the roughness also increased with increasing NR/HPIP blend ratio (Figure 5.7d, f, h and j). This could be explained in that PIP and HPIP in rubber blends may aggregate within the NR matrix, and thus phase separation and poor interaction occurs due to an incompatibility between the PIP, HPIP and the nonpolar NR chain. In addition, for rubber blends at a blend ratio of 80:20, the surface of NR/PIP (Figure 5.6e) was smoother than that of NR/HPIP (Figure 5.7e). The result shows that HPIP has a poor interaction with NR compared with PIP due to the incompatibility and the different morphology of HPIP and NR.

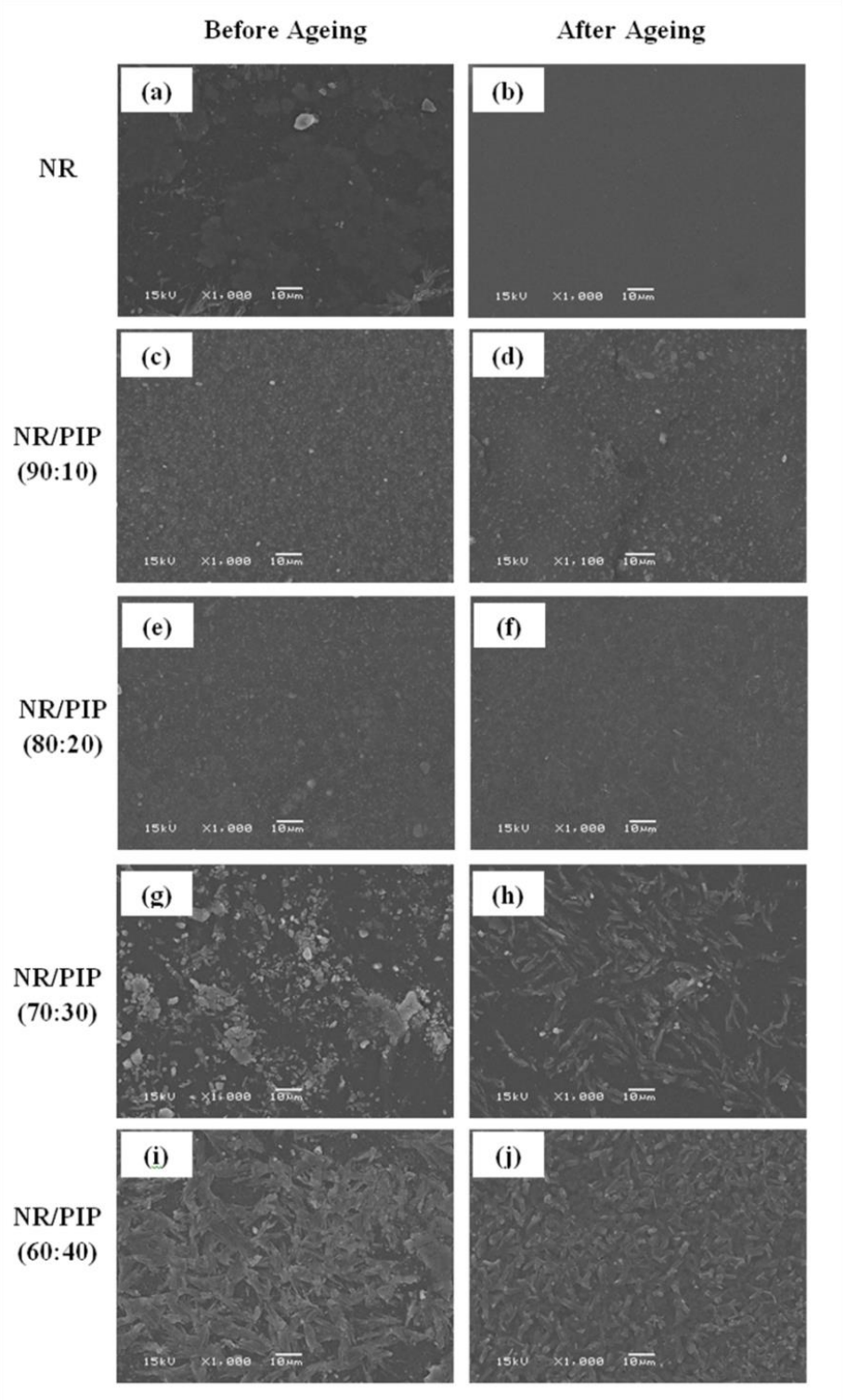

Figure 5.6 SEM micrographs of samples before and after ageing (x 1000). (a) NR, (b) aged NR, (c) NR/PIP (90:10), (d) aged NR/PIP (90:10), (e) NR/PIP (80:20), (f) aged NR/PIP (80:20), (g) NR/PIP (70:30), (h) aged NR/PIP (70:30), (i) NR/PIP (60:40), (j) aged NR/PIP (60:40).

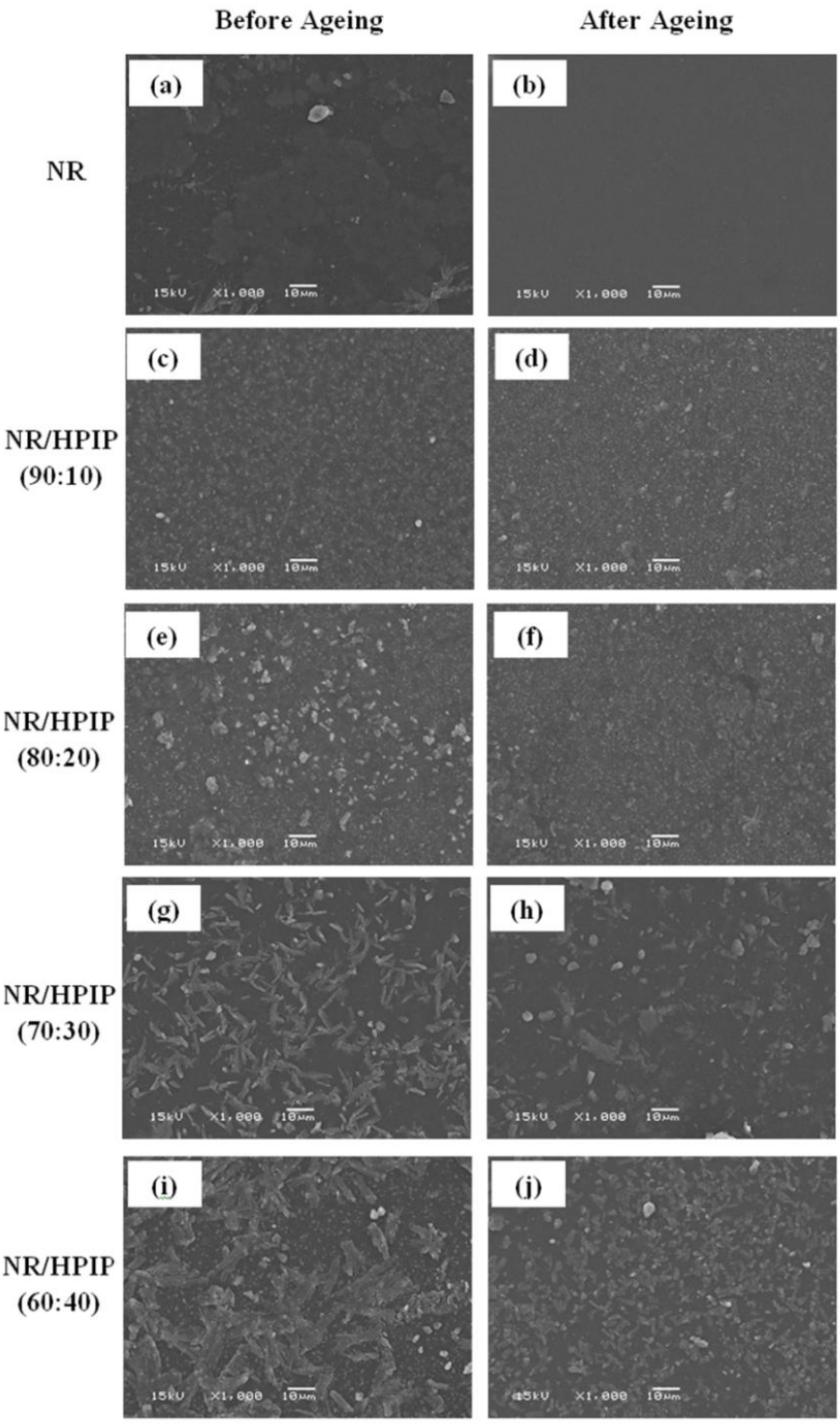

Figure 5.7 SEM micrographs of samples before and after ageing (x 1000). (a) NR, (b) aged NR, (c) NR/HPIP (90:10), (d) aged NR/HPIP (90:10), (e) NR/HPIP (80:20), (f) aged NR/HPIP (80:20), (g) NR/HPIP (70:30), (h) aged NR/HPIP (70:30), (i) NR/HPIP (60:40), (j) aged NR/HPIP (60:40).

5.7 Ozone Resistance of NR/PIP and NR/HPIP Blends

Many elastomers are vulnerable to degradation by ozone. The susceptibility to ozonation is due to the double bonds in the unsaturated rubber. This is also in the case for NR. To improve the ozone degradation of NR, HPIP may be an effective filler in NR. Optical photographs of the surfaces of the NR/PIP and NR/HPIP blend after ozone exposure for 72 h are shown in Figure 5.8. The photograph of unfilled NR showed macroscopic cracks (C-4 type) and numerous vertical cracking lines on the surface (Figure 5.8a). Similarly, the C-4 type cracking after 72 h also occurred for NR/PIP at blend ratio of 90:10, 80:20 and 70:30, as shown in Figure 5.8b-d. The appearance of ozone cracking was evident for the degradation of unfilled NR and NR/PIP blends. It is possible that the growth of surface cracks by ozonolysis was initiated from the rubber matrix and the PIP filler, and grew over the critical length resulting in failure. The ozonolysis is assumed to follow a bimolecular law, where each C=C bond functions as an independent kinetic unit (26–28). In addition, ozone also attacks, though more slowly, polymers containing hydrogen atoms. However, the reaction between ozone and the C–H bond is much slower than that between ozone and the C=C bond [72, 73].

On the other hand, all NR/HPIP blends showed better resistance towards ozone exposure compared with unfilled NR for a 72 h exposure. The NR/HPIP blends at ratios of 90:10, 80:20 and 70:30 exhibited less cracking of C-2, B-3 and B-2, respectively (Figure 5.8e-g). It is obvious that the ozone resistance of NR at high HPIP loading was much better than that of the unfilled NR due to the suppression of crack growth. It can be concluded that the incorporation of the HPIP could retard the surface cracking, resulting in more ozone resistance of the NR/HPIP blends.

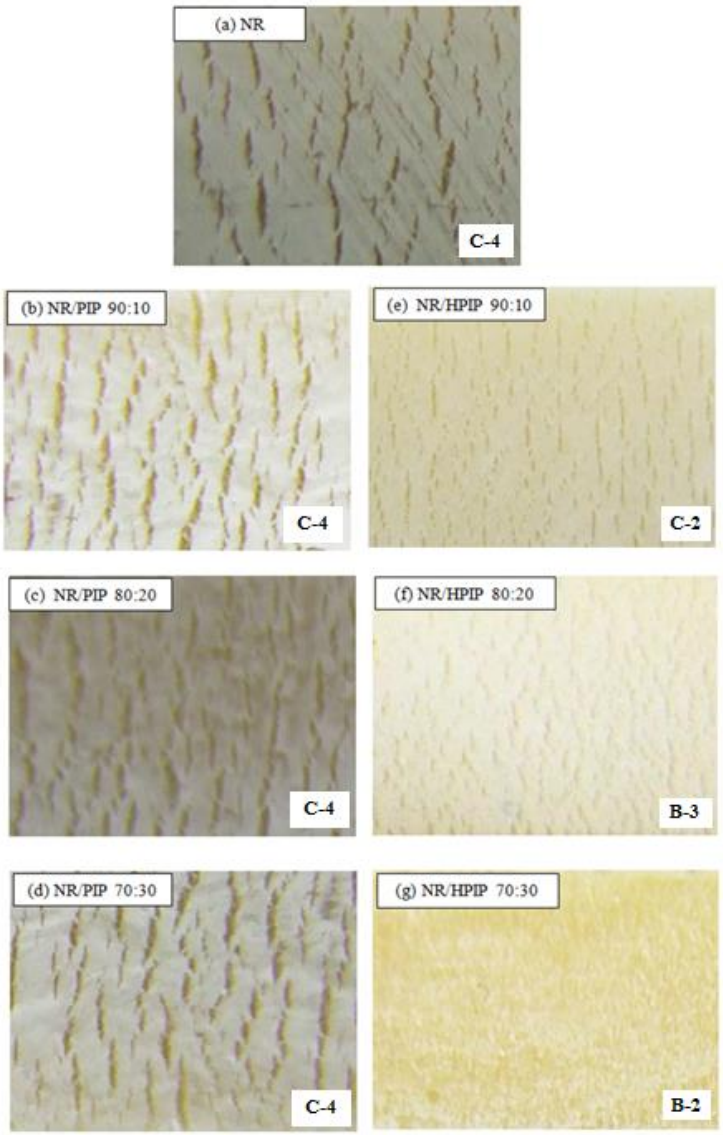

Figure 5.8 Surface of NR/PIP and NR/HPIP blends at various blend ratios after ozone exposure for 72 h. (a) NR, (b) NR/PIP (90:10), (c) NR/HPIP (90:10), (d) NR/PIP (80:20), (e) NR/HPIP (80:20), (f) NR/PIP (70:30), (g) NR/HPIP (70:30).

*Classification of cracking on the surface of rubber specimen are shown in Appendix E.

CHAPTER VI

CONCLUSIONS AND RECOMMENDATIONS

6.1 Conclusions

(i) Aqueous-Phase Hydrogenation of Nanosized Polyisoprene Emulsions Using Rhodium Catalysts

A high degree of hydrogenation (upto 90%) has been achieved for the hydrogenation of PIP employing water-soluble rhodium complexes in aqueous media, especially using $RhCl_3$/TPPMS as the catalyst precursor, while low conversion of carbon-carbon double bonds was obtained using $RhCl_3$/TPPTS as the catalyst. A Hartley ionic spherical micelle model was proposed to rationalize the observed results that the high polarity of TPPTS forces the rhodium atom to locate on the Stern layer despite the polymer micelle core.

Kinetic studies for the aqueous-phase hydrogenation of nanosized PIP showed that the reaction was first order with respect to [C=C]. The rate for the aqueous-phase hydrogenation catalyzed by $RhCl_3$/TPPMS increased with increasing catalyst concentration, reaction temperature and hydrogen pressure. The apparent activation energy for the hydrogenation of PIP was then calculated to be 117.0 kJ/mol. However, increasing the particle size of PIP had a negative effect on the hydrogenation rate, which can be explained in that the rhodium catalyst transferred through the smaller particles at a higher rate than through the larger particles of PIP.

For the thermal and dynamic mechanical properties of rubbers, an increase in the degradation temperature of the HPIP indicated that the hydrogenation increased the thermal stability of PIP. In addition, the HPIP had the highest storage modulus (231 MPa) owing to replacement of polyisoprene by ethylene-propylene units in the structure of HPIP. Thus, catalytic hydrogenation in aqueous media provides a method to improve the thermal stability and dynamic mechanical properties of polyisoprene.

(ii) Aqueous-Phase Hydrogenation of Natural Rubber Latex Using Rhodium Catalysts

For the organic solvent-free hydrogenation of NR and nanosized PIP catalyzed by water-soluble rhodium complexes, especially when using $RhCl_3$/TPPMS as a catalyst precursor, high degrees of hydrogenation (HD) of NR (85.8%) and PIP (89.7%) were achieved. However, hydrogenation using $RhCl_3/PPh_3$ or $RhCl_3$/TPPTS as a catalyst yielded lower HD for both polymers. A Hartley ionic spherical micelle model was applied to explain the observed results. The rhodium atom with the TPPMS ligand was located in a polymer micelle core layer despite being transferred to the Stern layer due to the low polarity of TPPMS.

For hydrogenation catalyzed by $RhCl_3$/TPPMS in the absence of organic solvent, an increase in the catalyst concentration, hydrogen pressure and reaction temperature had a beneficial effect on the NR and PIP hydrogenation and the highest HD (86% for NR and 90% for PIP) was achieved under an optimal condition. Moreover, the catalyst activity of $RhCl_3$/TPPMS in NR hydrogenation was lower than that for PIP hydrogenation for all conditions due to impurities, e.g. protein at the ω-terminal group of the NR structure in the latex.

For the thermal and dynamic mechanical properties of rubbers, thermal stability of HNR was improved, as shown by an increase in the maximum degradation temperature at 466 °C compared with the maximum degradation temperature of NR at 382 °C. Moreover, the HNR had the highest storage modulus of 429 MPa due to substitution of C=C unsaturation units with ethylene-propylene segments. Therefore, it can be generally concluded that the thermal stability and dynamic mechanical properties of NR as a "green polymer" can be improved by aqueous-phase hydrogenation as a "green process" which may lead to an alternative way in the future for the realization of a commercial process for green latex hydrogenation.

(iii) Mechanical Properties of NR/PIP and NR/HPIP Blends

In this work, the dynamic mechanical properties and thermal properties of NR/PIP blends and NR/HPIP blends was studied. The mechanical properties, thermal

resistance and ozone resistance of NR/PIP and NR/HPIP blends were also investigated.

For the dynamic mechanical analysis, the storage modulus of NR/PIP and NR/HPIP blends decreased with increasing PIP and HPIP amount due to the increase in free volume of the NR matrix. Moreover, for the same blend ratio, the storage modulus of the NR/HPIP blends were higher than that of the NR/PIP blends which led to an increase in the stiffness of the NR/HPIP blends. For the thermal properties of rubber blends, NR/HPIP blend had two maximum decomposition temperatures of 382 ºC and 450 ºC attributed to NR and HPIP, respectively, while NR/PIP blend had only one maximum decomposition temperature of 382 ºC a attributed to NR and PIP.

For the SEM micrographs, the roughness of the NR/PIP and NR/HPIP blends surface tended to increase with increasing PIP and HPIP content. This could be explained by an incompatibility among PIP, HPIP and the nonpolar NR chain. In addition, the surface of NR/PIP tended to be smoother than that of NR/HPIP. The results showed that HPIP had lower interaction with NR compared with PIP due to the incompatibility and the different morphology of NR and HPIP.

For the mechanical properties of NR/PIP and NR/HPIP blends, the tensile strength and modulus of the blends were lower than those of unfilled NR. Moreover, an increasing amount of PIP or HPIP tended to have a negative effect on mechanical properties, indicating that incompatibility among PIP, HPIP and NR occurred which resulted in an imbalance in the NR matrix.

However, the stability of the NR/HPIP blends after thermal ageing increased, maintaining 96% retention of their tensile strength and 94% retention of their modulus. With the reversed was observed for the mechanical properties of NR/PIP blends after thermal ageing (at 62% retention). In addition, incorporation of HPIP in NR could retard ozone-induced degradation resulting in an improvement of ozone resistance at the surface. Thus it can be concluded that HPIP can be used as a heat stabilizer and ozone resistant substance for NR composites to prevent polymer degradation at high temperature and ozone treatment.

6.2 Recommendations

A further study of the aqueous-phase hydrogenation of NR should be concerned with the following aspects:

1. The non-rubber contaminants including protein, which may act as the inhibitors, could affect the catalyst activity of hydrogenation. Therefore, the pretreatment of NR latex by deproteinization or neutralizing the impurities by adding *p*-toluenesulfonic acid should be further studied.
2. It is clear that a high hydrogenation degree and thermal stability of PIP and NR have been achieved for hydrogenation in aqueous media. Therefore, aqueous-phase hydrogenation of other elastomers such as polybutadiene rubber (PB) and styrene-butadiene rubber (SBR) in latex form should be further studied.

Although the heat and ozone resistance of vulcanized NR was improved by blending with HPIP, the mechanical properties of blends tended to be decreased. Therefore, mechanical properties improvement by adding a stiffness filler, such as silica or montmorillonite, should be further studied.

REFERENCES

[1] Morton, M. Rubber Technology. New York: Van Nostrand Reinhold Company, 1973.

[2] Anastas, P., and Warner, J. Green Chemistry: Theory and Practice. New York: Oxford University Press, 1998.

[3] Anastas, P.T., and Zimmerman, J.B. Design through the Twelve Principles of Green Engineering. Environmental Science and Technology 37 (2003): 94A-101A.

[4] Crabtree, R.H., and Mingos, D.M.P. Comprehensive Organometallic Chemistry III: From Fundamentals to Applications. Amsterdam: Elsevier, 2007.

[5] Browning, E. Toxic Solvents: A Review. British Journal of Industrial Medicine 16 (1959): 23-39.

[6] Rideout, D.C., and Breslow, R. Hydrophobic acceleration of Diels-Alder reactions. Journal of the American Chemical Society 102 (1980): 7816-7817.

[7] Thai Rubber Statistics. Gross Exports of Natural Rubber 2002-2010 [online]. Available from: http://www.thainr.com/en/detail-stat.php?statID=171 [2013, July, 23].

[8] Tarachiwin, L., Sakdapipanich, J., Ute, K., Kitayama, T., and Tanaka, Y. Structural Characterization of **α**-Terminal Group of Natural Rubber. 2. Decomposition of Branch-Points by Phospholipase and Chemical Treatments. Biomacromolecules 6 (2005): 1858-1863.

[9] Fisher, H.L. Chemistry of natural and synthetic rubber. New York: Reinhold Publishing Corporation, 1975.

[10] Tangpakdee, J., and Tanaka, Y. Characterization of sol and gel in *Hevea* natural rubber. Rubber Chemical Technology 70 (1997): 707-713.

[11] Allen, P.W., and Bristow, G.M. The gel phase in natural rubber. Journal of Applied Polymer Science 7 (1963): 603-615.

[12] Tangpakdee, J., and Tanaka, Y. Purification of natural rubber. Journal of Natural Rubber Research 12 (1997): 112-119.

[13] Schulz, D.N., Turner, S.R., and Golub, M.A. Recent Advances in the Chemical Modification of Unsaturated Polymers. Rubber Chemistry and Technology 55 (1982): 809-859.

[14] Schulz, D.N. Chemical modification of unsaturated polymer. Encyclopedia of Polymer 7 (1982): 7-12

[15] McManus, N.T., and Rempel, G.L. Chemical Modification of Polymers: Catalytic Hydrogenation and Related Reactions. Journal of Macromolecular Science, Part C 35 (1995): 239-285.

[16] Wideman, L.G. Process for hydrogenation of carbon-carbon double bonds in an unsaturated polymer in latex form. 4,452,950; 1984

[17] Parker, D.K.R., D.M. Process for the preparation of hydrogenated rubber. *Pat., U.S.* 5,424,356; 1995

[18] Zhou, S., Bai, H., and Wang, J. Hydrogenation of acrylonitrile–butadiene rubber latexes. Journal of Applied Polymer Science 91 (2004): 2072-2078.

[19] Mahittikul, A., Prasassarakich, P., and Rempel, G.L. Diimide hydrogenation of natural rubber latex. Journal of Applied Polymer Science 105 (2007): 1188-1199.

[20] Parker, D.K., Roberts, R.F., and Schiessl, H.W. A New Process for the Preparation of Highly Saturated Nitrile Rubber in Latex Form. Rubber Chemistry and Technology 65 (1992): 245-258.

[21] Simma, K., Rempel, G.L., and Prasassarakich, P. Improving thermal and ozone stability of skim natural rubber by diimide reduction. Polymer Degradation and Stability 94 (2009): 1914-1923.

[22] Xie, H.-Q., Li, X.-D., and Guo, J.-S. Hydrogenation of nitrile–butadiene rubber latex to form thermoplastic elastomer with excellent thermooxidation resistance. Journal of Applied Polymer Science 90 (2003): 1026-1031.

[23] Lin, X., Pan, Q., and Rempel, G.L. Hydrogenation of nitrile-butadiene rubber latex with diimide. Applied Catalysis A: General 276 (2004): 123-128.

[24] He, Y., Daniels, E.S., Klein, A., and El-Aasser, M.S. Hydrogenation of styrene-butadiene rubber (SBR) latexes. Journal of Applied Polymer Science 64 (1997): 2047-2056.

[25] Sumit Bhaduri, D.M. Homogeneous Catalysis: Mechanisms and Industrial Applications. New Jersey: Wiley & Sons, Inc., 2000.

[26] Mohammadi, N.A., and Rempel, G.L. Homogeneous catalytic hydrogenation of polybutadiene. Journal of Molecular Catalysis 50 (1989): 259-275.

[27] Šabata, S., and Hetflejš, J. Hydrogenation of low molar mass OH-telechelic polybutadienes catalyzed by homogeneous Ziegler nickel catalysts. Journal of Applied Polymer Science 85 (2002): 1185-1193.

[28] Rao, P.V.C., Upadhyay, V.K., and Pillai, S.M. Hydrogenation of polybutadienes catalyzed by $RuCl_2(PPh_3)_3$ and a structural study. European Polymer Journal 37 (2001): 1159-1164.

[29] Tsiang, R.C., Yang, W., and Tsai, M. Hydrogenation of polystyrene-*b*-polybutadiene-b-polystyrene block copolymers using a metallocene/n-butyllithium catalyst – the role of n-butyllithium. Polymer 40 (1999): 6351-6360.

[30] Escobar Barrios, V.A., Herrera Nájera, R., Petit, A., and Pla, F. Selective hydrogenation of butadiene–styrene copolymers using a Ziegler–Natta type catalyst: 1. Kinetic study. European Polymer Journal 36 (2000): 1817-1834.

[31] Guo, X., Scott, P.J., and Rempel, G.L. Catalytic hydrogenation of diene polymers : Part II. Kinetic analysis and mechanistic studies on the hydrogenation of styrene--butadiene copolymers in the presence of $RhCl(PPh_3)_3$. Journal of Molecular Catalysis 72 (1992): 193-208.

[32] Bhattacharjee, S., Bhowmick, A.K., and Avasthi, B.N. High-pressure hydrogenation of nitrile rubber: thermodynamics and kinetics. Industrial & Engineering Chemistry Research 30 (1991): 1086-1092.

[33] Mao, T.-F., and Rempel, G.L. Catalytic hydrogenation of nitrile-butadiene copolymers by cationic rhodium complexes. Journal of Molecular Catalysis A: Chemical 135 (1998): 121-132.

[34] Parent, J.S., McManus, N.T., and Rempel, G.L. $RhCl(PPh_3)_3$ and $RhH(PPh_3)_4$ Catalyzed Hydrogenation of Acrylonitrile–Butadiene Copolymers. Industrial & Engineering Chemistry Research 35 (1996): 4417-4423.

[35] Martin, P., McManus, N.T., and Rempel, G.L. A detailed study of the hydrogenation of nitrile-butadiene rubber and other substrates catalyzed by Ru(II) complexes. Journal of Molecular Catalysis A: Chemical 126 (1997): 115-131.

[36] Guo, X.-Y., and Rempel, G.L. Catalytic hydrogenation of nitrile–butadiene copolymer emulsion. Journal of Applied Polymer Science 65 (1997): 667-675.

[37] Tangthongkul, R., Prasassarakich, P., and Rempel, G.L. Hydrogenation of natural rubber with $Ru[CH=CH(Ph)]Cl(CO)(PCy_3)_2$ as a catalyst. Journal of Applied Polymer Science 97 (2005): 2399-2406.

[38] Hinchiranan, N., Prasassarakich, P., and Rempel, G.L. Hydrogenation of natural rubber in the presence of $OsHCl(CO)(O_2)(PCY_3)_2$: Kinetics and mechanism. Journal of Applied Polymer Science 100 (2006): 4499-4514.

[39] Mahittikul, A., Prasassarakich, P., and Rempel, G.L. Hydrogenation of natural rubber latex in the presence of $OsHCl(CO)(O_2)(PCy_3)_2$. Journal of Applied Polymer Science 100 (2006): 640-655.

[40] Kongparakul, S., Prasassarakich, P., and Rempel, G.L. Catalytic hydrogenation of methyl methacrylate-*g*-natural rubber (MMA-*g*-NR) in the presence of $OsHCl(CO)(O_2)(PCy_3)_2$. Applied Catalysis A: General 344 (2008): 88-97.

[41] Kongparakul, S., Prasassarakich, P., and Rempel, G.L. Catalytic hydrogenation of styrene-*g*-natural rubber (ST-*g*-NR) in the presence of $OsHCl(CO)(O_2)(PCy_3)_2$. European Polymer Journal 45 (2009): 2358-2373.

[42] Singha, N.K., De, P.P., and Sivaram, S. Homogeneous catalytic hydrogenation of natural rubber using $RhCl(PPh_3)_3$. Journal of Applied Polymer Science 66 (1997): 1647-1652.

[43] Mohammadi, N.A., and Rempel, G.L. Control, data acquisition and analysis of catalytic gas—liquid mini slurry reactors using a personal computer. Computers & Chemical Engineering 11 (1987): 27-35.

[44] Parent, J.S., McManus, N.T., and Rempel, G.L. Selectivity of the $OsHCl(CO)(O_2)(PCy_3)_2$ catalyzed hydrogenation of nitrile–butadiene rubber. Journal of Applied Polymer Science 79 (2001): 1618-1626.

[45] Tangthongkul, R., Prasassarakich, P., McManus, N.T., and Rempel, G.L. Hydrogenation of *cis*-1,4-polyisoprene catalyzed by $Ru(CH=CH(Ph))Cl(CO)(PCy_3)_2$. Journal of Applied Polymer Science 91 (2004): 3259-3273.

[46] Mohammadi, N.A., and Rempel, G.L. Homogeneous selective catalytic hydrogenation of C=C in acrylonitrile-butadiene copolymer. Macromolecules 20 (1987): 2362-2368.

[47] Singha, N.K., Talwar, S.S., and Sivaram, S. Solution Hydrogenation of Chloroprene Rubber Using a Wilkinson Catalyst. Macromolecules 27 (1994): 6985-6987.

[48] Joó, F. Aqueous Biphasic Hydrogenations. Accounts of Chemical Research 35 (2002): 738-745.

[49] Singha, N.K., Sivaram, S., and Talwar, S.S. A New Method to Hydrogenate Nitrile Rubber in the Latex Form. Rubber Chemistry and Technology 68 (1995): 281-286.

[50] Mudalige, D.C., and Rempel, G.L. Aqueous-phase hydrogenation of polybutadiene, styrene-butadiene, and nitrile-butadiene polymer emulsions catalyzed by water-soluble rhodium complexes. Journal of Molecular Catalysis A: Chemical 123 (1997): 15-20.

[51] Kotzabasakis, V., Georgopoulou, E., Pitsikalis, M., Hadjichristidis, N., and Papadogianakis, G. Catalytic conversions in aqueous media: a novel and efficient hydrogenation of polybutadiene-1,4-*block*-poly(ethylene oxide) catalyzed by Rh/TPPTS complexes in mixed micellar nanoreactors. Journal of Molecular Catalysis A: Chemical 231 (2005): 93-101.

[52] Kotzabasakis, V., Hadjichristidis, N., and Papadogianakis, G. Catalytic conversions in aqueous media: Part 3. Biphasic hydrogenation of polybutadiene catalyzed by Rh/TPPTS complexes in micellar systems. Journal of Molecular Catalysis A: Chemical 304 (2009): 95-100.

[53] Wei, Z., Wu, J., Pan, Q., and Rempel, G.L. Direct Catalytic Hydrogenation of an Acrylonitrile-Butadiene Rubber Latex Using Wilkinson's Catalyst. Macromolecular Rapid Communications 26 (2005): 1768-1772.

[54] Wang, H., Yang, L., Scott, S., Pan, Q., and Rempel, G.L. Organic solvent-free catalytic hydrogenation of diene-based polymer nanoparticles in latex form. Part II. Kinetic analysis and mechanistic study. Journal of Polymer Science Part A: Polymer Chemistry 50 (2012): 4612-4627.

[55] Suppaibulsuk, B., Prasassarakich, P., and Rempel, G.L. Factorial design of nanosized polyisoprene synthesis via differential microemulsion polymerization. Polymers for Advanced Technologies 21 (2010): 467-475.

[56] Papadogianakis, G., Verspui, G., Maat, L., and Sheldon, R.A. Catalytic conversions in water. Part 6. A novel biphasic hydrocarboxylation of olefins catalyzed by palladium TPPTS complexes (TPPTS=$P(C_6H_4$-m-$SO_3Na)_3$). Catalysis Letters 47 (1997): 43-46.

[57] Anastas, P.T., and Kirchhoff, M.M. Origins, Current Status, and Future Challenges of Green Chemistry†. Accounts of Chemical Research 35 (2002): 686-694.

[58] Gómez-Cisneros, M., Treviño, M.E., Peralta, R.D., Rabelero, M., Mendizábal, E., Puig, J.E., Cesteros, C., and López, R.G. Surfactant concentration effects on the microemulsion polymerization of vinyl acetate. Polymer 46 (2005): 2900-2907.

[59] Capek, I., Lin, S.-Y., Hsu, T.-J., and Chern, C.-S. Effect of temperature on styrene emulsion polymerization in the presence of sodium dodecyl sulfate. II. Journal of Polymer Science Part A: Polymer Chemistry 38 (2000): 1477-1486.

[60] He, G., Pan, Q., and Rempel, G.L. Synthesis of Poly(methyl methacrylate) Nanosize Particles by Differential Microemulsion Polymerization. Macromolecular Rapid Communications 24 (2003): 585-588.

[61] Drexler, K., Meisel, R., Grassert, I., Paetzold, E., Fuhrmann, H., and Oehme, G. Influence of poly(ethylene oxide)-poly(propylene oxide)-poly(ethylene oxide) triblock copolymers on stereoselective catalysis in water. Macromolecular Chemistry and Physics 201 (2000): 1436-1441.

[62] Grassert, I., Vill, V., and Oehme, G. Investigation of the influence of carbohydrate amphiphiles on the complex catalysed asymmetric hydrogenation of (Z)-methyl α-acetamidocinnamate in water. Journal of Molecular Catalysis A: Chemical 116 (1997): 231-236.

[63] Parac-Vogt, Tatjana N., Kimpe, K., Laurent, S., Piérart, C., Elst, Luce V., Muller, Robert N., and Binnemans, K. Gadolinium DTPA-Monoamide Complexes Incorporated into Mixed Micelles as Possible MRI Contrast Agents. European Journal of Inorganic Chemistry 2004 (2004): 3538-3543.

[64] Vangelis, C., Bouriazos, A., Sotiriou, S., Samorski, M., Gutsche, B., and Papadogianakis, G. Catalytic conversions in green aqueous media: Highly efficient biphasic hydrogenation of benzene to cyclohexane catalyzed by Rh/TPPTS complexes. Journal of Catalysis 274 (2010): 21-28.

[65] Charmondusit, K., Prasassarakich, P., McManus, N.T., and Rempel, G.L. Hydrogenation of *cis*-1,4-poly(isoprene) catalyzed by $OsHCl(CO)(O_2)(PCy_3)_2$. Journal of Applied Polymer Science 89 (2003): 142-152.

[66] Kongsinlark, A., Rempel, G.L., and Prasassarakich, P. Synthesis of nanosized ethylene–propylene rubber latex via polyisoprene hydrogenation. Journal of Applied Polymer Science 127 (2013): 3622-3632.

[67] Samran, J., Phinyocheep, P., Daniel, P., and Kittipoom, S. Hydrogenation of unsaturated rubbers using diimide as a reducing agent. Journal of Applied Polymer Science 95 (2005): 16-27.

[68] Hinchiranan, N., Charmondusit, K., Prasassarakich, P., and Rempel, G.L. Hydrogenation of synthetic *cis*-1,4-polyisoprene and natural rubber catalyzed by $[Ir(COD)py(PCy_3)]PF_6$. Journal of Applied Polymer Science 100 (2006): 4219-4233.

[69] Ahlford, K., Lind, J., Maler, L., and Adolfsson, H. Rhodium-catalyzed asymmetric transfer hydrogenation of alkyl and aryl ketones in aqueous media. Green Chemistry 10 (2008): 832-835.

[70] Hinchiranan, N., Lertweerasirikun, W., Poonsawad, W., Rempel, G.L., and Prasassarakich, P. Cure characteristics and mechanical properties of hydrogenated natural rubber/natural rubber blends. Journal of Applied Polymer Science 111 (2009): 2813-2821.

[71] Hinchiranan, N., Lertweerasirikun, W., Poonsawad, W., Rempel, G.L., and Prasassarakich, P. Hydrogenated natural rubber blends: Aspect on thermal stability and oxidative behavior. Journal of Applied Polymer Science 113 (2009): 1566-1575.

[72] Razumovsky, S.D., and Zaikov, G.E. Degradation & protection of polymeric materials in ozone. Developments in polymer stabilisation. in: G, S., (Ed.), Applied Science Publishers: London & New York, 1983: 239-93.

[73] Razumovsky, S.D., Podmasteriyev, V.V., and Zaikov, G. Kinetics of the growth of cracks on polyisoprene vulcanizates in ozone. Polymer Degradation and Stability 16 (1986): 317-324.

APPENDICES

APPENDIX A

Calculation of % Hydrogenation

cis-1,4 polyisoprene (Species 1)

Hydrogenated polyisoprene (Species 2)

Proton of repeating unit except =CH in Species 1 = 7 protons

Proton of repeating unit in Species 2 = 10 protons

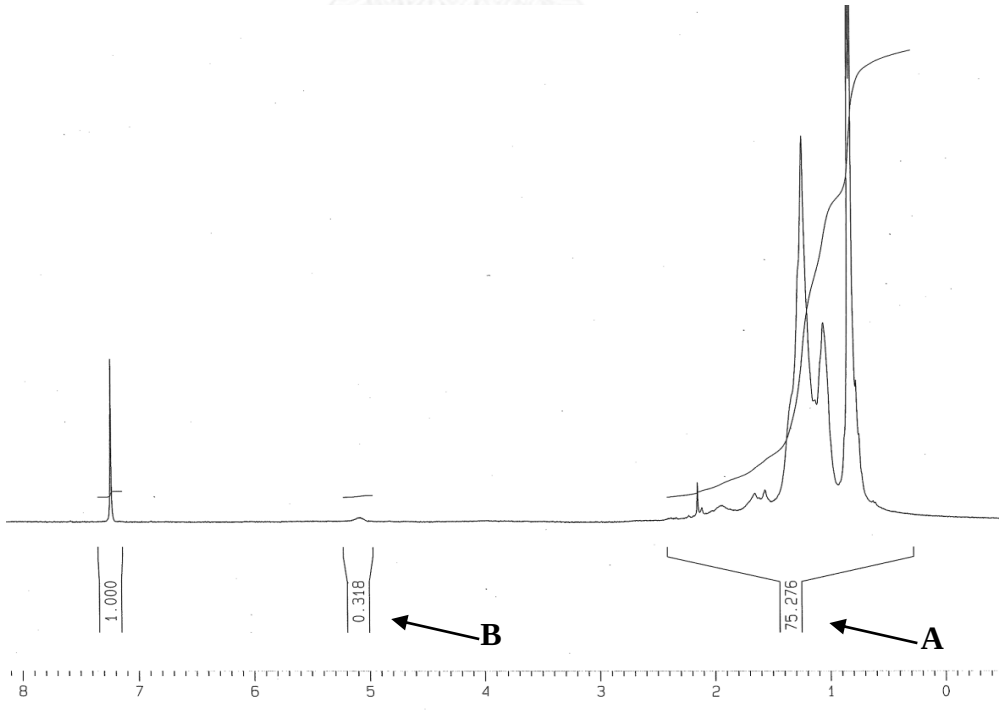

where A = Peak area except at 5.2 ppm

B = Peak area at 5.2 ppm

C = Peak area of saturated $-CH_2-$ and $-CH_3$

Hence, A = 10C + 7B

C = (A - 7B)/10

Total peak area = (Peak area of saturated $-CH_2-$ and $-CH_3$) + (Peak area at 5.2 ppm)

= [(A - 7B)/10] +B

= (A + 3B)/10

%Hydrogenation = [(Peak area of saturated $-CH_2$ and $-CH_3$)/(Total peak area)] ×100

$$= \frac{(A-7B)/10}{(A+3B)/10} \times 100$$

$$= \frac{(A-7B)}{(A+3B)} \times 100$$

For example: A = 75.276 and B = 0.318

$$\text{\% Hydrogenation} = \frac{[\,75.276 - 7(0.318)\,]}{[\,75.276 + 3(0.318)\,]} \times 100$$

= 95.83%

APPENDIX B

Derivation of the Expression from the Proposed Mechanism for Hydrogenation of PIP Catalyzed by $RhCl_3$/TPPMS

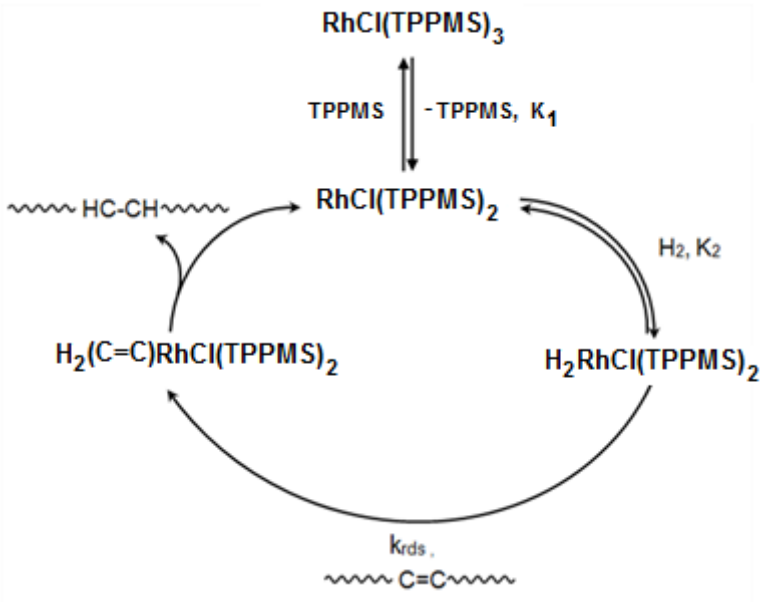

Using the steady state assumption for reaction intermediates, the following equilbria define the concentration of each catalytic species related to the rate determining step.

$$-\frac{d[C=C]}{dt} = k_{rds}[H_2RhCl(TPPMS)_2][C=C] \quad \text{(B-1)}$$

$$K_2 = \frac{[H_2RhCl(TPPMS)_2]}{[RhCl(TPPMS)_2][H_2]}$$

Hence; $$[RhCl(TPPMS)_2] = \frac{[H_2RhCl(TPPMS)_2]}{K_2[H_2]} \quad \text{(B-2)}$$

$$K_1 = \frac{[RhCl(TPPMS)_2][TPPMS]}{[RhCl(TPPMS)_3]}$$

Hence; $$[RhCl(TPPMS)_3] = \frac{[RhCl(TPPMS)_2][TPPMS]}{K_1}$$

or $$[RhCl(TPPMS)_3] = \frac{[H_2RhCl(TPPMS)_2][TPPMS]}{K_1 K_2[H_2]} \quad \text{(B-3)}$$

A material balance on the rhodium charged to the system yields;

$$[Rh]_T = [H_2RhCl(TPPMS)_2] + [RhCl(TPPMS)_2] + [RhCl(TPPMS)_3] \quad \text{(B-4)}$$

The rhodium species in Eq.(B-4) are substituted by Eq. (B-2) and (B-3), and transform to;

$$[Rh]_T = [H_2RhCl(TPPMS)_2]\left(1+\frac{1}{K_2[H_2]}+\frac{[TPPMS]}{K_1K_2[H_2]}\right)$$

$$= [H_2RhCl(TPPMS)_2]\left(\frac{K_1K_2[H_2]+K_1+[TPPMS]}{K_1K_2[H_2]}\right) \quad \text{(B-5)}$$

Rearranging Eq. (B-5) yields;

$$[H_2RhCl(TPPMS)_2] = \frac{K_1K_2[H_2][Rh]_T}{K_1K_2[H_2]+K_1+[TPPMS]}$$

$$= \frac{K_1K_2K_H P_{H_2}[Rh]_T}{K_1K_2K_{H_2}P_{H_2}+K_1+[TPPMS]} \quad \text{(B-6)}$$

where K_H is the Henry's Law constant for hydrogen in water, and P_{H2} is the hydrogen pressure.

The relationship of the hydrogenation rate to the operating conditions can be derived by substitution of Eq. (B-6) into Eq. (B-1) which is the rate determining step of the process.

$$-\frac{d[C=C]}{dt} = \frac{k_{rds}K_1K_2K_{H_2}P_{H_2}[Rh]_T[C=C]}{K_1K_2K_{H_2}P_{H_2}+K_1+[TPPMS]} \quad \text{(B-7)}$$

APPENDIX C

Results for the Aqueous-Phase Hydrogenation of Nanosized Polyisoprene Emulsion

Table C-1 Results for the synthesis of PIP: Effect of [SDS].

[SDS] (wt%)	Exp Run	D_n (nm)	Average D_n (nm)	Solid Content (%)	Average Solid Content (%)	Conversion (%)	Average Conversion (%)
0.25	1	50.0	49.3	13.6	13.4	67.7	69.3
0.25	2	48.6		13.2		70.9	
0.35	3	44.1	43.9	15.3	15.8	79.9	82.2
0.35	4	43.7		16.2		84.5	
0.69	5	32.4	32.8	16.3	15.9	85.7	83.6
0.69	6	33.2		15.5		81.5	
2.18	7	22.6	22.3	15.8	16.1	83.7	85.3
2.18	8	22.0		16.4		86.9	

Condition: IP/H_2O= 0.4 w/w; [SPS] = 0.3 wt%; [$NaHCO_3$] = 0.6 wt%; temperature=75°C; stirring speed=300 rpm; reaction time = 18 h.

Table C-2 Results for the aqueous-phase hydrogenation of PIP emulsion.

Entry	Initial D_n (nm)	[Rh] (μM)	T (^oC)	P (bar)	D_n (HPIP) (nm)	% HD
1	22.3	0	140	41.4	27.2	2.6
2	22.3	50	140	41.4	25.9	51.6
3	22.3	125	140	41.4	28.1	81.3
4	22.3	250	100	41.4	25.0	22.1
5	22.3	250	120	41.4	28.5	35.8
6	22.3	250	130	41.4	28.2	95.8
7	22.3	250	140	6.9	25.7	72.8
8	22.3	250	140	10.3	25.3	82.5
9	22.3	250	140	13.8	28.8	83.6
10	22.3	250	140	27.6	29.6	92.8
11	22.3	250	140	41.4	28.5	96.0
12	43.9	0	140	41.4	49.0	2.7
13	43.9	50	140	41.4	52.1	71.0
14	43.9	125	140	41.4	57.2	79.4
15	43.9	250	100	41.4	56.0	21.4
16	43.9	250	120	41.4	47.3	33.0
17	43.9	250	130	41.4	46.2	86.3
18	43.9	250	140	6.9	54.2	63.6
19	43.9	250	140	10.3	55.6	75.0
20	43.9	250	140	13.8	48.1	84.7
21	43.9	250	140	27.6	47.6	93.5
22	43.9	250	140	41.4	52.3	96.0

Hydrogenation conditions: [C=C] = 125 mM; catalyst precursor = $RhCl_3$/TPPMS (P/Rh molar ratio = 3); reaction time = 6 h.

Table C-3 Results for the kinetic study of HPIP: Effect of particle size and catalyst concentration.

Time (s)	% HD at Dn= 22.3 nm, [Rh]=250 μM	X	1-X	ln(1-X)	% HD at Dn= 38.1 nm, [Rh]=250 μM	X	1-X	ln(1-X)
1800	30.5	0.31	0.70	-0.36	3.1	0.03	0.97	-0.03
3600	43.2	0.43	0.57	-0.57	9.2	0.09	0.91	-0.10
5400	57.8	0.58	0.42	-0.86	18.9	0.19	0.81	-0.21
7200	61.0	0.61	0.39	-0.94	21.2	0.21	0.79	-0.24
10800	69.1	0.69	0.31	-1.17	54.0	0.54	0.46	-0.78
14400	77.4	0.77	0.23	-1.49	58.7	0.59	0.41	-0.89
18000	81.0	0.81	0.19	-1.66	66.2	0.66	0.34	-1.09
21600	93.1	0.93	0.07	-2.67	89.8	0.90	0.10	-2.28
28800	92.7	0.93	0.07	-2.61	87.2	0.87	0.13	-2.06
32400	95.7	0.96	0.04	-3.15	92.8	0.93	0.07	-2.63
43200	96.5	0.96	0.04	-3.35	95.5	0.96	0.05	-3.10

Time (s)	% HD at Dn= 49.3 nm, [Rh]=250 μM	X	1-X	ln(1-X)	% HD at Dn= 22.3 nm, [Rh]=125 μM	X	1-X	ln(1-X)
1800	3.7	0.04	0.96	-0.04	10.2	0.10	0.90	-0.11
3600	4.2	0.04	0.96	-0.04	15.0	0.15	0.85	-0.16
5400	15.0	0.15	0.85	-0.16	18.0	0.18	0.82	-0.20
7200	15.1	0.15	0.85	-0.16	25.5	0.25	0.75	-0.29
10800	20.6	0.21	0.79	-0.23	43.6	0.44	0.56	-0.57
14400	40.3	0.40	0.60	-0.52	49.9	0.50	0.50	-0.69
18000	63.2	0.63	0.37	-1.00	65.3	0.65	0.35	-1.06
21600	73.5	0.74	0.26	-1.33	76.0	0.76	0.24	-1.43
28800	83.9	0.84	0.16	-1.83	83.1	0.83	0.17	-1.78
32400	90.1	0.90	0.10	-2.31	88.4	0.88	0.12	-2.16
43200	95.1	0.95	0.05	-3.02	93.8	0.94	0.06	-2.78

Condition : [C=C] = 125 mM; catalyst precursor = $RhCl_3$/TPPMS (P/Rh molar ratio = 3); temperature = 140 $^{\circ}C$; H_2 pressrure = 41.4 bar

Table C-4 Results for the kinetic study of HPIP: Effect of temperature and H_2 pressure.

Time (s)	% HD at P= 13.8 bar, T=140 °C	X	1-X	ln(1-X)	% HD at P= 27.6 bar, T=140 °C	X	1-X	ln(1-X)	% HD at P= 41.4 bar, T=140 °C	X	1-X	ln(1-X)
1800	6.8	0.07	0.93	-0.07	7.9	0.08	0.92	-0.08	30.5	0.31	0.70	-0.36
3600	14.0	0.14	0.86	-0.15	21.4	0.21	0.79	-0.24	43.2	0.43	0.57	-0.57
5400	19.7	0.20	0.80	-0.22	25.4	0.25	0.75	-0.29	57.8	0.58	0.42	-0.86
7200	25.4	0.25	0.75	-0.29	37.8	0.38	0.62	-0.47	61.0	0.61	0.39	-0.94
10800	42.0	0.42	0.58	-0.54	57.8	0.58	0.42	-0.86	69.1	0.69	0.31	-1.17
14400	58.9	0.59	0.41	-0.89	63.5	0.64	0.36	-1.01	77.4	0.77	0.23	-1.49
18000	69.3	0.69	0.31	-1.18	80.2	0.80	0.20	-1.62	81.0	0.81	0.19	-1.66
21600	77.4	0.77	0.23	-1.49	86.2	0.86	0.14	-1.98	90.1	0.90	0.10	-2.31

Time (s)	% HD at P= 41.4 bar, T=130 °C	X	1-X	ln(1-X)	% HD at P= 41.4 bar, T=120 °C	X	1-X	ln(1-X)
1800	7.4	0.07	0.93	-0.08	7.7	0.08	0.92	-0.08
3600	8.5	0.09	0.91	-0.09	6.6	0.07	0.93	-0.07
5400	19.7	0.20	0.80	-0.22	12.3	0.12	0.88	-0.13
7200	21.8	0.22	0.78	-0.25	18.2	0.18	0.82	-0.20
10800	38.6	0.39	0.61	-0.49	21.9	0.22	0.78	-0.25
14400	46.0	0.46	0.54	-0.62	23.8	0.24	0.76	-0.27
18000	59.8	0.60	0.40	-0.91	26.3	0.26	0.74	-0.31
21600	78.4	0.78	0.22	-1.53	30.4	0.30	0.70	-0.36

Condition : [C=C] = 125 mM; particle size = 22.3 nm; catalyst precursor = $RhCl_3$/TPPMS (P/Rh molar ratio = 3); [Rh] = 250 μM

APPENDIX D

Results for the Aqueous-Phase Hydrogenation of Natural Rubber Latex

Table D-1 Results for the aqueous-phase hydrogenation of NR latex and PIP emulsion.

Entry	Polymer	[Rh] (μM)	P (bar)	T (°C)	D_n (nm)	% HD
1	NR	0	41.4	130	183.5	5.8
2	NR	25	41.4	130	175.7	8.3
3	NR	50	41.4	130	191.2	35.3
4	NR	125	41.4	130	188.4	66.6
5	NR	175	41.4	130	186.6	71.4
6	NR	250	6.9	130	163.8	12.9
7	NR	250	10.3	130	185.6	21.0
8	NR	250	13.8	130	180.4	73.1
9	NR	250	27.6	130	168.5	81.3
10	NR	250	41.4	100	175.9	23.1
11	NR	250	41.4	110	176.2	22.4
12	NR	250	41.4	120	175.1	24.2
13	NR	250	41.4	130	172.6	85.8
14	NR	250	41.4	140	179.0	83.0
15	NR	250	41.4	150	178.1	60.6
16	PIP	0	41.4	130	55.7	3.8
17	PIP	25	41.4	130	54.7	14.6
18	PIP	50	41.4	130	55.0	44.5
19	PIP	125	41.4	130	55.6	75.4
20	PIP	175	41.4	130	56.5	85.9
21	PIP	250	6.9	130	52.7	31.2
22	PIP	250	10.3	130	52.1	56.8
23	PIP	250	13.8	130	52.9	78.0
24	PIP	250	27.6	130	54.5	79.8
25	PIP	250	41.4	100	54.2	25.5
26	PIP	250	41.4	110	54.0	30.2
27	PIP	250	41.4	120	56.5	32.1
28	PIP	250	41.4	130	54.9	88.9
29	PIP	250	41.4	140	51.8	89.7
30	PIP	250	41.4	150	55.6	87.9

Hydrogenation conditions: [C=C] = 125 mM; initial D_n of NR= 169.1 nm, PIP = 49.3 nm; time = 6 h; catalyst precursor = $RhCl_3$/TPPMS P/Rh Molar ratio = 3

APPENDIX E

Results for the Mechanical Properties of NR/PIP and NR/HPIP Blends

Table E-1 Tensile strength of NR/PIP and NR/HPIP blends.

Rubber sample	NR/PIP or NR/HPIP	Tensile strength (MPa) before ageing					Tensile strength (MPa) after ageing				
		1	2	3	Mean	SD	1	2	3	Mean	SD
NR	-	21.6	21.4	20.2	21.1	0.8	13.0	12.9	13.5	13.1	0.3
NR/PIP	90/10	17.4	16.5	17.1	17.0	0.5	10.8	10.1	10.7	10.5	0.4
	80/20	15.2	14.7	15.3	15.1	0.3	8.5	7.8	8.9	8.4	0.6
	70/30	12.3	11.8	12.4	12.2	0.3	7.1	7.5	7.0	7.2	0.3
	60/40	8.1	8.9	8.4	8.4	0.4	4.5	5.6	5.1	5.1	0.5
NR/HPIP	90/10	15.6	14.9	16.3	15.6	0.7	12.0	13.6	12.9	12.8	0.8
	80/20	13.7	12.3	12.7	12.9	0.7	11.9	12.3	12.4	12.2	0.3
	70/30	9.2	8.3	8.0	8.5	0.6	8.4	7.9	8.3	8.2	0.3
	60/40	5.4	4.6	5.1	5.1	0.4	5.2	4.4	5.0	4.9	0.4

Table E-2 Modulus at 300% elongation of NR/PIP and NR/HPIP blends.

Rubber sample	NR/PIP or NR/HPIP	Modulus (MPa) before ageing					Modulus (MPa) after ageing				
		1	2	3	Mean	SD	1	2	3	Mean	SD
NR	-	1.79	1.72	1.67	1.73	0.06	1.29	1.32	1.34	1.32	0.03
NR/PIP	90/10	1.67	1.65	1.63	1.65	0.02	1.29	1.22	1.23	1.25	0.04
	80/20	1.54	1.63	1.49	1.55	0.07	1.21	1.10	1.15	1.15	0.06
	70/30	1.53	1.64	1.58	1.58	0.06	1.18	1.21	1.26	1.22	0.04
	60/40	1.43	1.38	1.47	1.43	0.05	1.18	1.11	0.93	1.07	0.13
NR/HPIP	90/10	1.49	1.48	1.55	1.51	0.04	1.21	1.19	1.25	1.22	0.03
	80/20	1.38	1.36	1.24	1.33	0.08	1.31	1.27	1.15	1.24	0.08
	70/30	1.14	1.16	1.02	1.11	0.08	1.11	1.12	0.97	1.07	0.08
	60/40	0.96	0.72	0.89	0.86	0.12	0.93	0.67	0.83	0.81	0.13

Table E-3 Elongation at break of NR/PIP and NR/HPIP blends.

Rubber sample	NR/PIP or NR/HPIP	Elongation at break (%) before ageing					Elongation at break (%) after ageing				
		1	2	3	Mean	SD	1	2	3	Mean	SD
NR	-	841	823	820	828	11.4	748	770	760	759	11.0
NR/PIP	90/10	797	811	823	810	13.0	745	764	766	758	11.6
	80/20	824	835	806	822	14.6	765	756	744	755	10.5
	70/30	784	805	791	793	10.7	728	752	744	741	12.2
	60/40	756	773	779	769	11.9	696	708	721	708	12.5
NR/HPIP	90/10	808	788	791	796	10.8	740	728	748	739	10.1
	80/20	762	775	784	774	11.1	735	744	758	746	11.6
	70/30	744	733	726	734	9.1	700	687	708	698	10.6
	60/40	649	639	626	638	11.5	598	629	617	615	15.6

APPENDIX F

Classification of Cracking on the Surface of Rubber Specimens for Ozone Resistance Tesing.

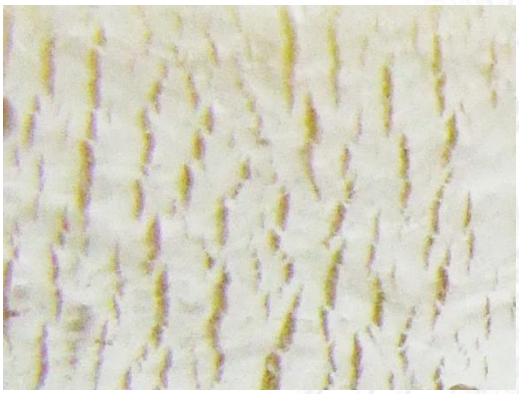

Number of Cracking

A : A small number of cracking.

B : A large of number cracking.

C : Numerous cracking.

Appearance of Cracking

1 : That which cannot be seen with eyes but can be confirmed with 10 times magnifying glass.

2 : That which can be confirmed with naked eyes.

3 : That which the deep and comparatively long (below 1 mm).

4 : That which the deep and long (above 1 mm and below 3 mm).

5 : That which about to crack more than 3 mm or about to severe.

VITA

Mr. Pornlert Piya-areetham was born on March 18th, 1983 in Bangkok, Thailand. He received his B.Sc. (Second class honors) degree from the Department of Chemical Technology, Chulalongkorn University in 2005. He became a production engineer at Thai Chemical Corp., Ltd. and AGC Chemicals (Thailand) Co., Ltd. in Samutprakan for 4 years. Pornlert resumed studying for a Doctoral Degree in Chemical Technology, Chulalongkorn University in 2009. He has received the Royal Golden Jubilee Scholarship from Thailand Research Fund for his Ph.D. study. He carried out some of his PhD research for one year (2010-2011) and four months (2012) at the "Advanced Rubber Technology and Applied Catalysis Laboratory" in Chemical Engineering, University of Waterloo, ON, Canada.

Journal Publication

1. Piya-areetham, P., Prasassarakich, P., and Rempel, G.L. Organic solvent-free hydrogenation of natural rubber latex and synthetic polyisoprene emulsion catalyzed by water-soluble rhodium complexes. Journal of Molecular Catalysis A: Chemical 372 (2013) 151-159.

2. Piya-areetham, P., Prasassarakich, P., and Rempel, G.L. Aqueous - Phase Hydrogenation of Nanosized Polyisoprene Emulsion Using Rhodium Catalysts. European Polymer Journal 49 (2013) 2584-2595

Conference Presentation

1. Piya-areetham, P., Prasassarakich, P., Rempel, G.L. (2012) "Aqueous - Phase Hydrogenation of Nanosized Polyisoprene Emulsion and Natural Rubber Latex Using Rhodium Catalysts" oral presentation conference on RGJ-Ph.D Congress XIII, 6 - 8 April, 2012 in Jomtien Palm Beach Hotel, Chonburi, Thailand.

2. Piya-areetham, P., Prasassarakich, P., Rempel, G.L. (2012) "Aqueous - Phase Hydrogenation of Nanosized Polyisoprene Emulsion and Natural Rubber Latex Using Rhodium Catalysts" poster presentation conference on 22nd Canadian Symposium on Catalysis, 13-16 May 2012 in Quebec City, Canada.